



## 저작자표시-비영리-변경금지 2.0 대한민국

이용자는 아래의 조건을 따르는 경우에 한하여 자유롭게

- 이 저작물을 복제, 배포, 전송, 전시, 공연 및 방송할 수 있습니다.

다음과 같은 조건을 따라야 합니다:



저작자표시. 귀하는 원저작자를 표시하여야 합니다.



비영리. 귀하는 이 저작물을 영리 목적으로 이용할 수 없습니다.



변경금지. 귀하는 이 저작물을 개작, 변형 또는 가공할 수 없습니다.

- 귀하는, 이 저작물의 재이용이나 배포의 경우, 이 저작물에 적용된 이용허락조건을 명확하게 나타내어야 합니다.
- 저작권자로부터 별도의 허가를 받으면 이러한 조건들은 적용되지 않습니다.

저작권법에 따른 이용자의 권리는 위의 내용에 의하여 영향을 받지 않습니다.

이것은 [이용허락규약\(Legal Code\)](#)을 이해하기 쉽게 요약한 것입니다.

[Disclaimer](#)

Doctoral Thesis

Spatiotemporal Integration of Early Visual Processing:  
Visual Phenomena beyond the Critical Fusion Frequency

Seonggyu Choe

Department of Biomedical Engineering  
(Human Factors Engineering)

Ulsan National Institute of Science and Technology

2023

# Spatiotemporal Integration of Early Visual Processing: Visual Phenomena beyond the Critical Fusion Frequency

Seonggyu Choe

Department of Biomedical Engineering  
(Human Factors Engineering)

Ulsan National Institute of Science and Technology

# Spatiotemporal Integration of Early Visual Processing: Visual Phenomena beyond the Critical Fusion Frequency

A thesis/dissertation submitted to  
Ulsan National Institute of Science and Technology  
in partial fulfillment of the  
requirements for the degree of  
Doctor of Philosophy

Seonggyu Choe

07.10.2023 of submission

Approved by



---

Advisor

Oh-Sang Kwon

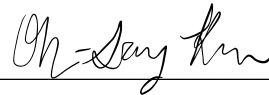
# Spatiotemporal Integration of Early Visual Processing: Visual Phenomena beyond the Critical Fusion Frequency

Seonggyu Choe

This certifies that the thesis/dissertation of Seonggyu Choe is approved.

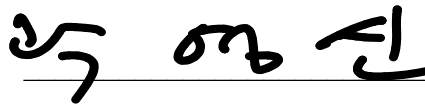
07.10.2023 of submission

Signature



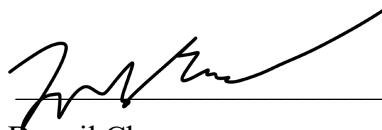
Advisor: Oh-Sang Kwon

Signature



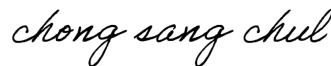
Youngshin Kwak

Signature



Dongil Chung

Signature



Sang Chul Chong

Signature



Sung Jun Joo

## Abstract

Our visual system integrates continuous signals to construct visual representation. This integration process involves combining visual inputs across both space and time. This spatiotemporal integration is inherently linked to motion. The movements of our eyes play a fundamental role in shaping our visual perception by spatially shifting the images projected on our retinas. The significance of considering the effects of eye movements on visual perception, resulting from these spatial modulations, has been consistently emphasized.

In the first part of the study, we focused on examining the influence of eye movements on the temporal sensitivity of the human visual system. Specifically, we assessed participants' ability to detect the flickering visual stimuli with and without the inclusion of eye movements. The findings revealed that the effects of eye movements varied depending on the spatial features of the stimuli. When eye movements were incorporated, participants were able to perceive flickering edges beyond their temporal limit, surpassing the critical fusion frequency (CFF). Furthermore, a significant positive correlation was observed between temporal sensitivity and the extent of eye movements executed during stimulus presentation.

To further elucidate the alterations in visual perception caused by the spatial characteristics of visual stimuli and the shifted retinal image resulting from eye movements, we developed a spatiotemporal integration model. This model aimed to emulate the spatiotemporal integration process occurring in our early visual system and was employed to encompass the observations made in this study.

In the second part of the study, we investigated the phenomena of visual persistence and the sense of reality associated with moving objects that move at a speed comparable to our eye movements (approximately 100 degrees per second). Introducing a Speedline, which connected two consecutively presented objects spatially, mitigated the smear effect on moving objects in terms of the range of visual persistence and perceived length. Additionally, the presence of the Speedline enhanced the resemblance between the moving objects in the display and the motion of objects in the real world, thereby amplifying the sense of reality in the object motion.

Overall, this study offers valuable insights into how eye movements impact visual perception, considering the spatial features of objects. The predictions made by the developed model suggest that the observed behavioral patterns, such as elevated temporal sensitivity to stimuli containing spatial edges, are outcomes of the spatiotemporal integration process

occurring in our early visual system. By investigating the intricate relationship between eye movements, object motion, spatial characteristics of visual stimuli, and visual perception, we deepen our understanding of how visual system processes and integrates visual information.





## Contents

<b>1. General Introduction</b>	<b>12</b>
1.1. Effects of eye movements on the visual perception	12
1.2. Spatiotemporal integration model of the visual receptive field	13
1.2.1. Spatiotemporal receptive (STRF) field model	14
1.2.2. Linear-Nonlinear (LN) model	14
1.3. Visual phenomena beyond the Critical Fusion Frequency (CFF)	15
<b>2. The effect of spatial modulations caused by eye movements on the temporal sensitivity of the human visual system</b>	<b>16</b>
2.1. Introduction	16
2.2. Effects of spatial edges and its orientation on CFFs during fixation	18
2.2.1. Participants	18
2.2.2. Apparatus	18
2.2.3. Stimuli	19
2.2.4. Procedure	19
2.2.5. Data Analysis	21
2.2.6. Results: The spatial edge increases CFFs regardless of the edge orientation	21
2.3. Effects of saccadic eye movements on CFFs for Flicker Containing Edge (FCE) stimuli	23
2.3.1. Participants, Apparatus, and Stimuli	23
2.3.2. Procedure	23
2.3.3. Data Analysis	23
2.3.4. Results: Saccadic eye movements selectively increase CFFs for FCE stimuli	23
2.4. Effects of the stimulus duration on CFFs for uniform and FCE stimuli	25
2.4.1. Participants, Apparatus, and Stimuli	25
2.4.2. Procedure	25
2.4.3. Data Analysis	25
2.4.4. Results: The longer stimulus duration increases CFFs for FCE stimuli while CFFs for uniform stimuli remain same	25
2.5. The relationship between the extent of fixational eye movements and the CFF elevation	27
2.5.1. Participants	27
2.5.2. Apparatus and Stimuli	27
2.5.3. Procedure	27
2.5.4. Data Analysis	28
2.5.5. Results: CFFs for FCE stimuli increase as the extents of fixational eye movements increase	28
2.6. A spatiotemporal integration model of retinal receptive fields	29

2.7. The eccentricity effect on the CFFs for uniform and FCE stimuli predicted by the spatiotemporal integration model .....	37
2.7.1. Methods and Procedure .....	37
2.7.2. Data Analysis .....	38
2.7.3. Model Prediction .....	38
2.7.4. Results: Increasing eccentricity increases CFFs for uniform stimuli but decreases CFFs for FCE stimuli despite the enhanced temporal sensitivity .....	38
2.8. Discussion .....	41
2.9. Conclusion .....	44
<b>3. Effects of Speedline on visual persistence and perceived quality of motion .....</b>	<b>45</b>
3.1. Introduction .....	45
3.2. Effects of Speedline on the range of persisting images .....	48
3.2.1. Participants .....	48
3.2.2. Apparatus .....	48
3.2.3. Stimuli .....	48
3.2.4. Procedure .....	49
3.2.5. Data Analysis .....	50
3.2.6. Results: Speedline reduces the range of concurrently perceived persisting images .....	50
3.3. Testing effects of stimulus size on the range of .....	52
3.3.1. Participants .....	52
3.3.2. Stimuli .....	52
3.3.3. Procedure .....	52
3.3.4. Data Analysis .....	52
3.3.5. Results: The persistence range is modulated by Speedline, not the stimulus size .....	53
3.4. Manipulating connectivity of line stimuli .....	54
3.4.1. Participants .....	54
3.4.2. Stimuli .....	54
3.4.3. Procedure .....	54
3.4.4. Data Analysis .....	54
3.4.5. Results: The connectivity between stimulus locations suppresses visual persistence .....	55
3.5. Effects of Speedline on the perceived length of moving stimuli .....	57
3.5.1. Participants .....	57
3.5.2. Stimuli .....	57
3.5.3. Procedure .....	58
3.5.4. Data Analysis .....	59
3.5.5. Results: Speedline reduces the perceived length of moving stimuli .....	59

3.6. A sense of reality with the presence or absence of Speedline .....	61
3.6.1.Participants .....	61
3.6.2.Apparatus and Stimuli .....	61
3.6.3.Procedure .....	61
3.6.4.Analysis of the distances between the internal representations from the 2IFC task .....	62
3.6.5.Speedline enhances the sense of reality of moving stimuli .....	64
3.7. Discussion .....	66
3.8. Conclusion .....	67
<b>4. General Discussion .....</b>	<b>68</b>
<b>5. Reference .....</b>	<b>70</b>
<b>6. Appendix.....</b>	<b>77</b>

## List of Figures

<b>Chapter 2</b> .....	
Figure 1. The three stimuli used in Experiment 1 .....	19
Figure 2. A schematic illustration of the 2IFC task structure in a single trial .....	20
Figure 3. Estimation of the critical fusion frequency in different stimulus conditions .....	21
Figure 4. Mean estimated CFF for the three types of stimuli .....	22
Figure 5. The effect of saccadic eye movements on CFFs for three types of stimuli .....	24
Figure 6. The effect of the stimulus duration on CFFs for the uniform and FCE stimuli .....	26
Figure 7. The effect of the eye movements extents on CFFs for the uniform and FCE stimuli .....	29
Figure 8. The spatiotemporal integration profile used in our model .....	30
Figure 9. Model prediction of the retinal responses to FCE stimuli presented at 120 Hz .....	33
Figure 10. Model prediction on the correction rate as a function of refresh rates .....	34
Figure 11. CFFs for FCE stimuli predicted by the spatiotemporal integration model .....	36
Figure 12. A schematic illustration of the experimental set-up .....	37
Figure 13. The effect of eccentricity on the estimated CFF for the uniform and FCE stimuli .....	39
Figure 14. Illustration of the phantom array .....	41
<b>Chapter 3</b> .....	
Figure 15. Illustration of the two stimuli used in Experiment 1 .....	49
Figure 16. A schematic illustration of the experimental task in Experiment 1 .....	50
Figure 17. The range of concurrently perceived persisting images for a moving dot and line .....	51
Figure 18. The range of concurrently perceived persisting images for different stimulus types .....	53
Figure 19. The range of concurrently perceived persisting images for the different length of line .....	56
Figure 20. The dot and line stimulus with varied number of elements .....	58
Figure 21. The perceived length of moving dot stimuli and dot stimuli as a function of the number of elements .....	60
Figure 22. The internal representation for moving objects presented at each refresh rates .....	64
Figure 23. The accumulated internal distance between refresh rates for dot and line stimuli .....	65

## 1. General Introduction.

### 1.1. Effects of eye movements on the visual perception

Our eyes are never steady, even when we try to maintain fixation. The primary function of eye movements is to position the region of interest in our visual field onto the retina, which is the area with the highest visual acuity. Extensive research has consistently demonstrated that eye movements have a significant impact on our visual perception (Keesey, 1971; Li et al., 2016; Schütz et al., 2009; West, 1968; Zhao et al., 2020). Eye movements can be categorized into different types based on their characteristics, including velocity, amplitude, dispersion, and duration.

Saccades are rapid, ballistic eye movements that redirect the gaze to a new target. They are characterized by short durations (20-200 ms) and high peak velocities (up to 1000 deg/s). Saccades play a crucial role in shifting attention and exploring the visual scene. Fixational eye movements encompass ocular drift and microsaccades. Ocular drift refers to slow, involuntary movements that occur when fixating on a stationary object. Microsaccades, on the other hand, are relatively fast, involuntary movements that occur within a very short time period. These small eye movements contribute to gaze stabilization and the maintenance of visual acuity. Smooth pursuit eye movements are voluntary tracking movements used to smoothly follow a moving target. They enable us to track and maintain fixation on a moving object.

The effects of eye movements on visual perception are observed in both the spatial and temporal domains. In the spatial domain, fixational eye movements, despite their inherent instability, actually enhance fine visual acuity (Clark et al., 2022; Intoy & Rucci, 2020). The small involuntary movements, such as ocular drift and microsaccades, help equalize the spectral power and reduce the power of low spatial frequency areas (Kuang et al., 2012; Zhao et al., 2020), resulting in clearer perception (Poletti et al., 2010). In fact, complete stabilization of the eyes leads to a significant decrease in visual acuity compared to normal vision conditions. However, there are instances such as saccadic suppression, where rapid eye movements degrade the detectability of visual stimuli and reduce the ability to discriminate the saccadic landing position (Henning et al., 2002; Krekelberg, 2010; Matin, 1974).

In terms of temporal sensitivity, different types of eye movements also play a crucial role. Saccades have been found to extend the range of temporal sensitivity (Burr & Morrone, 1996; Roberts & Wilkins, 2013; Zimmermann et al., 2014) by enhancing the critical fusion frequency (CFF), the frequency above which the flickering images appear continuous. Smooth pursuit eye movements increase the CFF compared to fixation conditions, indicating an enhancement in temporal sensitivity (Terao et al., 2010; Tong et al., 2009). Individuals with nystagmus, characterized by involuntary eye movements, exhibit an accelerated temporal impulse response function (TIRF) compared to those with

normal vision (Bedell et al., 2008; Waugh & Bedell, 1992), suggesting altered temporal sensitivity due to specific eye movement patterns.

The various types of eye movements, including saccades, fixational eye movements, and smooth pursuit eye movements, have notable effects on both spatial and temporal sensitivity. Understanding the relationship between these eye movements and visual perception provides valuable insights into how our visual system processes and integrates visual information over time.

## **1.2. Spatiotemporal integration model of the visual receptive field**

Eye movements shift retinal images and subsequently alter visual perception. Moreover, it is important to consider not only the shifted retinal images due to eye movements but also the process by which our visual perception of the external world is constructed. Evidence suggests that our visual system integrates continuous signals to construct visual perception. The construction of visual perception takes time, and the resulting perceptual representation remains active for a certain duration. This can be observed in the dynamics of visual perception (Burr, 1980; Ikeda, 1986; Rashbass, 1970) and neural activity (Cai et al., 1997; Linsenmeier et al., 1982). Particularly when it comes to the effects of eye movements on shifted retinal images, we employed a spatiotemporal integration model to capture this integration process both over time and space,

In this study, the spatiotemporal integration model refers to a computational framework designed to simulate the processes involved in integrating spatial and temporal information in the early stages of visual processing (DeAngelis et al., 1993; Wimbauer et al., 1997). The goal of the model is to replicate how the visual system combines and analyzes visual inputs across space and time, with a focus on fine detail and extremely short timescales. Motion is inherently involved in the dynamics of visual stimuli over both space and time, originating from two main sources: our own eye movements, which shift the retinal images in the opposite direction of the eye movements, and the motion of objects in the external world. The first part of our study focuses on the effects of eye movements whereas the second part focuses on the effect of object motion as fast as our eyes are moving.

In the context of eye movements and visual perception, the spatiotemporal integration model helps elucidate how the shifted retinal image resulting from eye movements is processed and integrated with the spatial characteristics of visual stimuli. It takes into account factors such as the receptive fields of retinal cells, the temporal dynamics of neural responses, and the linear and nonlinear processes that follow. By incorporating this model into our study, we were able to make predictions about how the visual system responds to stimuli with different spatial characteristics and how the perception of motion and spatial features is influenced by eye movements. The model provides a computational framework that enhances our understanding and interpretation of the observed behavioral patterns and phenomena

related to visual perception in the context of eye movements and object motion. It allows us to better understand the intricate interactions between eye movements, spatial information, and temporal dynamics, offering valuable insights into the mechanisms underlying visual perception.

### 1.2.1 Spatiotemporal receptive field (STRF) model

The Spatiotemporal receptive field (STRF) model is a valuable tool in understanding visual processing in the retina and the lateral geniculate nucleus (LGN), a relay station for visual information coming from the retina to the visual cortex.

The STRF characterizes the receptive fields of neurons in the lateral geniculate nucleus (LGN) and retina, incorporating both spatial and temporal properties. It describes how neurons integrate and process temporal information from visual stimuli and their sensitivity to different spatial locations and orientations. These receptive fields can be characterized in terms of their spatial and temporal properties.

The temporal receptive field refers to the neuron's sensitivity to changes in visual stimuli over time, commonly represented as temporal impulse response function (TIRF). It characterizes the temporal properties of the neuron's response, such as its preferred temporal frequency, phase, and duration. The temporal component of the STRF captures how the neuron integrates and processes temporal information from visual stimuli. The spatial receptive field refers to the region in the visual field that, when stimulated, leads to a response in the neuron. It is typically described as a two-dimensional area and represents the receptive field's sensitivity to different locations in the visual space. The spatial component of the STRF describes the receptive field's spatial properties, such as its size, center-surround organization, and preferred orientation.

### 1.2.2 Linear-Nonlinear (LN) model

The Linear-Nonlinear (LN) model simplifies the complex computations in retinal neurons by separating them into linear and nonlinear stages (Geisler & Albrecht, 1995; Kuo et al., 2016; Tolhurst et al., 1980). The linear stage involves the spatial and temporal filtering of visual inputs using linear filters, basically the convolution of the spatiotemporal receptive fields and 2-dimensional visual inputs over time and space. This captures the neuron's sensitivity to different spatial and temporal features. In constructing a retinal response model, the inclusion of nonlinear processes is necessary to accurately represent the behavior of the retinal cells and their responses to visual stimuli. The retinal cells, such as photoreceptors and ganglion cells, exhibit nonlinear characteristics in their response to light and visual stimuli. The nonlinear stage accounts for thresholding, saturation effects, and other nonlinear properties of retinal neurons. It introduces a nonlinear activation function that reproduces observed behaviors like contrast adaptation and response saturation.

### 1.3. Visual phenomena beyond the Critical Fusion Frequency (CFF)

Our visual system is highly sensitive both in terms of the spatial domain (Patel, 1966; Westheimer, 1975; Westheimer, 1981) and temporal domain (Sweet, 1953; Tadin et al., 2010; Westheimer & McKee, 1977; Zanker & Harris, 2002). In the one hand, there has been extensive study regarding the spatial resolution of the human visual system. For instance, in hyperacuity task (Westheimer, 1975), when two vertical lines are misaligned, we can detect this misalignment with a precision up to 10 times better than visual acuity. On the other hand, investigating the temporal limits of the human visual system has long been a central topic in visual research. The common method used to measure our temporal resolution is the temporal order judgment task, where participants were presented with two brief flashes and then asked to discriminate which flash occur earlier. Participants were able to discriminate 15 ms difference (Exner, 1895). Especially when two flashes are spatially separated, discrimination thresholds in time reduce to 5 ms (Sweet, 1953; Westheimer & McKee, 1977).

One of the properties characterizing the temporal sensitivity is the critical fusion frequency (CFF), which refers to the frequency above which a flickering stimulus appears continuous. If the stimulus flickers above the CFF, the observers no longer perceive the flickering stimulus, but instead perceives a continuous image. For instance, our smartphone is never continuous but appears so. CFF is known to vary depending on various factors such as stimulus brightness, stimulus size, and distance from the center of the field of view. Nevertheless, there has been a consensus that CFFs are generally reported to be in the range of 50-90 Hz (De Lange, 1952; De Lange, 1958; Eisen-Enosh et al., 2017; Hecht & Smith, 1936; Kelly, 1961, Kelly, 1971; Mankowska et al., 2021).

In our study, we aim to investigate the influence of spatial features on the visual perception of moving objects beyond our temporal limits, specifically the critical fusion frequency. In Chapter 2, we will focus on the ability of humans to perceive flickering stimuli that include high spatial frequency edges. We will examine how eye movements and the spatial characteristics of the stimuli interact to influence temporal sensitivity. In Chapter 3, we will examine the phenomena of visual persistence and the perceived sense of reality for fast-moving objects. We will investigate how the spatial features, the Speedline, influence the range of visual persistence and enhance the perceived sense of reality in object motion.



## **2. Chapter 2. The effect of spatial modulations caused by eye movements on the temporal sensitivity of the human visual system.**

In the first part of this study, we explored the effects of spatial properties and eye movements, and their interaction on the temporal sensitivity of the human visual system by measuring participants' ability to discriminate the flickering stimulus from the continuously presented visual stimuli with and without eye movements. We expected the different effect of eye movements depending on the spatial properties of the visual stimuli since the eye movements would modulate the retinal image and the ability to detect the flicker accordingly. Furthermore, to explain the observed effects of spatial features and eye movements, we constructed the spatiotemporal integration model simulating the responses of our visual system at the level of our retina or LGN, which is placed in the relatively early level in a series of information processing procedure.

### **2.1. Introduction**

The human visual system is highly sensitive to temporal changes in visual inputs (Sweet, 1953; Tadin et al., 2010; Westheimer & McKee, 1977; Zanker & Harris, 2002). The critical fusion frequency (CFF) threshold is one measurement used to quantify the temporal limits of the visual system, which represents the lowest frequency above which a flickering light stimulus can be perceived as continuous. CFFs have been measured in conditions where spatially uniform black and white blobs flickered (Kelly, 1971; Swanson et al., 1987) or in conditions where two counter-phasic Gabor patches flickered (Kelly, 1971; Watson & Nachmias, 1977). Extensive literature reveals that CFFs vary depending on various factors, such as stimulus contrast (Stromeyer & Martini, 2003; Watson, 2013), size (Rovamo & Raninen, 1988), distance from the center of the field of view (Emoto & Sugawara, 2012), and past visual experience (Seitz et al., 2005). Nevertheless, CFFs have consistently been reported to range from 50 to 90 Hz (De Lange, 1952; De Lange, 1958; Eisen-Enosh et al., 2017; Hecht & Smith, 1936; Kelly, 1961, Kelly, 1971; Mankowska et al., 2021).

However, recent research (Davis et al., 2015) has suggested that our visual system may have a higher temporal limit than previously believed, specifically in response to flickering edge stimuli. They presented two abutted black and white rectangles patches, which alternated their polarity at a given refresh rate. In the first frame, the left side is white and the right side is black whereas, in the second frame, the left side is black and the right side is white and so on (**Figure 1**). When abutted black and white patches are flickered, people can detect the edge in the middle of the stimulus at rates above 500 Hz.

This finding is surprising, as a sharp boundary enclosing the visual stimuli has previously been shown to enhance the CFF (Kelly, 1959; Keeseey, 1972) but approximately up to 60 Hz. The authors of the study suggested that the enhancement of CFFs may be attributable to saccadic eye movements. However, the role of eye movements in modulating CFF in response to FCE stimuli remains unexplored as they did not record participants' eye movements and employed the method of limits where participants matched the luminance level of the visual stimuli such that flickers were no longer visible without time limit.

Many studies have reported that eye movements can influence the temporal limits of the visual system (Keeseey, 1971; Li et al., 2016; West, 1968). Infantile nystagmus increases sensitivity to the low temporal frequency stimulus by accelerating temporal impulse response function to visual stimulation (Vaugh & Bedell, 1992; Bedell et al., 2008). Smooth pursuit and saccades also increase the speed of the impulse response function (Burr et al., 1994; Burr & Morrone, 1996; Tong et al., 2009). Smooth pursuit increases CFFs for color stimuli (Terao et al., 2010). Therefore, this study aimed to investigate whether eye movements executed during stimulus presentation can increase the CFFs for FCE stimuli beyond the commonly reported range. We tested whether CFFs for FCE stimuli scale positively with the extent of eye movements. To explain how eye movements increase CFFs for FCE stimuli, we built a filtering model that mimics the spatiotemporal integration process occurring in the low-level visual system (Cai et al., 1997; DeAngelis et al., 1993; Rust et al., 2005; Wimbauer et al., 1997).

The results of our experiments showed that, when participants executed saccade, CFF for the FCE stimuli significantly increased while those for the uniform stimuli did not. Furthermore, CFFs for the FCE stimuli systematically increased as the stimulus duration increased or the extent of fixational eye movements increased, supporting that eye movements can indeed increase CFFs for the FCE stimuli. The spatiotemporal integration model predicted the detection of flickering edge stimuli and captured the effects of eye movements on CFFs for FCE stimuli. The additional experiment replicated models' prediction by showing the opposite eccentricity effect on CFFs for uniform and FCE stimuli, providing an additional support for the model.

## 2.2. Experiment 1: Effects of spatial edges and its orientation on CFFs during fixation

Our initial objective was to replicate previous findings regarding the increase in critical flicker fusion thresholds (CFFs) with the presence of spatial edges. We conducted a study in which CFFs were measured for spatially uniform and flicker containing edge (FCE) stimuli while participants fixated their eyes at the center of the visual stimuli. To measure CFFs, we employed a 2-interval forced choice task in which participants were presented with two intervals of stimuli and had to indicate which interval contained the target stimulus.

We noted that the FCE stimuli used in previous literature, particularly those with a vertical edge, presented different images to the left and right hemispheres in each frame. This raised the possibility of hemispheric asymmetry affecting the results. Hemispheric differences in information processing have been widely reported in the perception of various visual stimuli, including temporal frequencies (Rebai et al., 1986), spatial frequencies (Christman et al., 1991; Peyrin et al., 2006), faces (Schonen et al., 1986), emotional contents (Atchley et al., 2003; Holtgraves & Felton, 2011), and speech and auditory stimuli (Gazzaniga, 1985; Hellige & Wong, 1983). In order to examine the potential effect of hemispheric asymmetry, we introduced a different type of stimulus, horizontal edge stimuli, as shown in Figure 1.

### 2.2.1. Participants

Nineteen individuals without any history of eye-related diseases within the past six months were recruited to participate in this study ( $21.44 \pm 1.95$  years; 9 men; 9 women). All participants reported having normal or corrected-to-normal visual acuity and provided informed consent prior to the start of the experiments. They were blinded to the study's objectives. The same group of participants participated in Experiments 1-3. All experimental protocols were approved by the UNIST Institutional Review Board. Although we did not conduct a power test, we observed a consistent pattern of CFFs for uniform and FCE stimuli across successive experiments with different groups of participants. Also, the sample size was comparable to that of the existing CFF studies (12 participants for Balestra et al., 2018; 10 participants for Eisen-Enosh et al., 2017; 13 participants for Seitz et al., 2005).

### 2.2.2. Apparatus

Visual stimuli were generated using MATLAB and the Psychophysics Toolbox (Brainard 1997, Pelli 1997), and displayed using a DLP projector (PROPixx;  $1920 \times 1080$ ; 120 Hz, linear gamma). The project can achieve a high refresh rate up to 1440 Hz by breaking up a single 120 Hz RGB signal into

12 multiple gray frames displayed in sequence. The details of the projector and its operation is described in Appendix (**Figure S1**). To ensure consistent viewing conditions, participants' head movements were restrained by a chin rest, and the viewing distance was fixed at 1.5 meters. Participants were asked to maintain fixation within a  $2^\circ$  fixation window located at the center of the fixation point, which was monitored by an infrared eye tracker (Eyelink 1000 Plus). Trials in which participants' gaze moved outside the fixation window were aborted and repeated at the end of the block.

### 2.2.3. Stimuli

A fixation dot with a diameter of  $0.15^\circ$  and a rectangular target stimulus ( $4^\circ \times 4^\circ$ ) was presented on a uniform gray background ( $11.84 \text{ cd/m}^2$ ). There were three types of target stimuli: a uniform target stimulus composed of a black ( $0.16 \text{ cd/m}^2$ ) and white ( $195.37 \text{ cd/m}^2$ ) patch with the maximum contrast (1 Michelson contrast), and vertical and horizontal edge stimuli consisting of two abutted black and white patches ( $2^\circ \times 4^\circ$  each and  $4^\circ \times 2^\circ$ , respectively) with the maximum contrast. In the absence of target stimuli, a steady gray patch ( $97.59 \text{ cd/m}^2$ ) with the same luminance as the mean luminance of the black and white patches was displayed. The refresh rate of the two intervals was randomly chosen from 48, 60, 96, 120, 144, 180, 240, 360, 480, 720, and 1440 Hz.

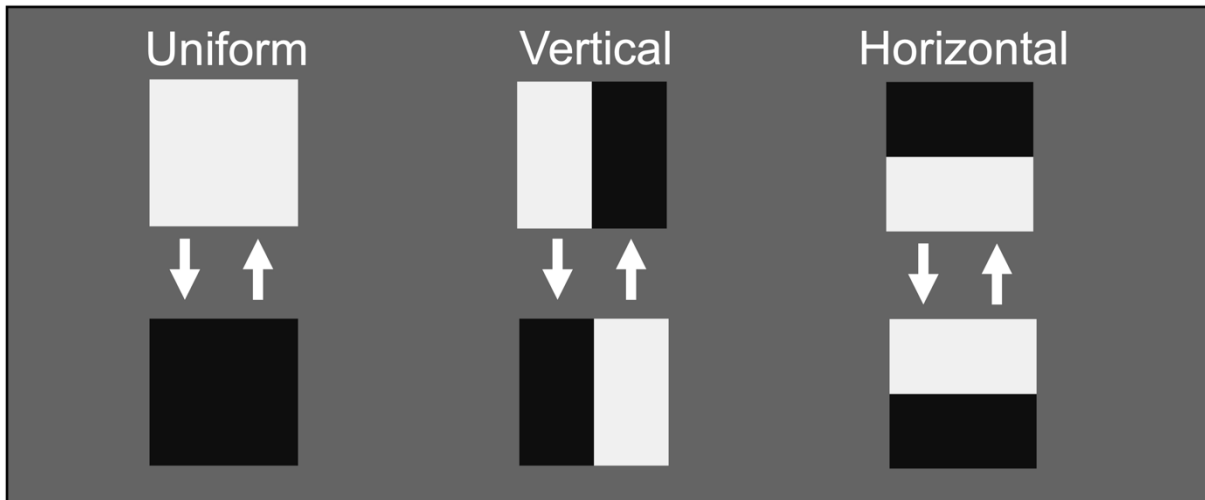


**Figure 1. The three stimuli used in Experiment 1.** The uniform (left), vertical FCE (middle), and horizontal FCE (right) stimuli. The uniform stimuli alternate between spatially uniform white and black square patches ( $4^\circ \times 4^\circ$ ). The vertical and horizontal FCE stimuli consist of the abutted white and black rectangular patches ( $2^\circ \times 4^\circ$  each and  $4^\circ \times 2^\circ$ , respectively). Given the refresh rate, a pair of stimuli was alternatively presented to participants.

#### 2.2.4. Procedure

Throughout the experiment, participants were asked to maintain fixation on the center of the screen. Each trial commenced with a 1-second presentation of a fixation dot at the center, followed by a 1-second blank screen. Two temporal intervals were then sequentially presented, with a 1-second interval featuring central fixation between them. The target stimulus was randomly presented at the center of either the first or second interval. Participants were required to indicate which interval contained the flickering stimulus by pressing the left arrow key for the first interval and the right arrow key for the second interval. Auditory feedback was provided to indicate the correctness of the participants' responses. After a 1-second blank screen, the next trial commenced. To test the three types of target stimuli (uniform, vertical edge, and horizontal edge), we employed a Latin-square design to assign the sequence of experimental conditions. We utilized the method of constant stimuli, which has been demonstrated to provide more reliable measurements of critical flicker fusion thresholds (Eisen-Enosh et al., 2017). Each experimental condition consisted of four consecutive blocks, with each block comprising 60 trials (~5 minutes) conducted on the same day. Additionally, each refresh rate was tested 20 times. Monocular eye movements of the participants were recorded throughout the 2IFC task. If their gaze deviated beyond the fixational window (radius:  $1^\circ$ ), the respective trial was excluded, and an additional trial was repeated at the end of the session.

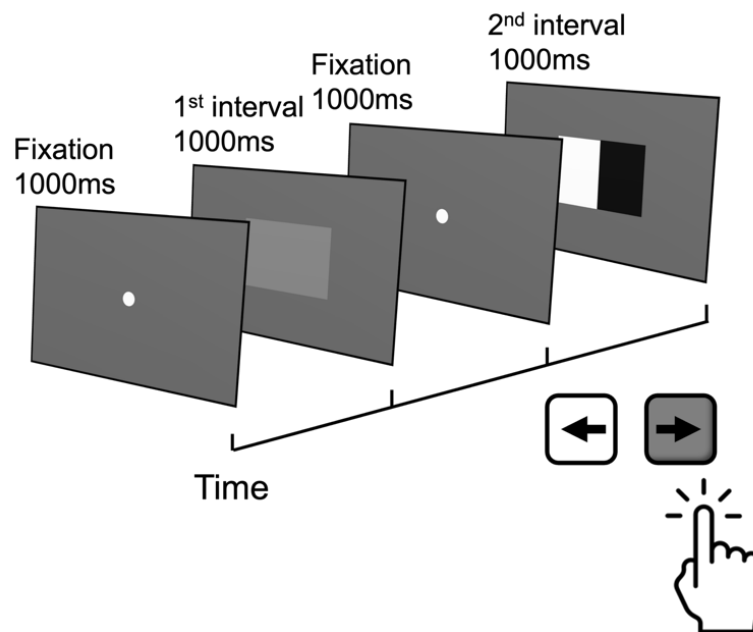


**Figure 2. A schematic illustration of the 2IFC task.** The target stimulus was randomly presented in the first or the second interval. After two stimulus intervals were presented, participants were asked to report the target interval. If the first interval included the target, they pressed the left arrow key and vice versa. The auditory feedback was given after the response.

### 2.2.5. Data Analysis

We analyzed the data by fitting a cumulative normal function to participants' 2IFC responses and identifying the refresh rate at which participants achieved a 75% correct answer rate as their CFFs (**Figure 3**). One participant's data was excluded because his or her estimated CFFs were 2.5 standard deviations away from the group mean. We used MATLAB (MathWorks, Inc.) to estimate the parameters that maximized the likelihood of models over psychophysically measured responses. We hierarchically fitted the cumulative normal function for each stimulus condition across participants to estimate reliable parameters, mean and standard deviation, at the group level. We then submitted the estimated thresholds obtained from each participant to ANOVA, with the type of stimulus as a fixed factor and participants as a random factor. Post-hoc analysis was conducted if statistical significance was observed. Significance tests were performed using RStudio (Version 1.1).

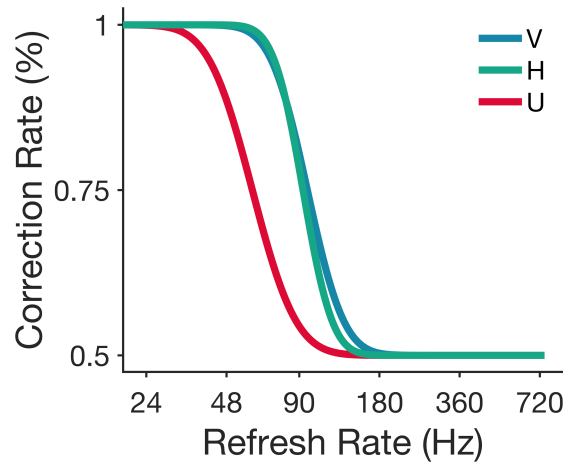


**Figure 3. Estimation of the critical fusion frequency in different stimulus conditions.** The x-axis represents the refresh rate, while the y-axis represents the proportion of correct responses. As the refresh rate increases, it becomes more challenging to differentiate between a flickering stimulus and a uniform gray stimulus, resulting in a decrease in the proportion of correct responses. Consistent patterns were observed across all three types of stimuli. The plotted results represent data collected from a single participant.

### 2.2.6. The spatial edge increases CFFs regardless of the edge orientation.

Figure 3 shows the mean of estimated CFFs of the three stimuli across all participants. The red, blue, and green bars represent the uniform, vertical FCE, and horizontal FCE stimuli, respectively. The results of the analysis of variance (ANOVA) indicated a significant effect of stimulus type ( $F_{2,34} = 23.93, p = 3.26e^{-7}, \eta_p^2 = .585$ ). Specifically, the CFFs for stimuli with spatial edges (vertical FCE:

93Hz; horizontal FCE: 95 Hz) were significantly higher than those for uniform stimuli (58 Hz, vs Vertical FCE:  $p = 4.27e^{-7}$ ; vs Horizontal FCE:  $p = 1.65e^{-6}$ ), consistent with the previous observation. Importantly, there was no significant difference between the CFFs for the vertical and horizontal FCE stimuli ( $p = 0.945$ ), suggesting that increased sensitivity to FCE stimuli was not due to hemispheric asymmetry in visual information processing (Sperry, 1968; Hellige, 1996; Mutha et al., 2011; Peterzell et al., 1989).

Although we replicated the key observation that the presence of the spatial edge significantly increased CFFs, it must be noted that the observed CFFs for FCE stimuli were remarkably lower than those reported in Davis et al.'s study (93 Hz vs. 500 Hz). Our conjecture is that the difference between CFFs arose due to the control over participants' eye movements. Davis et al.'s study did not control participants' eye movements and the stimulus duration until participants responded, leaving much room for eye movements to increase CFFs of FCE stimuli. In contrast, we excluded the trials in which participants' eye deviated out from the fixation window.

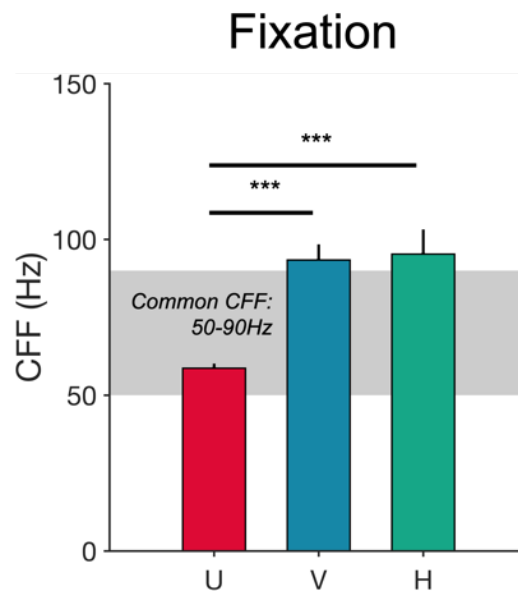


**Figure 4. Mean estimated CFF for the three types of stimuli (N = 18).** CFFs for the three stimuli were estimated while participants fixated their eyes at the center of the stimuli. In all figures, error bars represent the mean value of measurements with their standard error of the means. The gray shaded area indicates the commonly reported range of CFFs. Red, blue, and yellow indicate the uniform, vertical FCE, and horizontal FCE stimuli. The uniform stimuli produced significantly smaller CFF compared to the vertical and horizontal FCE stimuli. An asterisk indicates the statistical significance (\*:  $p < .05$ ; \*\*\*:  $p < 0.001$ ).

## 2.3. Experiment 2: Effects of spatial edges and its orientation on CFFs during saccade

To investigate the impact of participants' eye movements on the elevated CFFs observed for FCE stimuli in Davis et al.'s study, we conducted a new experiment where participants move their eyes. In this experiment, we ensured that the fixation point remained visible during the presentation of the stimulus, and we presented it alternately on either the left or right side of the stimulus.

### 2.3.1. Participants, Apparatus, and Stimuli

Participants, apparatus, and stimuli were identical to those of Experiment 1.

### 2.3.2. Procedure

To test the effect of eye movement, we manipulated the presentation of the fixation point. The fixation appeared on the left side of the center of the screen ( $6^\circ$ ) and shifted horizontally from left to right ( $6^\circ$ ) and then right to left every 0.5 seconds during the stimulus presentation (1.5 second). Participants were asked to follow the fixation point with their eyes and conduct a 2IFC task.

### 2.3.3. Data Analysis

The analyses and criteria for data exclusion were the same as those in Experiment 1. We aggregated the results of Experiment 1 and 2 to compare the effect of eye movements on CFFs. We conducted a paired t-test to compare the CFFs measured with and without eye movements for each type of stimuli. We also conducted an ANOVA, considering the type of stimuli and presence or absence of eye movements as fixed factors and participants as a random factor.

### 2.3.4. Saccadic eye movements selectively increased CFFs for FCE stimuli.

Participants were asked to move their eyes following the jumping fixation point while conducting 2IFC task. We measured CFFs for the three types of stimuli: uniform, vertical FCE, and horizontal FCE stimuli. The results of this eye movement condition are presented in **Figure 5**. A two-way ANOVA was conducted to examine the effect of stimulus type on CFFs. The analysis revealed a significant main effect of the stimuli type ( $F_{2,17} = 87.12$ ,  $p = 4.16e^{-14}$ ,  $\eta_p^2 = .860$ ). Post-hoc test showed a significant difference between the uniform and the vertical FCE stimuli (61 Hz vs 351 Hz,  $p \ll .001$ ) and the vertical FCE and horizontal FCE stimuli (351 Hz vs 112 Hz,  $p \ll .001$ ) while there was no significant difference in CFFs between the uniform stimuli and horizontal FCE stimuli (61 Hz vs 112 Hz,  $p = 0.096$ ).



In the right panel of **Figure 5**, we combined the data collected when participants fixated their eyes (fixation condition) and moved their eyes horizontally (saccade condition) during the stimulus presentation. Compared to CFFs measured with the stationary eye, only the vertical FCE stimuli showed significantly increased CFFs when participants made eye movements (93 Hz vs 351 Hz,  $t_{17} = 9.2871, p = 4.526e^{-8}$ ) while the uniform and horizontal FCE stimuli did not (uniform: 58 Hz vs 61 Hz,  $t_{17} = 2.0899, p = .05197$ ; horizontal FCE: 95 Hz vs 112 Hz,  $t_{17} = 1.6637, p = .1145$ ). Notably, some participants showed that their CFFs for the vertical FCE stimuli were even higher than 500 Hz. A repeated measures ANOVA shows that there was a significant main effect of the stimuli type ( $F_{2,34} = 89.55, p = 2.81e^{-14}, \eta_p^2 = .840$ ) and the eye movements condition ( $F_{1,34} = 77.75, p = 9.47e^{-08}, \eta_p^2 = .736$ ). There was a significant interaction effect between the type of the stimuli and the presence of eye movements ( $F_{2,34} = 76, p = 2.84e^{-13}, \eta_p^2 = .817$ ), implying that the effect of eye movements differed depending on the type of the stimuli. The association between the direction of the eye movements and the orientation of FCE stimuli suggests that the spatiotemporal integration processing of the visual stimulation plays a key role in modulating the observed effects, which will be discussed in later sections.

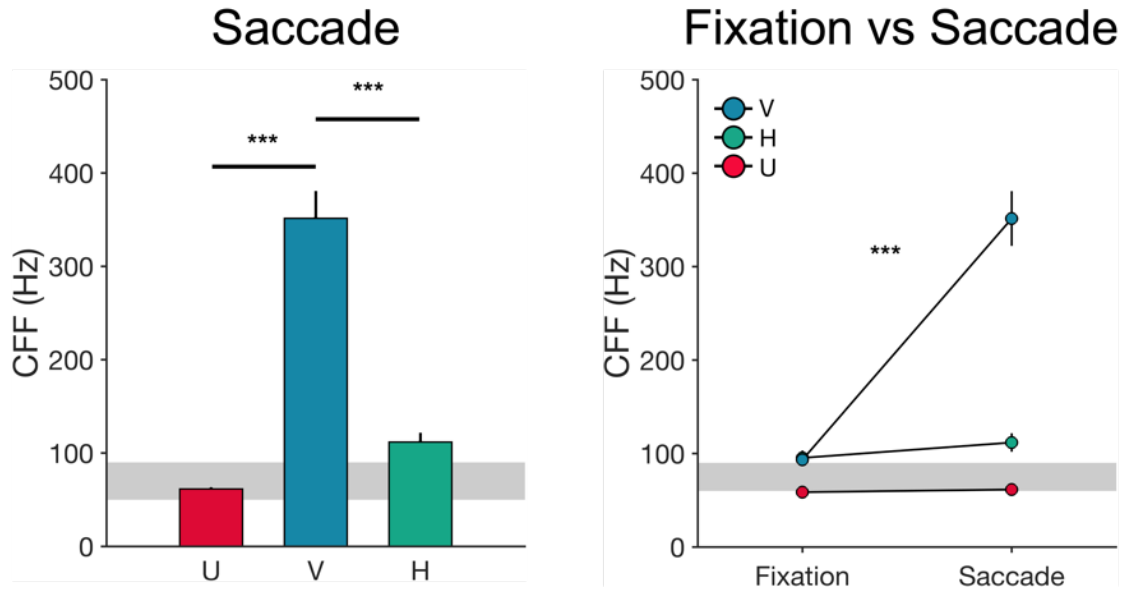


**Figure 5. The effect of saccadic eye movements on CFFs for three types of stimuli: uniform, vertical FCE, and horizontal FCE stimuli.** (Left) The mean CFFs of three stimuli when participants performed saccadic eye movements. Note that the scale of the y-axis is different from the previous figure. (Right) Aggregated CFFs in the fixation condition (Experiment 1) and in the saccadic eye movements condition (Experiment 2).

## 2.4. Experiment 3: Effects of the stimulus duration on CFFs for uniform and FCE stimuli

If inducing eye movements increases the CFF for FCE stimuli, it is reasonable to expect that suppressing eye movements would have the opposite effect, leading to a decrease in CFF thresholds. One effective method for reducing the impact of eye movements on perception is to shorten the stimulus duration (Mayfrank et al., 1987; Hoffman & Subramaniam, 1995; Deubel & Schneider, 1996). Based on this understanding, we hypothesized that as the stimulus duration decreases, the CFF thresholds for FCE stimuli would also decrease.

### 2.4.1. Participants, Apparatus, and Stimuli

Participants, apparatus, and stimuli of Experiment 3 were identical to those of Experiment 1 except that we presented only two types of the stimuli, the uniform stimuli and the vertical FCE stimuli.

### 2.4.2. Procedure

We adjusted the stimulus duration from 100, 316, 600, and 1000 ms and conducted the identical 2IFC task in Experiment 1. Participants were asked to fixate their eyes at the center of the stimuli during the stimulus duration. If their eyes moved out the fixation window (radius: 1 °), we excluded such trials and repeated those trials at the end of the session.

### 2.4.3. Data Analysis

The analyses and the criteria for data exclusion were the same as those in Experiment 1. We conducted a repeated measures ANOVA to test the effect of the stimulus type and the stimulus duration.

### 2.4.4. The longer stimulus duration increases CFFs for FCE stimuli while CFFs for uniform stimuli remain same.

We presented the uniform and vertical FCE stimuli in fovea for varied durations while participants fixated their eyes at the center of the stimuli. We measured CFFs for the uniform and vertical FCE stimuli in each stimulus duration (**Figure 6**). ANOVA shows significant effects of the stimulus type ( $F_{1,10} = 11.22, p = 7.38e^{-03}, \eta_p^2 = .529$ ) and stimulus duration ( $F_{3,30} = 7.59, p = 6.40e^{-04}, \eta_p^2 = .432$ ). There is also a significant interaction effect between the stimulus type and stimulus duration ( $F_{3,30} = 6.00, p = 0.0025, \eta_p^2 = .375$ ). The effect of the stimulus duration was marginally significant in that CFFs for the vertical edge stimuli significantly increased as the stimulus duration increased ( $p = 0.003$ ) while CFFs for the uniform stimuli remained same ( $p = 0.148$ ). CFFs

for vertical FCE stimuli gradually decrease as the stimulus duration decrease. Intriguingly, when the stimulus duration is 100 ms, CFFs for the FCE stimuli did not show a significant difference compared to those for uniform stimuli ( $p = 0.580$ ) otherwise the two stimuli show significant differences in their estimated CFFs. A short stimulus duration can effectively restrict the effect of eye movements and selectively decreased CFFs of vertical FCE stimuli.

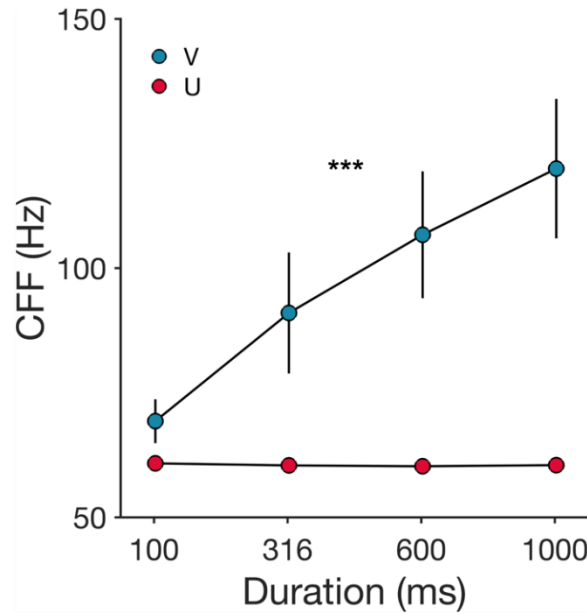


**Figure 6. The effect of the stimulus duration on CFFs for the uniform (red) and FCE stimuli (blue).** The x-axis and y-axis indicate the stimulus duration and estimated CFFs for the two stimuli. CFFs for the FCE stimuli significantly increased as the stimulus duration increased while CFFs for the uniform stimuli remained constant across the stimulus duration.

## **2.5.Experiment 4: The relationship between the extent of fixational eye movements and the CFF elevation.**

The results of this study consistently demonstrate that the presence of eye movements significantly influenced the elevated CFFs for FCE stimuli, while it did not have a significant effect on the CFFs for uniform stimuli. However, a question may arise regarding why the CFFs for FCE stimuli still increased in Experiment 1, even when participants were asked to maintain fixation at the center of the stimuli. One possible explanation is the presence of fixational eye movements, which are continuous and involuntary eye movements that occur even when individuals attempt to fixate their gaze on a specific point. It is known that fixational eye movements, such as microsaccades and drifts, can affect visual perception (Clark et al., 2022; Intoy & Rucci, 2020). Therefore, based on this hypothesis, we aimed to investigate whether there is a systematic relationship between the extent of fixational eye movements and the CFFs of FCE stimuli.

To explore this relationship, we conducted a follow-up experiment using the same procedure as in Experiment 1, but with an additional focus on recording participants' eye movements. By collecting a large number of trials and analyzing the data on fixational eye movements, we examined whether there is a consistent pattern between the extent of these eye movements and the observed CFFs for both uniform and FCE stimuli.

### **2.5.1. Participants**

Four individuals without any history of eye-related diseases within the past six months were recruited to participate in this study ( $27.25 \pm 1.71$  years; 3 men; 1 woman).

### **2.5.2. Apparatus and Stimuli**

Experimental apparatus and stimuli of Experiment 4 were identical to those of Experiment 1 except that we presented only two types of the stimuli, the uniform stimuli and the vertical FCE stimuli. We recorded participants' eye movements while they were conducting the 2IFC task.

### **2.5.3. Procedure**

Participants completed the identical 2IFC task as in Experiment 1. Each block consisted of 110 trials (~8 min). On a single day, participants completed 5 blocks with an interim break (at least ~2 min). The FCE stimulus condition and uniform stimulus condition took 9 days and 2 days to finish 4950 trials and 990 trials, respectively.

#### 2.5.4. Data Analysis

The analyses and the criteria for data exclusion were the same as those in Experiment 1. We recorded and used participants' eye movements to quantify the extent of fixational eye movements executed during the stimulus presentation. We employed specific criteria to identify and analyze fixational eye movements, particularly microsaccades and drifts, during the presentation of stimuli. For microsaccades, we defined them as fast eye movements with a velocity exceeding 10 degrees per second, a variance of velocity greater than 5 °/s, and a minimum duration of 6 milliseconds. We then calculated several measures related to microsaccades, including the number of occurrences, peak velocity, amplitude, and duration observed during the stimulus presentation. In addition to microsaccades, we also computed measures related to drift, which is a slow and continuous eye movement. For drift, we calculated peak velocity, amplitude, and duration. These measures provide insights into the characteristics of drift eye movements during the stimulus presentation. Furthermore, we quantified the overall extent of eye movements by computing the total traveled distance of the eyes. This measure captures the cumulative distance covered by the eyes throughout the stimulus presentation and provides an indication of the overall eye movement activity. To assess the dispersion and stability of gaze, we employed the Bivariate Contour Ellipse Area (BCEA) metric. BCEA calculates a confidence ellipse that encompasses the distribution of recorded eye positions in two-dimensional space. A larger BCEA indicates a more dispersed gaze pattern, while a smaller BCEA suggests a more stable gaze. By employing these measures, we aimed to quantitatively estimate the extent and characteristics of fixational eye movements during the stimulus presentation.

#### 2.5.5. CFFs for FCE stimuli increase as the extents of fixational eye movements increase.

Using the recorded eye movements, we quantified the extent of eye movements during the stimulus duration such as the mean velocity of eye movements, dispersion of eye movements, the number of microsaccade, and so on (see Methods). As eye movement features are highly correlated, we only considered the number of microsaccades and the bivariate contour ellipse area (BCEA), which quantified the spatial dispersion of fixations. We then subdivided the trials into 4 groups depending on the extent of each measurement and estimated CFFs separately. CFFs for the two stimuli show a consistent pattern that FCE edge stimuli had significantly higher CFFs compared to uniform stimuli (  $t_3 = 4.3256, p = .0228$  ). CFFs for FCE stimuli significantly increased as the number of microsaccade (**Figure 7**, left panel) and the BCEA (**Figure 7**, right panel) increased ( $F_{3,9} = 5.62, p = 0.0189, \eta_p^2 = .652$ ;  $F_{3,9} = 4.06, p = 0.0443, \eta_p^2 = .575$ ) while CFFs for uniform stimuli did not ( $p = 0.939$ ;  $p = 0.485$ ). A systematic increment in CFFs for FCE stimuli implied that CFFs differs not only depending on the voluntary and explorative saccade but also incessant and involuntary fixational eye movements.

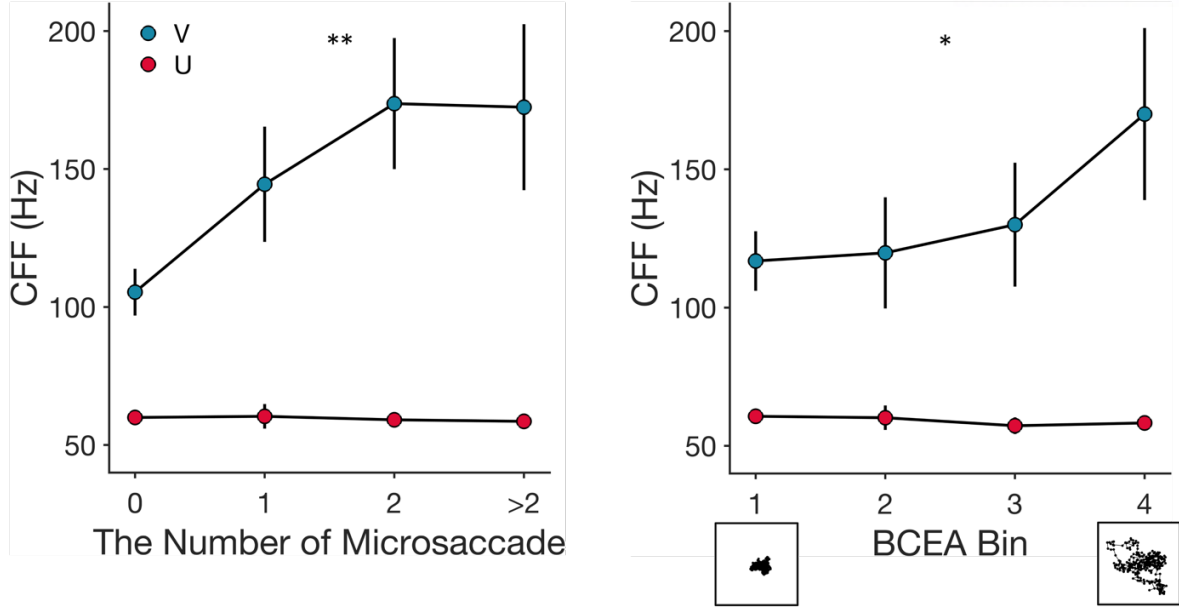


**Figure 7. The effect of the eye movements extents on CFFs for the uniform (red) and FCE stimuli (blue).** The x-axis represents the extent of fixational eye movements in ascending order, while the y-axis indicates CFFs. The left panel displays estimated CFFs for the uniform and FCE stimuli when we divided collected trials depending on the number of microsaccade occurring during the stimulus presentation. The right panel shows estimated CFFs for the two stimuli when we divided collected trials depending on the bivariate contour ellipse area (BCEA). The small boxes below the x-axis represent the x-y coordinates of fixation points during the stimulus presentation. The smaller bin represents stable fixation, while the larger bin represents dispersed fixation, respectively.

## 2.6.A spatiotemporal integration model of retinal receptive fields

To encompass the observations, we established the filtering model which integrates dynamic visual stimulations using the spatiotemporal response profile, followed by a nonlinear process and decision stage. The temporal response profile is the difference of two gamma functions, whose peaks correspond to the peak and undershoot, and thus biphasic (**Figure 8**, left).

$$Profile_{time} = \alpha \cdot \exp^{-\alpha t} \cdot \frac{(\alpha t)^5/5!}{(\alpha t)^7/7!}$$

The parameter  $\alpha$  determines the latency width of temporal response profile. The spatial response profile is the difference of two gaussian function, whose Mexican hat structure indicates the center-surround antagonism of retinal receptive fields.

$$Profile_{space} = \frac{1}{2\pi\sigma_{center}^2} e^{\frac{-x^2}{2\sigma_{center}^2}} - \frac{1}{2\pi\sigma_{surround}^2} e^{\frac{-x^2}{2\sigma_{surround}^2}}$$

Two gaussian distributions have the zero mean, and  $\sigma_{center}$  and  $\sigma_{surround}$  correspond to the standard deviation of each gaussian distribution (**Figure 8**, middle). Note that  $\sigma_{surround}$  was always larger than  $\sigma_{center}$  to mimic the center-surround antagonism. We assumed time-space separability such that spatiotemporal filter is represented by the product of linear spatial and temporal response functions (**Figure 8**, right). We set this assumption to estimate parameters for individuals' spatial and temporal filters but see Wandell's study for the time-space inseparability (Wandell, 1995).

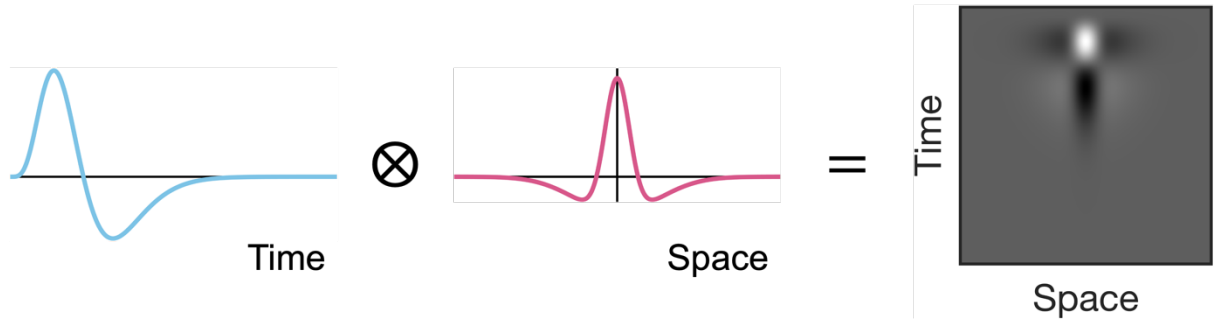


**Figure 8. The spatiotemporal integration profile used in our model.** The spatiotemporal integration filter is constructed by multiplying a bi-phasic temporal filter (left, cyan) and a Mexican hat spatial filter (middle, magenta) based on the time-space separability assumption.

In order to predict the perception of FCE stimuli in the presence of eye movements, we utilized a spatiotemporal integration model to simulate the retinal responses. This involved simulating the images of the FCE stimuli as they would be projected onto the retina. For simplicity, we focused on FCE stimuli with a vertically oriented edge and a horizontal shift in the edge's position. **Figure 9** illustrates the retinal image of the FCE stimuli, with the x-axis representing spatial positions and the y-axis representing time. The polarity of the visual inputs is indicated by white and black regions. The spatial distinction along the x-axis represents the edge position, while the swapping of polarity along the y-axis reflects the alternating nature of the FCE stimuli with the given refresh rate. In this case, Figure 9 is generated for FCE stimuli with a refresh rate of 120 Hz, meaning that the polarity of the left and right sides alternates approximately every 8.33 ms. To account for eye movements and their influences on retinal images, we incorporated recorded eye movement data to shift the spatial location of the high frequency edge accordingly. If the eye moved from left to right, the spatial location of the FCE stimuli was shifted from left to right to align with the eye movement. The upper row of **Figure 9** represents the retinal responses of the FCE stimuli with saccadic eye movements, while the bottom row represents the responses with fixational eye movements.

To estimate the retinal responses to the visual inputs at specific locations and times, we convolved the 2-dimensional retinal image with a spatiotemporal response profile. This process mimics the integration of spatial and temporal information in retinal processing. The resulting retinal responses were then logarithmically transformed to enhance sensitivity to low-intensity stimuli and introduce saturation at high-intensity stimuli. Furthermore, rectification was applied to convert negative values in the retinal responses to positive values. Additionally, responses above a certain threshold were retained, while those below the threshold were set to zero. By eliminating negative responses and rectifying them, the model emphasized information related to increments in stimulus intensity and enhanced the efficiency of encoding visual information. By implementing these steps, we aimed to simulate the retinal responses to FCE stimuli, accounting for the effects of eye movements and the subsequent changes in retinal images.

$$l(x, t) = \sum_{space} \left( \sum_{time} s(x, t) \cdot Profile_{time}(t - \tau) \right) \cdot Profile_{space}(x - \xi)$$

$$r(x, t) = \log(m * |l(x, t)|)$$

$$r'(x, t) = \begin{cases} r(x, t), & \text{if } r(x, t) \geq threshold \\ threshold, & \text{if } r(x, t) < threshold \end{cases}$$

We used simulated responses to the retinal images of the FCE stimuli and uniform stimuli to predict participants' detectability of the target interval. We assumed that the target interval which included the flickering stimuli have the maximum response across space and time,

$$R = \max(r'(x, t))$$

whereas the reference interval which included the gray patch without luminance change have no response. We additionally assumed retinal responses are noise-contaminated such that  $R_{target} = R + \mathcal{N}(0, \sigma^2)$  and  $R_{reference} = \mathcal{N}(0, \sigma^2)$ , and the noise for the two intervals had the identical variance,  $\sigma_r$ . If the difference between two retinal responses were larger than 0, the model predicts that participants correctly reported the target interval. As the standard deviation of the difference between the two retinal responses is  $\sqrt{2}\sigma$ , the likelihood can be calculated using percent correct value assuming the Gaussian distribution whose mean and standard deviation is 0 and  $\sqrt{2}\sigma$ , respectively. Percent correct values can be calculated according to the maximum values of retinal responses of  $i$ th trial.

$$p(R_i, \sqrt{2}\sigma) = \frac{1}{2\sigma\sqrt{\pi}} \int_{-\infty}^{R_i} \exp\left(-\frac{r^2}{4\sigma^2}\right) dr$$

$p$  is the probability of a correct response, which is an integration of normal distribution across response domain.  $R_i$  indicates the maximum response of  $i$ th trial. Then the likelihood function over  $N$  trials is proportional to



$$likelihood = \prod_{i=1}^N [p(R_i, \sqrt{2}\sigma)]^{r_i} * [1 - p(R_i, \sqrt{2}\sigma)]^{1-r_i}$$

where  $r_i=1$  when model predicts that a participant makes a correct response in  $i$ th trial, and  $r_i = 0$  when model predicts that the participant makes an incorrect response. We then took the logarithm of the equation above and compute the log likelihood.

$$\log likelihood = \sum_{i=1}^N r_i * \log (p(R_i, \sqrt{2}\sigma)) + (1 - r_i) * \log (1 - p(R_i, \sqrt{2}\sigma))$$

The simulation results depicted in the rightmost column of **Figure 9** indicate that eye movements had an influence on the perception of FCE stimuli, resulting in increased retinal responses in the vicinity of the FCE. The extent of this increment depended on the properties of the eye movements. The model's behavior exhibited locally enhanced retinal responses, particularly when the participants' eyes moved rapidly over a large amplitude. It is worth noting that the modulation of retinal responses varied depending on the spatial characteristics of the visual stimuli. For FCE stimuli, the receptors experienced changes in their input signals due to the spatial variations, whereas for uniform stimuli that did not vary in space, the receptors experienced no such changes.

According to the model's predictions, if participants observed FCE stimuli while making saccadic eye movements, they would perceive a set of blurred and wider edges around the center of the stimuli, rather than perceiving a single sharp edge in the middle. The width and number of concurrently perceived FCE varied based on the refresh rates and velocity of eye movements (as shown in **Figure S2 and Figure S3**). Consistent with the model's prediction, participants reported perceiving several lines resembling Gabor blobs, although the study did not include experimental measurements of their subjective percepts.

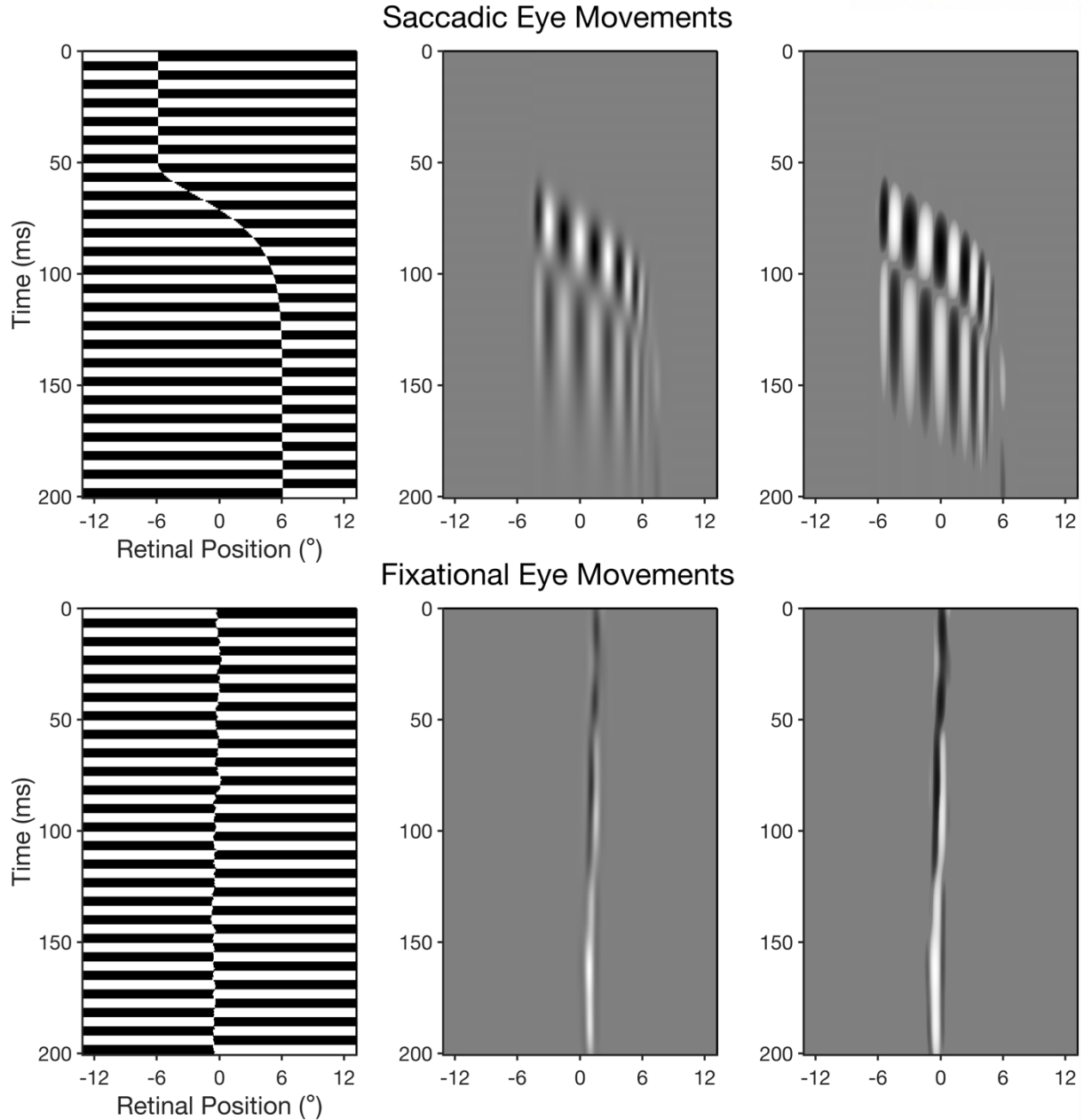


**Figure 9. Model prediction of the retinal responses to FCE stimuli presented at 120 Hz.**

The x-axis represents the retinal position, while the y-axis represents time. The upper row corresponds to saccadic eye movements, while the bottom row corresponds to fixational eye movements. On the left side, retinal images of FCE stimuli are shown, indicating the refresh rates and the horizontal position of the eye. The polarity of the stimuli alternates based on the given refresh rate, and the location of the FCE shifts according to the recorded eye movements. In the middle, the retinal images of FCE stimuli are convolved with the spatiotemporal integration filter. On the right side, the retinal responses of the FCE stimuli are shown after the application of logarithmic transformation and rectification.

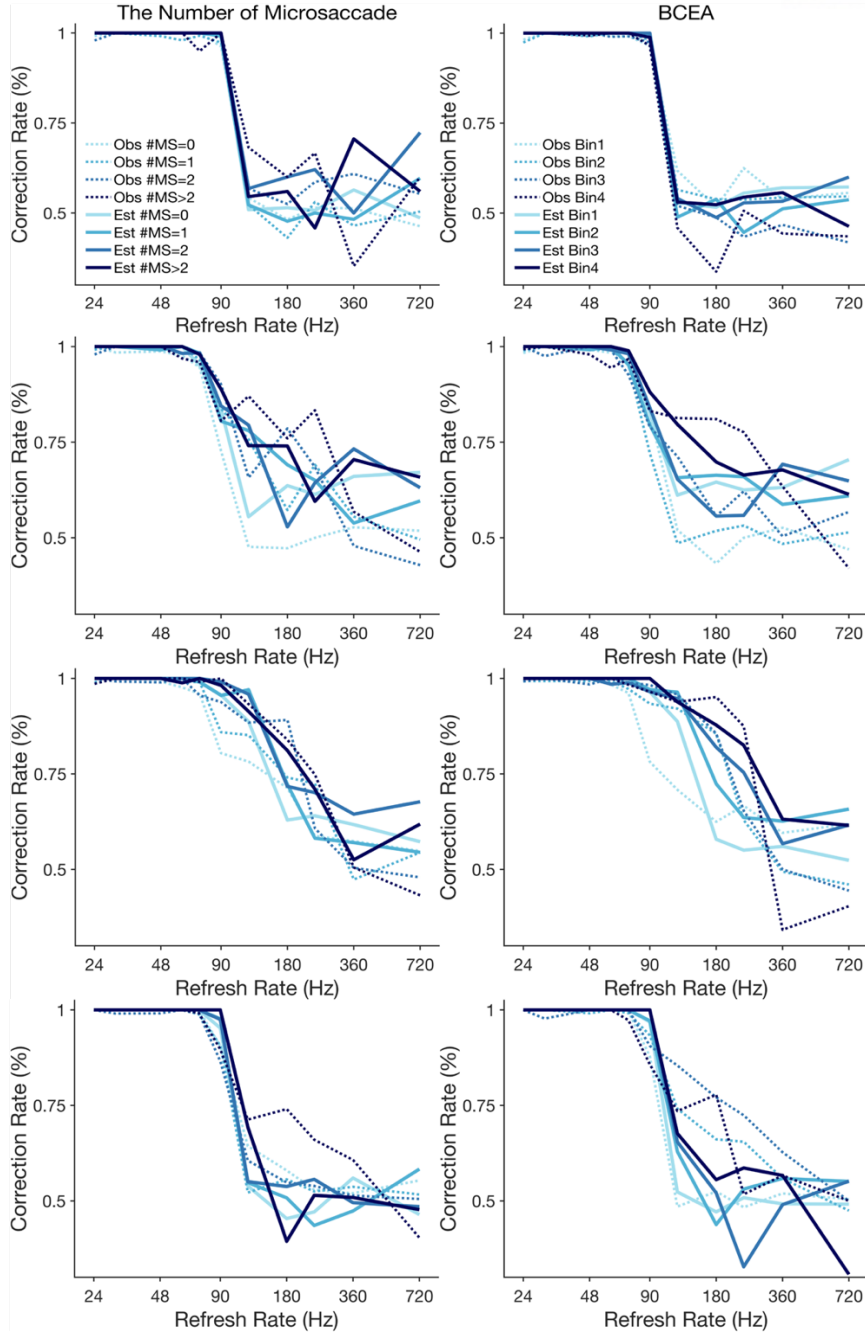


**Figure 10. Model prediction on the correction rate as a function of refresh rates.** The left column and right column represent the model predictions based on the number of microsaccades and BCEA (bivariate contour ellipse area), respectively. Each row corresponds to a different participant. The color intensity in the figure indicates the extent of fixational eye movements, where brighter colors represent smaller extents of fixational eye movements and darker colors represent larger extents. The dashed line represents the observed correction rate, while the solid line represents the model's predictions.

Since the spatiotemporal integration model enabled us to construct the retinal responses of a single trial with FCE stimuli and predict the detectability of the flickering target using the maximum retinal responses, we could compute the percentage of correct responses for the FCE condition using recorded eye movements and the given refresh rate. We used the 2IFC responses and recorded fixational eye movements in Experiment 4. The trials were divided into four groups based on the number of microsaccades and BCEA percentile.

**Figure 10** presents the correction rates for each refresh rate in the FCE condition for each participant. Each row represents the results for an individual participant. The left column displays the correction rates estimated for different trial sets divided based on the number of microsaccades, while the right column shows the correction rates for different trial sets divided based on BCEA. The dashed line represents the observed correction rate, while the solid line represents the predicted correction rate. Psychometric functions were fitted to the data to estimate CFFs.

**Figure 11** displays the estimated CFFs for FCE stimuli (shaded error bars) in relation to the extent of fixational eye movements, along with the observed CFFs (error bars). Notably, the model predicts a systematic pattern where CFFs for FCE stimuli increase proportionally with the extent of fixational eye movements. There is a significant increase in CFFs as the number of microsaccades ( $F_{3,9} = 5.15, p = 0.0241, \eta_p^2 = .632$ ) or BCEA ( $F_{3,9} = 4.50, p = 0.0344, \eta_p^2 = .600$ ) increases. These findings indicate that there is a clear relationship between the extent of fixational eye movements and the perceived CFFs for FCE stimuli. The model's predictions align well with the observed data, further supporting the influence of eye movements on the perception of FCE stimuli and their effect on temporal frequency processing.

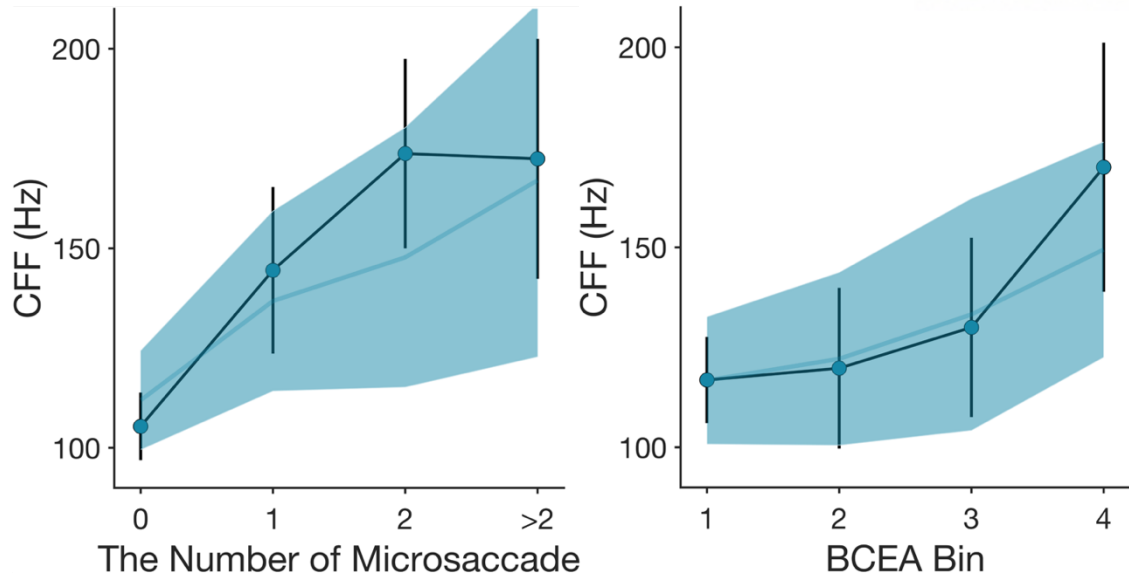


**Figure 11. CFFs for FCE stimuli predicted by the spatiotemporal integration model.** Consistent with the previous data analysis, the trials were divided into subgroups depending on the number of microsaccade (left) or BCEA (right). The error bars represent the observed CFF values, while the shaded error bars indicate the model's predictions.

## 2.7. Experiment 5: The eccentricity effect on the CFFs for uniform and FCE stimuli predicted by the spatiotemporal integration model

The spatiotemporal integration model successfully captures the behavioral pattern that CFFs for FCE stimuli systematically increases as the extent of fixational eye movements increase, suggesting that the elevated CFFs for FCE stimuli may be a byproduct of the spatiotemporal integration procedure that occurs in our early visual system. According to this model, the spatiotemporal integration profile modulates the retinal responses and detectability, which derived a novel prediction on the eccentricity effect on CFFs for uniform and FCE stimuli. The temporal and spatial characteristics of the visual system differ between the fovea and the periphery. The periphery is known to have a faster temporal filter (Carrasco et al., 2003; Hartmann et al., 1979; Tyler, 1987) and wider spatial filter (McKee & Nakayama 1984; Rentschler & Treutwein, 1985), compared to the fovea, leading to differences in CFFs between the fovea and periphery for both types of stimuli (see the Model prediction below). To further test the predictive ability of the spatiotemporal integration model on the eccentricity effect, we conducted an additional experiment where participants observed the flickering stimulus in their periphery while conducting the 2IFC task and compared the CFFs for the two stimuli.

### 2.7.1. Methods and Procedure

Participants, apparatus, and stimuli used in Experiment 5 were identical to those used in Experiment 4. We measured CFFs for uniform and FCE stimuli using 2IFC task. Compared to the experimental procedure of Experiment 1, the only thing manipulated is the location of the fixation (Figure 12). We placed the fixation to the right ( $12^\circ$ ) of the target stimulus and measured the critical flicker fusion threshold using a 2IFC task.

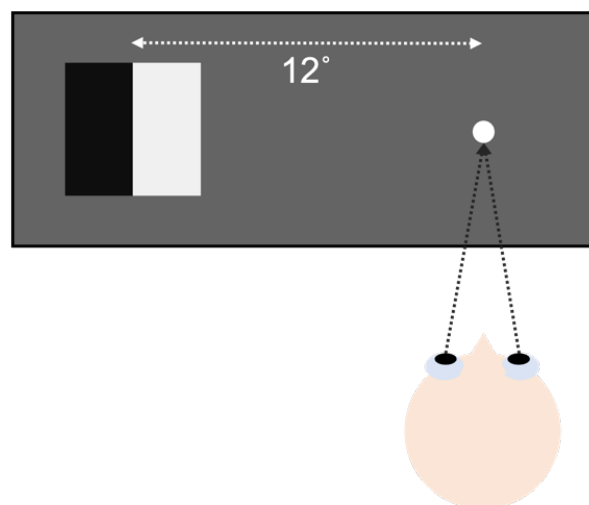


**Figure 12. A schematic illustration of the experimental set-up.** Participants were asked to fixate their gaze at the fixation point, which is located  $12^\circ$  away from the center of the target.

### 2.7.2. Data Analysis

The analyses and the criteria for data exclusion were the same as those in Experiment 1. To test the effect of the eccentricity, we used paired t-test. We aggregated the results of Experiment 1 and Experiment 5 and submitted them to ANOVA, considering the type of stimuli and eccentricity as fixed and participants as a random factor.

### 2.7.3. Model prediction

In the model simulation for Experiment 5, the retinal responses and predicted correctness in response to the given stimulus conditions (stimulus type, eccentricity, refresh rate, and eye movements) were generated. The left panels of **Figure 13** depict the temporal and spatial filters used in the simulation. The upper panel represents the temporal filter, while the bottom panel represents the spatial filter. The filters are differentiated for the fovea (yellow) and periphery (purple). For the fovea condition, the recorded fixation eye movements and their estimated spatiotemporal integration filters from Experiment 4 were employed. For the periphery condition, the same fixational eye movements were used, but with different spatiotemporal integration filters. The filters for the periphery have a relatively faster temporal response and a wider spatial response compared to those of the fovea. These parameters were set based on the findings of the previous study (Bonin et al., 2005) about the spatial filters in the LGN (lateral geniculate nucleus) at the periphery.

According to this model, the spatiotemporal integration profile modulates the increment of retinal responses. The narrower and faster filter results in a more accentuated response, whereas the wider and slower filter results in a less accentuated response. The spatial filter has a more dominant influence on the retinal responses compared to the temporal filter. It is because the high spatial frequency edge plays a critical role in accentuating the local retinal responses. For uniform stimuli, the retinal responses are not influenced by the shape of the spatial filter since there are no spatial features in these stimuli. Therefore, only the faster temporal filter in the periphery condition will enhance the response and increase the CFFs for uniform stimuli. However, for FCE stimuli, the wider spatial filter becomes more influential and cancels out the effect of the faster temporal filter. As a result, the CFFs for FCE stimuli decrease due to the wider spatial filter's dampening effect on the response.

### 2.7.4. Increasing eccentricity increases CFFs for uniform stimuli but decreases CFFs for FCE stimuli despite the enhanced temporal sensitivity.

Our model predicted that in the periphery, where the temporal filter is accelerated and the spatial filter is flattened, CFFs for uniform and FCE stimuli would change differently. The accelerated temporal filter will increase the responses and CFFs for uniform stimuli, which are not affected by eye

movements and, consequently, the shape of the spatial filter. However, for FCE stimuli, the flattened spatial filter will decrease the increment in retinal responses (Baylor et al., 1971b; Enroth-Cugell et al., 1983; Mastronarde, 1987b; Ruksenas et al., 2000), canceling out the effect of the accelerated temporal filter, resulting in a decrease in CFFs.

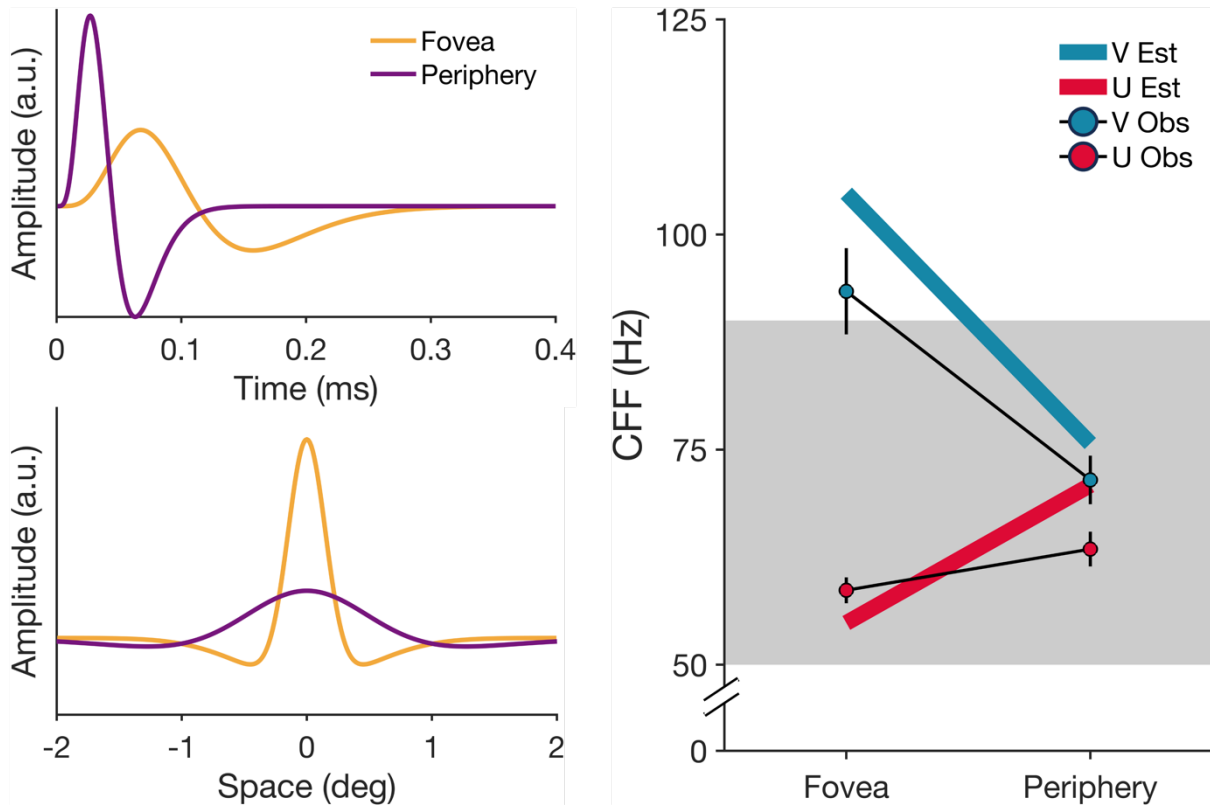


**Figure 13. The effect of eccentricity on the estimated CFF for the uniform (red) and FCE stimuli (blue).** The upper left and bottom panels depict the temporal and spatial filters used in the model simulation. The yellow and purple colors represent the fovea and periphery conditions, respectively. In the right panel, the solid line represents the model prediction for the two stimuli across different eccentricities (fovea and periphery). The error bar indicates the mean observed CFFs for the two stimuli with the standard error of the means. The effect of eccentricity on the CFFs was found to be significant for both stimuli, which is consistent with the model prediction. As eccentricity increases, the uniform stimuli exhibit increasing CFFs, while the vertical edge stimuli show decreasing CFFs. An asterisk denotes statistical significance ( $p < .05$ ).



In Experiment 5, where participants fixated their eyes at a point 12 degrees away from the center of the flickering stimuli, the CFFs for both uniform and FCE stimuli were measured and analyzed. The aggregated data from Experiment 1 and 5 were used for analysis. **Figure 13** depicts CFFs for both uniform and FCE stimuli. We aggregated and analyzed the CFF data of Experiment 1 and Experiment 5 together. CFFs for FCE stimuli were significantly higher than CFFs for uniform stimuli at fovea (58 Hz vs 93 Hz,  $t_{17} = 6.3428, p = 5.6284e^{-04}$ ) and periphery (64 Hz vs 71 Hz,  $t_{17} = 2.4862, p = .02361$ ). Importantly, the observed eccentricity effect on CFFs aligns with the model's predictions. There was a significant interaction between stimulus type and eccentricity ( $F_{1,17} = 17.89, \eta_p^2 = .513, p = .000565$ ), indicating opposite patterns of CFFs for the two stimuli. Additionally, there were significant main effects of the type of stimuli ( $F_{1,17} = 80.99, p = 7.09e^{-8}, \eta_p^2 = .729$ ) and eccentricity ( $F_{1,17} = 11.24, p = .00377, \eta_p^2 = .303$ ) individually.

Specifically, the uniform stimuli showed significantly higher CFFs in the periphery than in the fovea (53 Hz vs 64 Hz,  $t_{17} = 2.4426, p = .0258$ ), while the FCE stimuli showed significantly lower CFFs in the periphery (93 Hz vs 71 Hz,  $t_{17} = 4.0599, p = .0008144$ ). The fact that the model can account for the opposite patterns of CFFs for the two stimuli provides strong evidence for the spatiotemporal integration framework proposed in the study.

## 2.8. Discussion

The aim of this study was to explore the relationship between temporal sensitivity of the human visual system and eye movements by examining critical fusion frequencies (CFF). Our finding revealed that saccadic eye movements had a significant impact on elevating CFFs for flicker containing edge (FCE) stimuli, while no such effect was observed for uniform stimuli. Moreover, the extent of eye movements positively correlated with CFFs for FCE stimuli, and CFFs decreased as the stimulus duration decreased. These observations align with the predictions of the spatiotemporal integration model, which posits that eye movements enhance CFFs by accentuating the local retinal responses of high-frequency edges during early visual processing. The contrasting effects of eccentricity on CFFs for FCE stimuli provide further support for the model's predictive capability.

An alternative account for observed elevation of CFFs for FCE stimuli involves the perception of a smeared spatial pattern, known as a phantom array, during eye movements (**Figure 14**, Hershberger & Jordan, 1996; Hershberger & Jordan, 1998). Other relevant studies also conjectured that this phenomenon enables individuals to discriminate the flickering target stimulus from a continuous gray target (Davis et al., 2015; Roberts & Wilkins, 2013; Wang et al., 2017). The appearance of the phantom array may partially account for this finding, as the spatiotemporal representations take time to build up, and the spatial distribution of visual stimuli can be altered by eye movements during this period. Experiment 2 provided support for this possibility by demonstrating that horizontal saccades selectively increased CFFs for vertical FCE stimuli. Furthermore, participants described perceiving a set of Gabor blobs instead of a single sharp spatial edge if FCE stimuli were presented. However, it is important to note that the model's success in predicting the detectability of flicker is based on the locally accentuated retinal responses resulting from transient eye movements, rather than solely relying on the appearance of the pattern.



**Figure 14. Illustration of the phantom array.** As the eyes execute a saccade from left to right, a flashing light at the center of the screen creates the perception of a horizontal array of lights in sequence. Within the sequence, each individual light appears to move to the left, known as *phi* motion. Simultaneously, the entire sequence of flashing lights appears to move to the right, in the direction of the attended saccade. This phenomenon highlights the interaction between saccadic eye movements and the perception of motion.

Our findings advanced our understanding of the role of fixational eye movements in enhancing visual sensitivity of the human visual system. We demonstrated that fixational eye movements can increase CFFs for FCE stimuli in a manner similar to saccadic eye movements (Roberts & Wilkins, 2013). Fixational eye movements occur naturally even when we have no intention to move our eyes, but rather to maintain gaze. Intuitively, one might assume that these movements would degrade the sensitivity of our visual system due to smeared percepts. However, recent studies have reported that humans tune their fixational eye movements to perceive the fine details of high-frequency stimuli. It has been shown that perfect stabilization of the image, compensating for fixational eye movements and retinal images shifts, cannot achieve normal visual acuity (Clark et al., 2022; Intoy & Rucci, 2020). Interestingly, our study also showed counterintuitive effects of fixational eye movements' instability. We found that CFFs for FCE stimuli increased significantly as fixation stability decreased or the number of microsaccades increased. This indicates that the role of fixational eye movements extends beyond simply relocating visual stimuli to fovea, where visual acuity is highest (Steinman & Levinson, 1990), highlighting their role in modulating the retinal inputs and enhancing visual sensitivity.

The current model in our study simulated retinal responses to visual stimuli based on their retinal position and applied the spatiotemporal integration process. However, to gain a better understanding of how the flickering stimuli are represented in our visual system, further exploration is needed. One important consideration is how to realign the retinal image to its physical position. This poses a challenge as it is difficult to compute how the brain encodes the perceived spatial location of visual objects during eye movements. It may not be sufficient to shift retinal images in the opposite direction of recorded eye movements with the same amplitude, known as forward remapping (Duhamel et al., 1992; Marino & Mazer, 2016). Moreover, to accurately reflect the effects of eye movements on the visual representation, we need to consider shifts of attention and other dynamic cognitive processes which may affect the encoding process, as highlighted by previous studies (Golomb, 2019; Golomb & Mazer, 2021). Nevertheless, we want to emphasize that our model successfully captures the changes in CFFs for FCE stimuli depending on the recorded eye movements. The subsequent process involving the later spatial alignment may not alter the prediction power of our model because it relies on maximum response across retinal images, which is not affected by realignment in our visual representation.

The spatiotemporal integration model employed in our study uses recorded eye movements to predict correctness of participants' responses in reporting the target interval containing the flickering stimuli, based on the maximum value of retinal responses. We used the model's predictions to calculate the percentage of correct responses and applied a psychometric function to estimate CFFs (**Figure 10**). The estimated CFFs from the model show a strong agreement with the CFFs obtained from the observed behavioral data. However, a noticeable discrepancy in the percentage of correct responses between the observed data and the model's predictions emerges for refresh rates ranging from 90 to 360 Hz. The

modulation induced by eye movements exerts the most significant influence on the detectability of flickering stimuli within this range although the CFFs did not change as they were estimated based on a 75 % correction rate. Further refinement and elaboration of our model are necessary to effectively capture the changes in retinal responses influenced by these executed eye movements.

Despite the overall agreement between the model predictions and observed CFFs, it remains unclear why there is no significant difference between CFFs for uniform and FCE stimuli with a duration of 100 ms. To address this, we conducted an additional experiment to validate our findings and confirmed that the statistically significant difference between CFFs for uniform and FCE stimuli did not occur at this particular stimulus duration (see Appendix for a detailed explanation). **Figure S4** represents the estimated CFFs for both types of stimuli obtained through maximum likelihood estimation of model parameters. While the model seems to capture the general pattern, a closer analysis of the filter parameters raises concerns. Specifically, the widths of estimated spatial filters in **Figure S4** are too wide compared to the reported size of retinal receptive fields in previous literature (Freeman & Simoncelli, 2011; Winawer & Horiguchi, 2015). This discrepancy suggests the need for further elaboration of the spatiotemporal integration model to explain the observed changes in CFFs for FCE stimuli as a function of stimulus duration. We conjecture that our visual systems may operate differently for short durations, employing a faster temporal filter and wider spatial filter that gradually stabilize into a fixed form. When the stimulus duration exceeds a critical value, post-processing mechanisms may come into play, leading to the establishment of fixed filter shapes. However, the question of how and why this transition occurs still remains open for further investigation.

Further studies can investigate the following questions to gain a deeper understanding of the spatiotemporal integration of dynamic visual signals in our visual system. Firstly, how does modulating the sharpness of the flicker containing edge affect CFFs for FCE stimuli? As the interaction between the high frequency edge and the spatial filter played a key role in elevating the retinal responses to the flickering stimulus and increased CFFs, we expect that reducing the sharpness of the edge would result in the less dramatic decreases in CFFs for FCE stimuli. Secondly, what would be the effect of spatially enveloping FCE stimuli to exclude interruptions of surrounding edges lying between the stimuli and the background? Although we assumed that the effect of these low-contrast edges was minimal, varying the spatial properties of these edges would allow us to eliminate any potential interruption and solely focus on the effect of FCE in the middle. Thirdly, how CFFs differ when we could create FCE stimuli using the equiluminant red and green patches instead of white and black abutted patches. We can entirely prevent the motion system from involving because motion system is known to be color blind. Lastly, how does presenting stabilized images help disentangle the effect of eye movements and shifts in retinal images on elevated CFFs? A recent study (Li et al., 2016) reported that motion signals preparing for saccadic eye movements directly mediated the representation of visual features. It would

be worthwhile to test whether the increase in CFFs originated from the activated motion signals that govern eye movements or changes in retinal images induced by eye movements.

## **2.9. Conclusion**

Our study reveals that eye movements play a crucial role in elevating critical fusion frequencies (CFFs) for flicker containing edge (FCE) stimuli. This finding strongly supports the spatiotemporal integration model, which elucidates how eye movements enhance local retinal responses and improve temporal sensitivity in the visual system. Additionally, we challenge the traditional view that fixational eye movements degrade visual sensitivity, as our results demonstrate that they can actually enhance CFFs for flickering stimuli. Our study highlights the importance of considering eye movements in understanding visual perception, and future research delve deeper into the relationship between eye movements and visual processing to expand our knowledge of human vision.

### **3. Chapter 2. Effects of Speedline on visual persistence and perceived quality of motion**

In the second part of this study, we aimed to investigate the influence of fast object motions, comparable to eye movements (~200 degrees per second), on the perception of moving objects. We examined two aspects of perceived motion quality through different measurements. The first measurement focused on visual persistence, which refers to the ability to detect the presence of a moving object even after its visual stimulus has disappeared. Due to the rapid motion of the objects, they transitioned to the next location before their visual representation in the previous location disappeared. The second measurement assessed the perceived sense of reality of the moving objects in the display compared to that of real physical objects in the external world.

Specifically, we focused on manipulating a spatial feature known as the Speedline, which connects two spatially separate objects. The Speedline has been extensively utilized in the video game industry and animated films (Lake et al., 2000; Lasseter, 1987; Masuch, 1999) to enhance the perceived quality of object motion in displays. While a previous psychophysical study reported that increasing the width of a moving bar reduced observers' sensitivity to discriminate stroboscopic motion from continuous motion (Mackin et al., 2017), there has been limited quantification of the tangible effects of Speedline on our perception of object motion, and the underlying mechanisms remain unclear.

#### **3.1.Introduction**

When objects are presented through a digital display, their motion is perceived as a series of spatially and temporally separated still images, resulting in stroboscopic motion. The fast-moving objects used in this experiment aimed to evoke a subjective impression of motion. Visual persistence is a prominent phenomenon observed in stroboscopic representations. Briefly presented objects can persist in visual perception, even after they have disappeared, and may overlap with the appearance of subsequent objects, leading to the perception of multiple objects instead of a single object (Burr, 1980; Coltheart, 1980; Sperling, 1976). This persistence of visual perception can have implications for motion perception, resulting in smeared and unclear motion. The duration of visual persistence is influenced by various factors, including size, luminance, and spatial frequency (Bowling et al., 1979; Di Lollo & Woods, 1981; Francis & Grossberg, 1996; Francis, 1999; Kim & Francis, 1998). Importantly, the estimated durations of visible persistence increase as the distance between successive stimuli becomes larger (Castet et al., 1993; Di Lollo & Hogben, 1985; Farrell, 1984; Ferrell et al., 1990;).

One possible explanation for this observation is that when the distance between successive stimuli is small, the visual system prioritizes temporal fidelity over stimulus sensitivity. This prioritization allows for the preservation of temporal stimulus information and helps reduce the blur that may be caused by moving objects. However, when the distance between successive stimuli is large, the visual system prioritizes stimulus sensitivity over temporal fidelity, similar to the case of briefly presented stationary objects. This allows more time for extracting the necessary spatial information for object identification (Bowling et al., 1979; Castet, 1994).

Another possible explanation is an inhibition-based account. According to this account, when two brief stimuli are successively presented in adjacent locations, the activity elicited by the second stimulus inhibits the persisting activity elicited by the first stimulus. To explain the suppression of visual persistence with adjacent stimuli, this model posits the existence of two channels: the transient channel and the sustained channel. The transient channel exhibits a short latency and brief activation, while the sustained channel has a longer latency and longer activation. The sustained channel's activation, which lasts longer, contributes to visual persistence. In the case of objects in stroboscopic motion, the transient activity induced by the adjacent trailing stimulus overlaps and inhibits the sustained activity of the leading stimulus. The extent of suppression depends on the spatiotemporal integration profile of the two channels. This is plausible because the efficiency of persistence suppression varies based on two known principles governing the strength of inhibition: the development of inhibitory interactions takes some time, and inhibitory strength increases with proximity. Building upon previous research, we hypothesized that the addition of Speedline would further suppress the perception of visual persistence in the successive presentation of moving objects.

Regarding the sense of reality for moving objects in display environments, previous research has demonstrated that the perceived quality of the display increases with higher refresh rates (Burt & Sperling, 1981; Kuroki et al., 2007; Sperling, 1976; Wilcox et al., 2015) or decreased duty frame (Denes et al., 2020; Hoffman et al., 2011; Hoffman et al., 2014), which refers to the proportion of time a stimulus is presented within a single frame. While most studies have focused on the temporal properties of the screen and their impact on the perceived quality of motion, there has been limited investigation into how the spatial features of moving objects influence the perceived quality of motion. Furthermore, many studies have relied heavily on subjective ratings, which are susceptible to biases such as experimenter expectations, contextual cues, and individual predispositions to rate certain conditions more favorably. In order to address these issues, we conducted experiments to examine the effect of Speedline on the perceived quality of moving objects, while also psychophysically estimating the objective quantity of perceived motion quality.

In our study, we designed a series of experiments to measure the visual persistence of dot stimuli that moved rapidly along a horizontal axis, both with and without Speedline. The Speedline was

created by connecting the spatial separation between two consecutive frames, resembling a comet tail. We hypothesized that the Speedline would decrease visual persistence since there is no spatial separation between the two stimuli. Our results revealed that the presence of the Speedline decreased the range of concurrently perceived persisting images. Importantly, this reduction in persistence was not attributable to the size or light intensity of the Speedline, but rather to the absence of spatial separation between the two stimuli. Control experiments further confirmed the crucial role of connectivity in maintaining persistence. Additionally, we manipulated the number of moving objects and measured their perceived length, finding that the Speedline decreased the perceived length of moving objects. Finally, through our perceptual quality assessment, we demonstrated that object motion accompanied by the Speedline evoked a stronger sense of reality compared to object motion without the Speedline, likely due to the shortened persistence of moving objects.



### 3.2. Experiment 1: Effect of Speedline on the range of persisting images

We aimed to test the effect of Speedline on the visual perception of the fast-moving stimulus which moves as fast as our eyes. We used a line stimulus created by connecting two consecutively displayed dots. Psychophysical measurements were conducted to assess and compare the range of visual persistence between a single dot and a line stimulus. These stimuli were presented at refresh rates.

#### 3.2.1. Participants

Nine individuals without any history of eye-related diseases within the past six months were recruited to participate in this study ( $26.4 \pm 2.7$  years; 7 men; 2 women). All participants reported having normal or corrected-to-normal visual acuity and provided informed consent prior to the start of the experiments. They were blinded to the study's objectives. No participant was excluded. The study was approved by the Ulsan National Institute of Science and Technology Institutional Review Board. All participants signed a written consent form before the experiment.

#### 3.2.2. Apparatus

All visual stimuli used in this study were created in MATLAB and the Psychophysics Toolbox (Brainard, 1997; Pelli, 1997), and were presented by a digital light processing projector (PROPixx;  $1920 \times 1080$ ; 1440 Hz, linear gamma) against a black background ( $0.16 \text{ cd/m}^2$ ). Trackpad was used to collect participants' responses to visual stimuli. In all experiments, participants sat in a comfortable position in a dark room, with their chin on a chin rest, looking at the screen with binocular vision. The viewing distance was 150 cm.

#### 3.2.3. Stimuli

Two types of visual stimuli were used in Experiment 1, as shown in **Figure 15**. The first type consisted of dots without Speedline, with a radius of  $0.1^\circ$  and luminance of  $189.59 \text{ cd/m}^2$ . The second type consisted of lines with Speedline, with a width of  $0.2^\circ$  and varying length ranging from  $0.2^\circ$  to  $4^\circ$ , and same luminance as the dots. These stimuli moved horizontally at constant speeds of 60, 90, and  $120^\circ/\text{s}$ , covering a visual angle of 40 degrees. The line stimulus was designed to mimic a camera analogy, where the motion is recorded at a specific refresh rate by connecting the preceding and subsequent dots from consecutive frames. The motion pathway was positioned at an orthogonal distance of  $8^\circ$  from the fixation point, considering the longer duration of the visual persistence in the periphery than the fovea (Di Lollo & Hogben, 1985). The stimuli were presented at varied refresh rate, including 24, 48, 60, 90, 120, 240, 360, and 1440 Hz. The length of line stimuli was determined by connecting the positions of two consecutively presented dots. At a refresh rate of 1440 Hz, the length of the line stimulus was matched to the diameter of the dot stimulus.

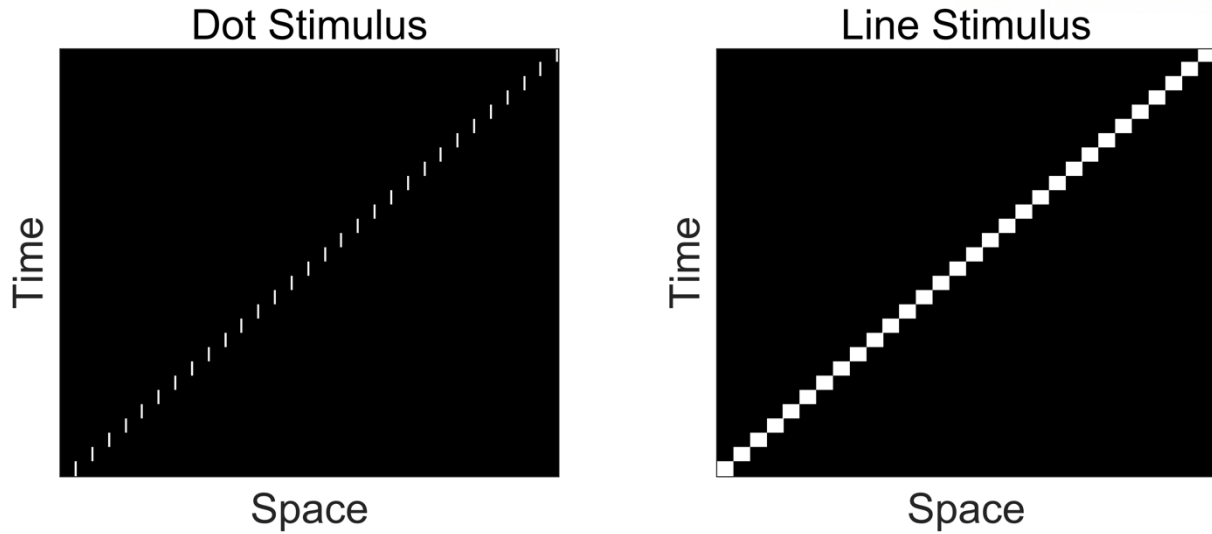


**Figure 15. Illustration of the two stimuli used in Experiment 1 in the time (x-axis) and space (y-axis) domains.** On the left side, there is a dot stimulus, while on the right side, there is a line stimulus. Both stimuli exhibit rightward translation along the horizontal pathways at the same speed. The line stimulus is constructed by filling the spatial separation between the positions of the two consecutively presented dot stimuli. This illustration highlights the difference between the dot and line stimuli and their temporal and spatial characteristics.

#### 3.2.4. Procedure

Throughout the experiments, participants were asked to maintain their fixations on a white fixation cross (width:  $0.1^\circ$ , length:  $0.25^\circ$ , luminance:  $189.59 \text{ cd/m}^2$ ) positioned 4 degrees below the center of the screen. A trial began contingent on 1 s of participants' fixation (**Figure 16**). The stimulus, either a dot or line stimulus, was presented and moved horizontally, extending 8 degrees beyond the center of the screen. The duration of the stimulus varied depending on the speed, with durations of 0.4, 0.5, or 0.67 seconds. This fast-moving stimulus resulted in a stroboscopic representation. Immediately after the stimulus ended, two white bars appeared at the location of the fixation cross. Participants were asked to adjust the spatial interval between the bars to match the perceived range of persisting images using a trackpad and then press a button. Each trial was followed by a 1-second intertrial interval. Participants completed three blocks, with each block consisting of 160 trials (2 stimulus types  $\times$  8 refresh rates  $\times$  10 repetitions) in randomized order, and the blocks were designed to have different speeds. The order of the blocks was counterbalanced among participants. The entire experimental session lasted a maximum of 50 minutes.

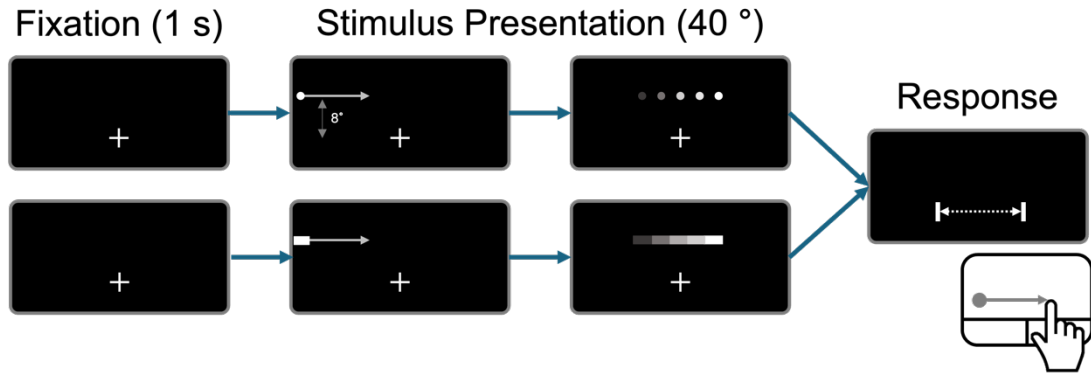


**Figure 16.** A schematic illustration of the experimental task in Experiment 1. Initially, a fixation cross is displayed for 500 ms and then disappears. Following this, a dot stimulus (upper) or a line stimulus (bottom) horizontally moves across a 40° visual angle. Immediately after the stimulus offset, the fixation cross transforms into a pair of bars. Participants are asked to adjust the spatial interval between the bars and report the range of concurrently persisting images they perceive.

### 3.2.5. Data Analysis

A repeated-measures ANOVA was performed on the participants' responses with participants as a random factor. As we intentionally set the size of dot and line stimuli as the same at 1440 Hz to test the reliability of participants' responses, data collected at 1440 Hz were excluded after we examined that there is no significant difference between the two stimulus types at 1440 Hz ( $F_{1,8} = 0.83, p = 0.389, \eta_p^2 = 0.010$ ). The means of persistence range were calculated separately for each participant, stimulus type, and speed and submitted to repeated measures ANOVA. Fixed factors were a stimulus type (dot and line), speed (60, 80, and 100 °/s), and refresh rate (24, 48, 60, 90, 120, 240, 360, and 1440 Hz).

### 3.2.6. Speedline reduces the range of concurrently perceived persisting images.

Participants were asked to report the range of persisting images after being exposed to stroboscopic representations of moving objects with and without Speedline (line and dot stimuli). Consistent with previous research (reference), our analysis revealed that the range of persisting images increases with higher refresh rates ( $F_{6,48} = 20.26, p = 1.21e^{-11}, \eta_p^2 = 0.810$ ) or faster speeds ( $F_{2,16} = 16.11, p = 1.47e^{-4}, \eta_p^2 = 0.799$ ). Notably, the persistence range of the line stimuli was found to be shorter compared to that of the dot stimuli (**Fig 17**, Green: dot stimulus; Red: line stimulus;  $F_{1,8} = 20.80, p = 0.00185, \eta_p^2 = 0.763$ ). The shaded gray area represents the refresh rate at which the two

stimuli exhibited a significantly different persistence range. Particularly, for the highest speed and lowest refresh rate condition, a significant difference was observed, with the persisting dot stimuli having approximately twice the range compared to the persisting line stimuli (120 °/s, 24 Hz, mean response: 13.9 vs. 7.4 °). The difference in the persistence range of the two stimuli increases as refresh rate decreases or speed increases, evidenced by a significant interaction of the stimulus type with refresh rate ( $F_{6,48} = 11.30, p = 7.8e^{-8}, \eta_p^2 = 0.579$ ) and speed ( $F_{2,16} = 9.568, p = 0.00185, \eta_p^2 = 0.524$ ). In summary, our findings indicate that the addition of Speedline parallel to the axis of motion resulted in a perceptual reduction in the range of persisting images.

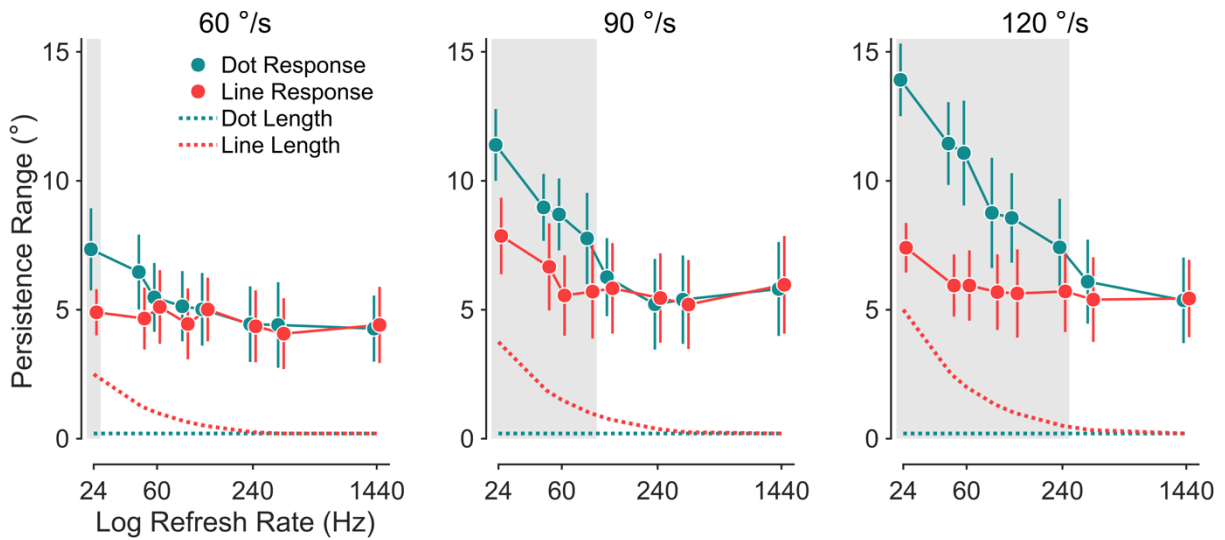


**Figure 17. The range of concurrently perceived persisting images for a moving dot (green) and line (red).** Each panel corresponds to different speed conditions. The dashed lines indicate the actual length of the two stimuli, while the error bars represent the average value of the persistence range along with the standard error of the means. The gray shaded area indicates conditions where there was a significant difference between line and dot stimuli ( $p < 0.05$ ).

### 3.3. Experiment 2: Testing effects of the stimulus size on the range of visual persistence

Results of Experiment 1 showed that Speedline added behind a moving dot significantly reduced the range of the visual persistence compared to dot stimuli. As the previous study reported (Francis & Grossberg, 1996; Francis, 1999; Kim & Francis, 1998), one may concern that the difference in the persistence range of the two stimuli may be attributable to the different size of the two stimuli. In order to address concerns about the size difference between the dot and line stimuli, we conducted an additional experiment. We included a vertical line stimulus that was the same length as the horizontal line stimulus but oriented orthogonally. This allowed us to examine whether the reduction in persistence range observed with Speedline was specific to the parallel orientation of the line. The experimental procedure was similar to Experiment 1, and we measured and compared the persistence ranges of all three stimuli (dot, horizontal line, vertical line) under various conditions.

#### 3.3.1. Participants

Twelve individuals without any history of eye-related diseases within the past six months were recruited to participate in this study ( $26.5 \pm 2.6$  years; 10 men; 2 women).

#### 3.3.2. Stimuli

On top of the two stimuli used in Experiment 1, we added vertical line stimuli which are equivalently long as the horizontal line stimulus ( $0.2^\circ$  to  $4^\circ$ ). Stimuli were presented at six refresh rates (24, 48, 60, 90, 120, 1440 Hz). We set the speed of visual stimuli as  $120^\circ$  because the difference between the horizontal line stimuli and dot stimuli was most prominent in the condition with the fastest speed.

#### 3.3.3. Procedure

The experimental procedure was identical to that of Experiment 1. Participants completed one block (180 trials, 3 stimulus types x 6 refresh rate x 10 repetitions), which lasted at most 15 min.

#### 3.3.4. Data Analysis

Data collected at 1440 Hz were excluded after we examined that there is no significant difference between the three stimulus types at 1440 Hz ( $F_{2,22} = 0.70, \eta_p^2 = 0.006, p = 0.509$ ). The means of persistence range were calculated separately for each participant, stimulus type, and speed and submitted to repeated measures ANOVA. A stimulus type (dot, horizontal line, and vertical line) and refresh rate (24, 48, 60, 90, 120, 240, 360, and 1440 Hz) were treated as a fixed factors whereas participant was treated as a random factor. If factors including more than three levels showed a significant main effect, we run Tukey's HSD to figure out which specific groups' means are different.

### 3.3.5. The persistence range is modulated by Speedline, not the stimulus size.

The results of the additional experiment provide evidence that the reduction in persistence range observed with Speedline is not solely due to the size difference between the stimuli. The persistence ranges of the vertical and horizontal line stimuli were expected to be the same, based on the properties of visual persistence depending on the stimulus size. A repeated-measures ANOVA shows that there is a significant effect of the three types of stimuli ( $F_{2,22} = 9.51, p = 0.00106, \eta_p^2 = 0.46$ ). As depicted in **Figure 18**, we replicated the observation of Experiment 1 in that the horizontal line stimuli had a significantly shorter persistence range than the dot stimuli (Tukey's test:  $p = 0.001$ ). However, the vertical line stimuli did not differ significantly from the dot stimuli in terms of persistence range ( $p = 0.545$ ), but they did differ significantly from the horizontal line stimuli ( $p = 0.010$ ). These findings suggest that the presence of Speedline modulates the persistence range independently of the stimulus size. We also found a significant main effect of refresh rate ( $F_{6,66} = 4.653, p = 0.000531, \eta_p^2 = 0.30$ ) such that the persistence range decreases as refresh rate increases, and a significant interaction effect between the stimulus type and refresh rate ( $F_{12,132} = 2.28, p = 0.0117, \eta_p^2 = 0.17$ ). The result of this experiment suggests that the size of the visual stimuli did not mediate the visual persistence.

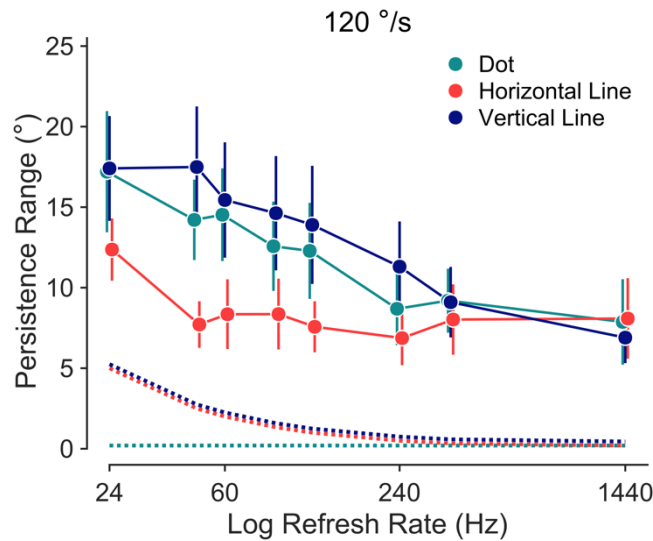


**Figure 18. The range of concurrently perceived persisting images for different stimulus types.** Three different stimulus types are represented by different colors: navy for vertical line, red for horizontal line, and green for dot. The x-axis corresponds to the refresh rate, while the y-axis represents the persistence range. Error bars are included to indicate the standard error of the means.

### 3.4. Experiment 3: Manipulating connectivity of line stimuli

Through the two previous experiments, we showed that the line stimuli with Speedline have a shorter persistence range and ruled out the possible effect of the stimulus size. We now consider the potential influence of the connectivity between the two stimuli on the persistence range. To investigate the role of connectivity between stimuli on persistence range, we conducted Experiment 3. We focused on line stimuli with Speedline and varied the length of the line segment. The stimulus speed was fixed at 120 °/s to maximize the impact of Speedline. We hypothesized that the extent of connectivity between the line segments would influence the persistence range.

#### 3.4.1. Participants

Ten individuals without any history of eye-related diseases within the past six months were recruited to participate in this study ( $27.2 \pm 2.8$  years; 6 men; 4 women).

#### 3.4.2. Stimuli

The white lines (luminance: 189.59 cd/m<sup>2</sup>) moved horizontally at a constant speed of 120 °/s and were presented at refresh rates of 60 Hz and 240 Hz. The line stimuli were created by connecting two consecutively presented dots, and the length of the line segment was manipulated in 8 steps relative to the distance between the dots (length ratios: 0, 0.2, 0.4, 0.6, 0.8, 1.0, 1.2, 1.4). The shortest condition (zero-ratio) had a line length equal to the dot diameter, while the ratio of one corresponded to the line length being equal to the dot distance. Ratios greater than one indicated that the line length exceeded the dot distance, resulting in partial overlap between consecutive lines. The length of the line stimulus varied depending on the refresh rates (60 Hz: 0.2 ° to 2.8 °, 240 Hz: 0.2 ° to 0.7 °). Additionally, we included a control condition where line stimuli were presented at 1440 Hz and varied in length as follow: 0.1 ° (dot diameter), 0.4 ° (minimum length at 60 Hz), 2.8 ° (maximum length at 60 Hz), 0.2 ° (minimum length at 240 Hz), and 0.7 ° (maximum length at 240 Hz).

#### 3.4.3. Procedure

The experimental procedure is as same as that of Experiment 1. We measured the persistence range separately for each stimulus type by employing a randomized block design. Within a day, participants completed three blocks of which each lasted at most 15 min (See **Figure S9** in Appendix for results when all trials were intermixed).

#### 3.4.4. Data Analysis

The means of persistence range were calculated separately for each participant, stimulus type,

and speed and submitted to repeated measures ANOVA. The length ratio of the line stimulus (0, 0.2, 0.4, 0.6, 0.8, 1.0, 1.2, and 1.4) and refresh rate (60 and 240 Hz) were treated as a fixed factor, while participant was treated as a random factor. If factors including more than three levels, in this case the length ratio of the line stimulus, showed a significant main effect, we run Tukey's HSD to figure out which specific groups' means are different. For responses to 1440 Hz condition, we applied ANOVA considering the length ratio as a fixed factor and participant as a random factor.

### 3.4.5. The connectivity between stimulus locations suppresses visual persistence

We examined how the range of persisting images varied with the length of the line segment at 60 Hz and 240 Hz (**Figure 19**, left). A repeated-measures ANOVA on the combined data revealed a significant main effect of line length ( $F_{7,84} = 17.04, p = 7.99e^{-14}, \eta_p^2 = 0.591$ ) and refresh rate ( $F_{1,12} = 5.831, p = 0.0326, \eta_p^2 = 0.330$ ). Furthermore, there was a significant interaction effect between the line length and refresh rate ( $F_{7,84} = 2.999, p = 0.00735, \eta_p^2 = 0.200$ ). Post-hoc analysis demonstrated a gradual decline in the persistence range as the line length increased (**Table S18**, **Table S19**). The decline reached an asymptote for longer line lengths. Importantly, the zero-ratio stimuli, which matched the dot stimuli from Experiment 1, showed similar persistence ranges (60 Hz:  $11.1^\circ$  vs  $13.2^\circ$ ,  $t_{20} = 0.604, p = 0.552, \text{cohen}'d = 0.262$  ; 240 Hz:  $7.4^\circ$  vs  $8.7^\circ$ ,  $t_{20} = 0.551, p = 0.588, \text{cohen}'d = 0.239$ ). Similarly, the ratio-one stimuli, which matched the line stimuli from Experiment 1, displayed comparable responses (60 Hz:  $5.9^\circ$  vs  $7.2^\circ$ ,  $t_{20} = 0.632, p = 0.535, \text{cohen}'d = 0.274$  ; 240 Hz:  $5.7^\circ$  vs  $6.6^\circ$ ,  $t_{20} = 0.447, p = 0.659, \text{cohen}'d = 0.194$ ). Additionally, in a control condition with line stimuli presented at 1440 Hz, where the line length was always same as or exceeded the spatial separation between stimuli, there was no significant effect of line length on persistence range (**Figure 19**, **Table S20**;  $F_{4,20} = 0.17, p = 0.951, \eta_p^2 = 0.03$ ). This suggests that elongation beyond the spatial separation does not impact the range of visual persistence.



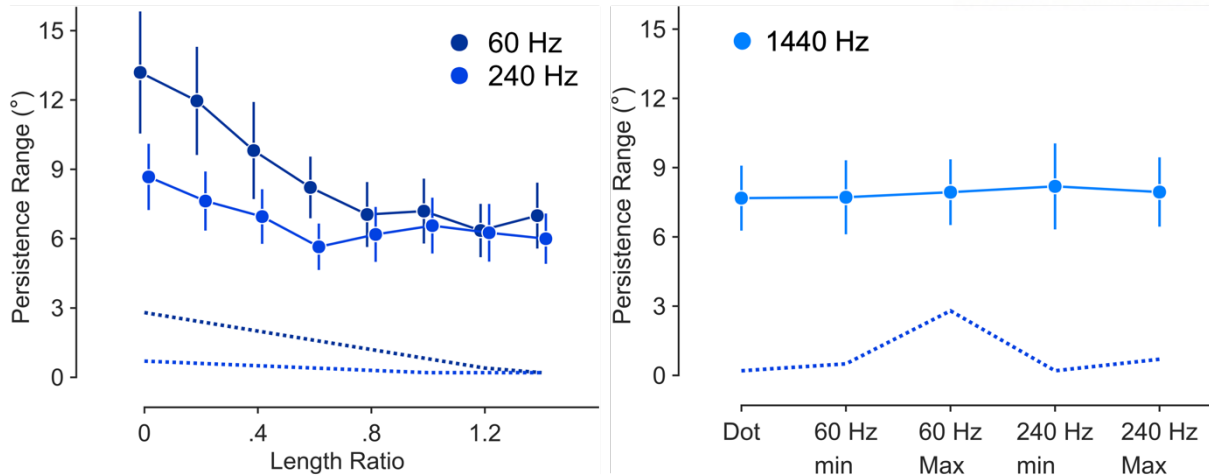


**Figure 19. The range of concurrently perceived persisting images for the different length of line.** The length ratio indicates the length of the line stimuli relative to the distance between two consecutively presented dots in two refresh rate conditions. X-axis indicates the length ratio, while y-axis represent the persistence range. Dashed lines are included to indicate the physical lengths of the moving lines. The fixed speed of the stimuli causes the actual length of the line stimuli to differ based on the refresh rate (refer to the Methods section for details). A ratio of zero corresponds to the dot diameter, while ratios greater than one indicate that the preceding and subsequent lines are connected. The observations at 60 Hz and 240 Hz are displayed on the left panel, and those at 1440 Hz are displayed on the right.

### 3.5. Experiment 4: Effects of Speedline on the perceived length of moving stimuli

In the previous three experiments, we asked participants to report the range of the concurrently perceived images, which is vulnerable to individual's bias. For instance, some participants may have always reported the longer range for line stimuli over dot stimuli. In Experiment 4, we aimed to directly measure the perceived length of moving stimuli by manipulating the actual number of elements comprising dot and line stimuli. We varied the number of elements from 1 to 4 for both dot and line stimuli. Importantly, when the number of elements was equal for both stimuli, the overall length from the start point to the end point of the stimulus remained constant. By assessing the perceived length of the stimuli, we aimed to minimize individual biases that may have influenced the range reports in the previous experiments.

#### 3.5.1. Participants

Six individuals without any history of eye-related diseases within the past six months were recruited to participate in this study ( $23.7 \pm 2.7$  years; 5 men; 1 woman).

#### 3.5.2. Stimuli

The two types of visual stimuli, dots (without the artificial streak, radius:  $0.1^\circ$ , luminance:  $189.59 \text{ cd/m}^2$ ) and lines (with the artificial streak, width:  $0.2^\circ$ , luminance:  $189.59 \text{ cd/m}^2$ ), rotated along a circular trajectory (radius:  $4^\circ$ ). We adjusted the number of elements constituting the to-be-presented visual stimulus from one to four (**Figure 20**). When the number of elements was one, the line stimulus was identical to the dot stimulus. We increased the number of elements by adding a dot separated by  $14.4^\circ$  or extending the arc along the circular pathway by  $14.4^\circ$ . Since we fixed the angular difference between two adjacent elements as  $14.4^\circ$ , four different refresh rates (72, 80, 120, 160 Hz) have the corresponding four tangential speeds (18, 20, 30,  $40^\circ/\text{s}$ , respectively). The stimulus duration was 1 second across all conditions.

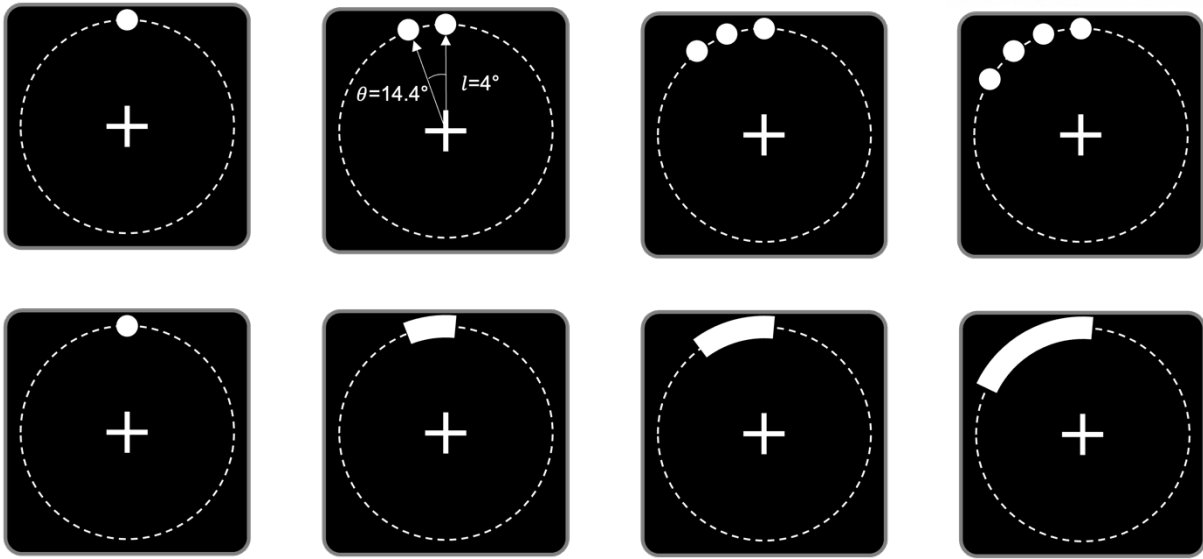


**Figure 20. The dot (upper row) and line (bottom row) stimulus with varied number of elements.** Each element was displaced by  $14.4^\circ$  from each other. A dashed line represents an invisible circular trajectory with a radius of  $4^\circ$ , along which the entire set of the visual stimuli rotates together.

### 3.5.3. Procedure

Throughout the experiments, participants were asked to fixate their eyes on a white fixation cross (width:  $0.1^\circ$ , length:  $0.25^\circ$ , luminance:  $189.59 \text{ cd/m}^2$ ) located at the center of the screen. Instead of using horizontal motion as in previous experiments, we employed rotating motion to eliminate the potential influence of eccentricity. Eye movements were not recorded during the experiment. Each trial began with a 1-second fixation period, followed by the appearance of the stimulus (either a set of dot or line stimuli) rotating for 1 second. The fixation point and visual stimuli disappeared simultaneously. A white marker was then presented at a random position along the circular trajectory. Participants were asked to use the trackpad to draw an arc starting from the white marker and continue until they believed the arc length matched the perceived length of the previously presented stimuli. They clicked a button to indicate their response.

Participants completed four blocks of trials in a single day, with each block consisting of 100 trials. The trials included different combinations of stimulus types (dot or line), number of elements (ranging from 1 to 4), and repetitions (10 repetitions per condition). Additionally, 20 catch trials were included where both dot and line stimuli were presented at a slow speed of  $3^\circ/\text{s}$  and 12 Hz. The purpose of the catch trials was to ensure participants set consistent criteria for the perceived length of stimuli across different speed conditions. The order of blocks was counterbalanced across participants. The entire experimental session lasted a maximum of 45 minutes.

### 3.5.4. Data Analysis

Because the two stimuli were identical when the number of moving stimuli was 1, we found no main effect of the stimulus type in this condition ( $F_{1,5} = 0.065, p = .809, \eta_p^2 = .006$ ) and excluded corresponding data in the following analysis. The means of perceived length in arc were calculated separately for each participant, stimulus type, and speed and submitted to repeated measures ANOVA (fixed factor: stimulus type (dot, line), the number of elements (1, 2, 3, 4), refresh rate (72, 80, 120, 160 Hz); random factor: participant). If factors including more than three levels showed a significant main effect, we run Tukey's HSD to figure out which specific groups' means are different.

### 3.5.5. Speedline reduces the perceived length of moving stimuli.

Participants were aware that the number of elements varied and asked to report the perceived length by answering the angle subtended by an arc of moving stimuli. The results of Experiment 4 in **Figure 21** demonstrate that the perceived length of moving lines is significantly shorter than that of moving dots. A repeated measures ANOVA showed a significant main effect of stimulus type ( $F_{1,5} = 7.676, p = .0393, \eta_p^2 = .734$ ), indicating that the perceived length of lines is consistently shorter than dots. Additionally, there was a significant interaction effect between the number of elements and stimulus type ( $F_{2,10} = 4.345, p = .0438, \eta_p^2 = .734$ ), suggesting that the difference in perceived length between lines and dots increases as the number of elements increases. The gray shaded area in **Figure 21** indicates the conditions where the perceived lengths of the two stimuli are significantly different. It is no surprise that there is a significant effect of the number of elements ( $F_{2,10} = 77.32, p = 8.27e^{-07}, \eta_p^2 = .954$ ). This finding is consistent with the results obtained when participants were asked to report the number of elements instead of the perceived length of moving stimuli (**Fig S8**,  $F_{1,5} = 6.811, p = .0477, \eta_p^2 = .412$ ). In summary, the presence of Speedline significantly reduces the perceived length of moving stimuli, and this effect is influenced by both the stimulus type (line vs. dot) and the number of elements.

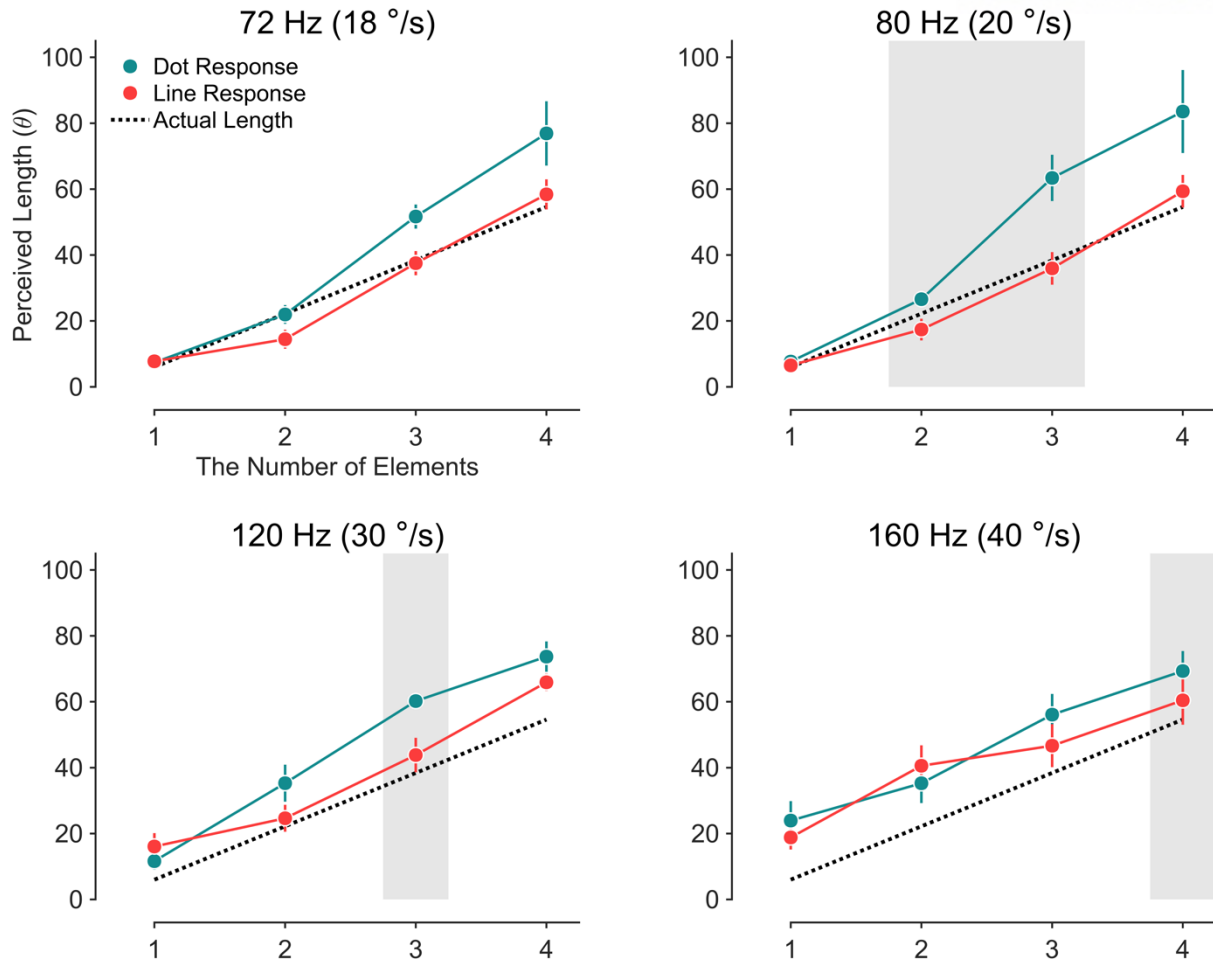


**Figure 21. The perceived length of moving dot stimuli in green and line stimuli in red as a function of the number of elements.** Each panel corresponds to different refresh rate conditions. The grey unity line indicates the actual length of the stimuli. It is worth noting that the physical length of line stimuli and dot stimuli with the same number of elements was set to be identical. The shaded area in gray represents the refresh rate condition where the perceived length of line stimuli was shorter than that of dot stimuli.

### 3.6. Experiment 5: A sense of reality with the presence or absence of Speedline

Our results encompassed within an argument that Speedline reduced suppressed the visual persistence in a way that both the range of perceived concurrently persisting images and the perceived length of moving objects decreases. In Experiment 5, the focus shifted to the perceived quality of motion and specifically the similarity with real motion in the world. To assess this, we employed a Thurstonian modeling approach, which involves pairwise comparison responses to assign numeric values to the perceived sense of reality. By using this approach, we aimed to compare the perceived sense of reality of moving objects with and without Speedline and investigate how the presence or absence of Speedline influences the perception of motion and its resemblance to real-world motion.

#### 3.6.1. Participants

Eight individuals without any history of eye-related diseases within the past six months were recruited to participate in this study ( $24.0 \pm 2.7$  years; 5 men; 3 women).

#### 3.6.2. Apparatus and Stimuli

A single dot (without Speedline, radius:  $0.1^\circ$ , luminance:  $189.59 \text{ cd/m}^2$ ) or a single line (with Speedline, width:  $0.2^\circ$ , luminance:  $189.59 \text{ cd/m}^2$ ) rotated along an imaginary circular trajectory (radius:  $4^\circ$ ). The combination of 4 tangential speeds (3, 6, 12, and  $24^\circ/\text{s}$ ) and 13 refresh rates (24, 48, 60, 96, 120, 144, 180, 240, 288, 360, 480, 720, and 1440 Hz) made 48 conditions. The initial locations of the dot and line stimuli were randomly sampled from the uniform distribution. Note that if the refresh rate is 1440 Hz, the dot and line stimuli were exactly the same stimuli.

#### 3.6.3. Procedure

We used 2-interval forced choice (2IFC) tasks to measure individual's preference for one refresh rate over the others. Throughout the experiments, participants were asked to fixate their eyes on a centrally located white fixation cross (width:  $0.1^\circ$ , length:  $0.25^\circ$ , luminance:  $189.59 \text{ cd/m}^2$ ). After a white fixation cross was presented for 1 s, the first stimulus interval was presented for 1 s followed by a 1-s interstimulus interval with the central fixation before the second stimulus was presented. Following the offset of the second stimulus, a beep sound was given to signal the end of the stimulus presentation. Participants were asked to report which of the two intervals included more realistic motion. As an example of real motion, we suggested Jwibulnori (**Figure S12**), a Korean game in which participants create streaks of light by swinging cans filled with burning items. According to the previous finding (Sperling et al., 1985; Watson et al., 1986), if refresh rates of two intervals were largely different, participants mostly preferred and selected the higher refresh rate. The 2IFC task for each refresh rate

was completed in pairs within three levels. For instance, 96 Hz was compared only with 24 (-3 levels), 48 (-2 levels), 60 (-1 level), 120 (+1 level), 144 (+2 levels), 180 (+3 levels) Hz. A combination of each speed and each stimulus type was conducted in separate blocks, 8 blocks in total (330 trials each, ~30 min). The order of blocks was counterbalanced across participants.

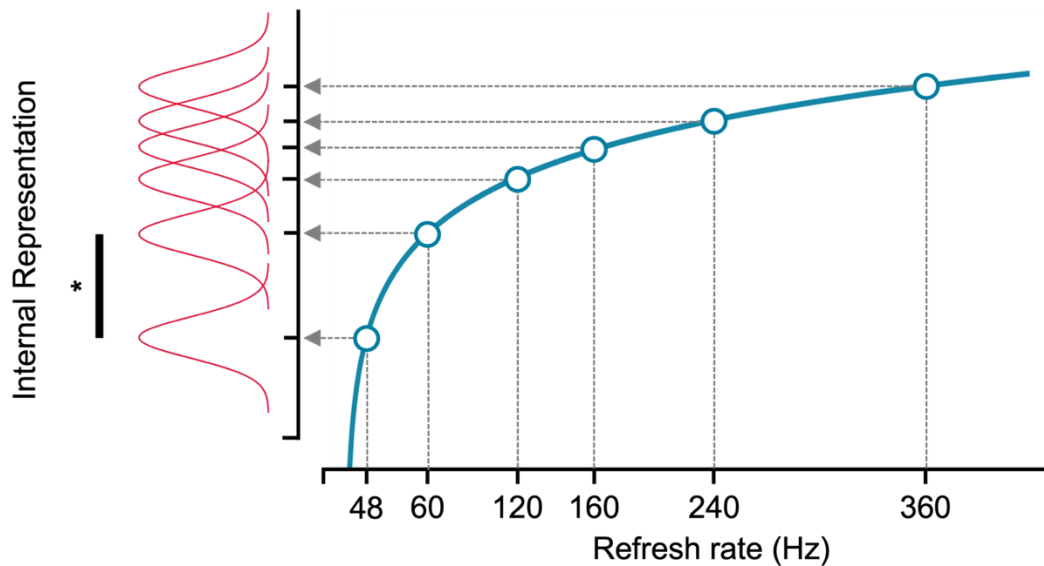


**Figure 22. The internal representation for moving objects presented at each refresh rates.**

The x-axis represents the refresh rate, while the y-axis represents the estimated internal representation based on responses collected from a psychophysical experiment. As the refresh rate increases, the internal representation of the sense of reality also increases, indicating a higher quality of perceived motion. If the distributions of internal representation are significantly different, there is a noticeable difference in the perceived sense of reality for moving objects. The distance between their distributions indicates the extent of difference in the perceived sense of reality. For instance, between the refresh rates of 48 Hz and 60 Hz, the distance is distant enough such that there is a significant difference in the perceived sense of reality between 48 Hz and 60 Hz.

#### 3.6.4. Analysis of the distances between the internal representations from the 2IFC task.

We used the participants' responses collected during the 2IFC task and computed the probability of preference compared to three adjacent refresh rates. Thurstonian modeling was used to analyze these pairwise comparison responses and obtain a quantitative measure of the perceived sense of reality. It was assumed that participants had preferences for the stimuli being compared, with a

preference for the stimulus that was perceived to have a higher sense of reality. Two assumptions were made in the analysis of the internal representation of the sense of reality. First, it was assumed that each refresh rate used in the experiment has its own internal representation, represented by a numeric number. These internal representations were assumed to follow a standard normal distribution with a mean of 0 and a fixed variance of 1 across all refresh rates. Second, it was assumed that the mean of the normal distribution representing the internal representation may or may not differ depending on the refresh rate, but the variance remains constant at 1 across all refresh rates. For the comparison between two refresh rate conditions, a probability of 0.5 indicated that the internal representations of the two conditions were not distinguishable. On the other hand, a probability of 1 indicated that the internal representations of the two conditions were widely different. We used this probability to examine the internal representation for the sense of reality across different refresh rate conditions. **Figure 22** shows the results of this analysis, depicting the distinguishability of the internal representations.

To estimate the internal representations, we set the internal representation of the lowest refresh rate as 0. Then, they estimated 12 psychological distance values in terms of the internal representation, representing the differences between adjacent refresh rates. As the standard deviation of the difference between two normal distributions is  $\sqrt{2}$ , each distance follows a normal distribution with a mean of 0 and a fixed variance of  $\sqrt{2}$ . The likelihood of the distance between two adjacent refresh rates was calculated using the responses to the pairwise comparisons. This calculation was similar to the maximum likelihood estimation used in the spatiotemporal integration model in the earlier part of the study. The probability of choosing the higher refresh rate for each refresh rate  $p_i$  was computed based on these likelihood calculations.

$$p_i(D_i, \sqrt{2}) = \frac{1}{2\sqrt{\pi}} \int_{-\infty}^{D_i} \exp\left(-\frac{D^2}{4}\right) dD$$

$D_i$  indicates the distance parameter from the estimated sense of reality in  $i$ th refresh rate to that of  $i + 1$ th refresh rate. The likelihood function over  $N_f$  levels of refresh rate is proportional to

$$likelihood = \prod_{i=1}^{N_f} [p(D_i, \sqrt{2})]^{r_i} * [1 - p(D_i, \sqrt{2})]^{1-r_i}$$

where  $r_i=1$  when a participant reports that the objects presented at the higher refresh rate appears more realistic than those presented at  $i$ th refresh rate, and  $r_i = 0$  when the participant reports that the objects presented at  $i$ th refresh rate appears more realistic than those presented at the higher refresh rate. We then took the logarithm of the equation above and compute the log likelihood.

$$\log likelihood = \sum_{i=1}^{N_f} r_i * \log(p(D_i, \sqrt{2})) + (1 - r_i) * \log(1 - p(D_i, \sqrt{2}))$$



MCMC sampling was used to estimate the parameters that maximize the likelihood estimation on the posterior probability distribution of the 12 distance values. This approach accounted for individual variability and provided a robust estimation of the parameters by considering the uncertainty in the data. The posterior distribution obtained from the MCMC sampling allowed for inferences about the internal representations of the sense of reality for stimuli with and without Speedline. By considering the relative judgments made by participants in pairwise comparisons, this modeling approach provides a numerical representation of the perceived quality of motion, offering a more objective measure.

### 3.6.5. Speedline enhances the sense of reality of moving stimuli.

The other aspect characterizing the effect of the Speedline on the perceived motion is a sense of reality. It is worthwhile to examine whether the line stimuli elicit a higher sense of reality than the dot stimuli. In terms of the internal representation, psychological distance between two levels was computed based on pairwise comparison data (see Methods). Assuming that the lowest refresh rate has 0 value, we accumulated the estimated distances separately depending on the stimulus type (dot vs., line) and speed (**Figure 23**; left panel: dot stimuli; right panel: line stimuli). It seems obvious that the higher refresh rates result in more realistic motion for both dot and line stimuli. Since our main interest lies in comparison between dot and line stimuli, we intentionally presented the identical stimuli at the 1440 Hz condition. The internal representation for both stimuli must be the same at 1440 Hz because they are identical stimuli. The apparent differences in two panels arise from the assumption that the lowest refresh rate has zero value and the distance between adjacent refresh rate was estimated separately. By tracing back from the 1440 Hz condition, we can compare the relative internal representation. The internal representation of the dot stimuli estimated at 240 Hz was significantly different from that estimated at 1440 Hz, indicating that dot stimuli need to be presented at a higher refresh rate to achieve a sense of reality comparable to stimuli presented at 1440 Hz. In contrast, the internal representation of the line stimuli estimated at 120 Hz was not significantly different from that estimated at 1440 Hz, suggesting that line stimuli presented at 120 Hz were perceived as real as dots presented at 1440 Hz. These findings support the conclusion that moving lines have a higher sense of reality compared to dots.

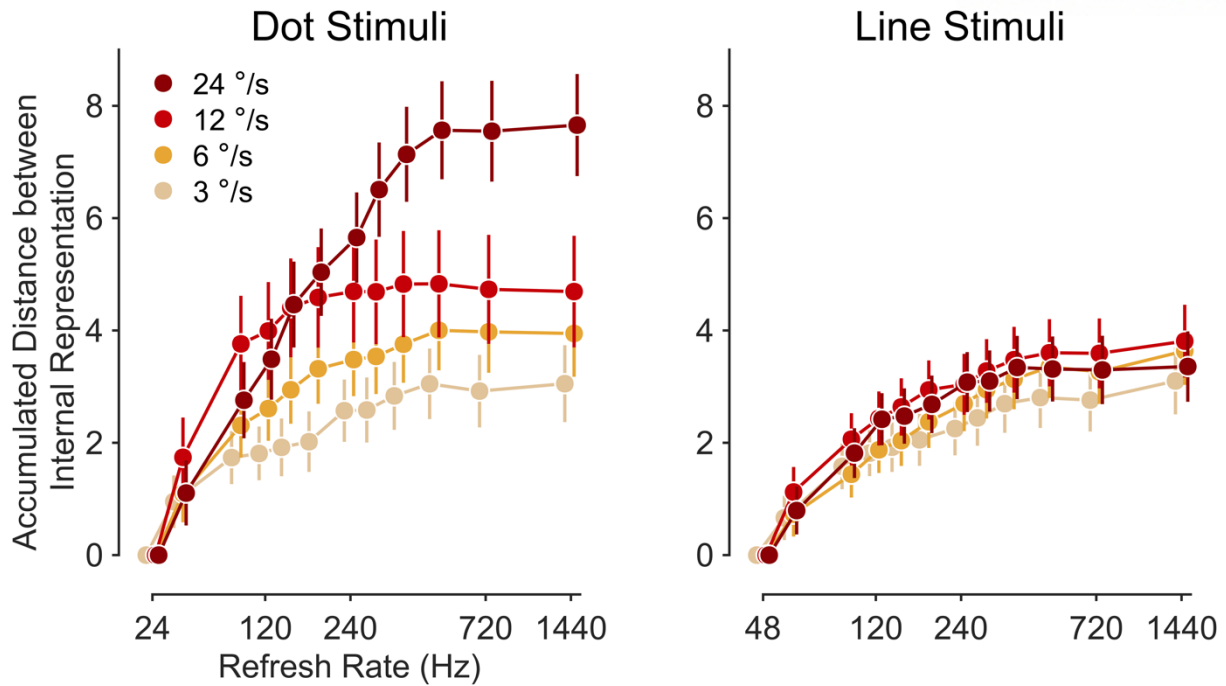


**Figure 23.** The accumulated internal distance between refresh rates for dot (left) and line (right) stimuli. The x-axis represents the refresh rate, while the y-axis represents the accumulated distance between the internal representations for the sense of reality. Each color corresponds to a different speed condition. The error bars in the figure represent the credible interval, indicating the level of uncertainty associated with the estimated distances.

### 3.7. Discussion

We observed that the presence of Speedline, characterized by line stimuli created through the connection of consecutive positions, had a significant impact on visual persistence. Specifically, the line stimuli exhibited a shorter persistence range compared to dot stimuli. This suggests that Speedline influences the spatiotemporal integration of visual information and reduces the ranges over which images persist in the visual system. Control experiments ruled out the possibility that the observed effects were solely due to differences in stimulus size. Instead, the connectivity between the two consecutively presented stimuli played a crucial role in modulating visual persistence. Furthermore, our study examined the perceived sense of reality in the motion of dot and line stimuli. The results demonstrated that line stimuli elicited a higher sense of reality compared to dot stimuli in a way that the motion of lines appeared as realistic as the motion of dots presented at a much higher refresh rate.

In Experiment 2, we observed that line stimuli of equal length exhibited different persistence ranges depending on whether they were aligned parallel to the motion axis. This finding is consistent with previous research indicating that the motion system processes oriented signals to code the direction of motion. Studies using Glass patterns (Krekelberg et al, 2003), RDK stimuli (Bae & Luck, 2022; Kwak & Curtis, 2022; Tang et al., 2015), and streak-free motion cloud stimuli (Moon et al., 2022) have reported the involvement of oriented signals in motion perception. We speculated that the horizontal line along the motion axis in our study provided an oriented signal that facilitated motion processing. An additional experiment comparing the persistence range of dot stimuli, horizontal line stimuli, and square stimuli supported this conjecture. The results showed no significant difference in persistence range between line stimuli and square stimuli (**Figure S10**, Tukey's test:  $p = 0.931$ ), suggesting that orientation information plays a role in motion processing, particularly along the axis parallel to the motion trajectory, rather than the expansion of stimulus size along the axis perpendicular to the motion trajectory. However, the exact mechanism by which the motion signal facilitated by oriented signals along the motion axis leads to the shortening of the persisting image remains elusive and requires further investigation. We also found that the persistence suppression induced by Speedline did not vary depending on stimulus duration (**Figure S11**), which contrasts with previous findings on motion smear, where the motion system deblurred the motion smear after a certain duration.

Moreover, compared to the dot stimulus, the line stimulus with Speedline had a relatively lower spatial frequency. Previous studies have shown that spatial frequency is another important factor that affects visual persistence. Higher spatial frequencies tend to increase visual persistence. This effect can be explained within the framework of inhibition-based accounts and the involvement of transient and sustained channels. The transient channel, being less sensitive to high-frequency components, is expected to elicit less inhibition, resulting in longer visual persistence for dot stimuli. Building a

spatiotemporal integration model that incorporates these two channels would provide a more detailed understanding of the underlying mechanisms of persistence suppression induced by Speedline.

Our findings from Experiment 5 demonstrate that the perceptual quality of motion in displays can be enhanced by inserting a tail-like Speedline along the motion axis. This supports previous proposals that subjective ratings for motion quality increase when the spatial displacement between consecutive frames matches the width of the line (Mackin et al., 2016). These findings validate common techniques used in the animation and video game industry (Kuroki et al., 2007; Wilcox et al., 2015), such as drawing motion lines or superimposing images of multiple frames. Furthermore, our study revealed that the subjective sense of reality increases with higher refresh rates and stimulus speeds. Previous research has reported that higher refresh rates lead to higher subjective ratings of motion in displays (Sperling et al., 1985; Watson et al., 1986). Similarly, the effect of speed aligns with previous studies, where the refresh rate at which sampled motion becomes indistinguishable from continuous motion increases as the speed of the stimulus increases. In summary, there are two effective approaches to enhance the perceptual quality of motion in displays: inserting a tail-like Speedline and increasing the refresh rate. While increasing the refresh rate can be costly in terms of technical requirements, drawing a Speedline is a more efficient way to achieve a higher sense of reality.

### **3.8. Conclusion**

In conclusion, our study contributes to the understanding of motion perception by investigating the impact of the Speedline technique on visual persistence. We have demonstrated that the presence of a Speedline, which connects consecutive stimuli, influences the perceived persistence and length of moving objects. Furthermore, we have shown that the Speedline technique enhances the sense of reality in motion perception compared to dot stimuli. These findings have implications for various domains including animation, video games, and virtual reality, where the incorporation of Speedline can improve the perceptual quality of moving objects.

## 4. General Discussion

Eye movements play a crucial role in visual perception, influencing various aspects of visual processing, including the perception of critical fusion frequency (CFF) - the threshold at which a flickering light source appears to be continuously illuminated. Our study has demonstrated that eye movements can modulate CFF, with fixational eye movements and saccadic eye movements exerting a significant influence on the perception of flickering stimuli. These findings suggest that the dynamic nature of eye movements contributes to the spatiotemporal integration of visual information, ultimately shaping our perception of flickering stimuli.

The results of this study raise the possibility that the eye tremors in individuals with low vision may not be random but rather strategic, perhaps to gather more information by increasing their sensitivity. It would be interesting to explore whether the individuals with low vision cease tremors when the retinal image is stabilized and there is no use of eye movements in manipulating the retinal shift. The biological reasons behind these phenomena are still unclear. From a neurological perspective, it is intriguing to consider that if observers consciously make an effort to see better, it could lead to dopamine secretion, potentially enhancing eye movements. This area requires further exploration and beyond the scope of early visual processing.

Furthermore, the interaction between eye movements and the spatial feature of the visual scene holds particular significance. Our eye movements, which continuously shift the gaze across the visual scene, result in a dynamic retinal input and subsequently influence the visual experience of observers. The spatial characteristics of the scene, such as the distribution and arrangement of visual elements, can further influence the occurrence and characteristics of eye movements. This interplay between eye movements and the spatial feature of the visual scene emphasizes the importance of considering both temporal and spatial factors in understanding the perception of motion and flickering stimuli. Based on understanding about the intricate relationship between eye movements and the spatial context, we can obtain a more comprehensive understanding of how visual information is processed and integrated, ultimately shaping our perception of the visual world.

In addition to eye movements, the presence of speed lines has been found to have a profound effect on visual persistence and the perceived quality of motion. Speed lines, which are tail-like streaks that connect successive stimuli, have been shown to alter the persistence range and perceived length of moving objects. Our study further extends this understanding by demonstrating that speed lines not only affect visual persistence but also enhance the sense of reality in motion perception compared to dot stimuli. The incorporation of speed lines in visual displays, such as animations, video games, and virtual reality, can greatly enhance the perceptual quality of motion, providing a more immersive and engaging experience for viewers.

These results have implications for understanding the mechanisms underlying visual perception and the influence of Speedline on our perception of moving objects. Future studies could further investigate the neural correlates and computational processes involved in the integration of motion information and the generation of a sense of reality in the presence of Speedline. Additionally, exploring the perceptual effects of Speedline in other contexts, such as dynamic scenes or real-world stimuli, could provide a broader understanding of their impact on visual perception. Overall, our study highlights the complex interplay between motion processing, oriented signals, spatial frequency, and visual persistence. Further investigations and modeling approaches are necessary to fully elucidate the underlying mechanisms and provide a comprehensive understanding of the observed effects.

The effects of eye movements on CFF and the influence of speed lines on visual persistence and perceived motion quality highlight the importance of considering temporal and spatial factors in understanding how the visual system integrates and processes motion information. Future research should delve deeper into the underlying mechanisms that mediate these effects, such as the role of motion-sensitive neurons, neural adaptation, and the interaction between fixational eye movements and motion processing. Moreover, by elucidating the mechanisms underlying motion perception and highlighting the benefits of the Speedline technique, our study could provide an opportunity for designing more immersive visual experiences by increasing the perceived quality of motion.

## References

1. Atchley, R. A., Ilardi, S. S., & Enloe, A. (2003). Hemispheric asymmetry in the processing of emotional content in word meanings: The effect of current and past depression. *Brain and language*, 84(1), 105-119.
2. Balestra, C., Machado, M. L., Theunissen, S., Balestra, A., Cialoni, D., Clot, C., ... & Lafère, P. (2018). Critical flicker fusion frequency: a marker of cerebral arousal during modified gravitational conditions related to parabolic flights. *Frontiers in physiology*, 9, 1403.
3. Bedell, H. E., Ramamurthy, M., Patel, S. S., Subramaniam, S., Vu-Yu, L. P., & Tong, J. (2008). The temporal impulse response function in infantile nystagmus. *Vision research*, 48(15), 1575-1583.
4. Bonin, V., Mante, V., & Carandini, M. (2005). The suppressive field of neurons in lateral geniculate nucleus. *Journal of Neuroscience*, 25(47), 10844-10856.
5. Bowling, A., Lovegrove, W., & Mapperson, B. (1979). The effect of spatial frequency and contrast on visual persistence. *Perception*, 8(5), 529-539.
6. Brainard, D. H., & Vision, S. (1997). The psychophysics toolbox. *Spatial vision*, 10(4), 433-436.
7. Burr, D. (1980). Motion smear. *Nature*, 284(5752), 164-165.
8. Burr, D. C., Morrone, M. C., & Ross, J. (1994). Selective suppression of the magnocellular visual pathway during saccadic eye movements. *Nature*, 371(6497), 511-513.
9. Burr, D. C., & Morrone, C. (1996). Temporal impulse response functions for luminance and colour during saccades. *Vision research*, 36(14), 2069-2078.
10. Burt, P., & Sperling, G. (1981). Time, distance, and feature trade-offs in visual apparent motion. *Psychological review*, 88(2), 171.
11. Cai, D., Deangelis, G. C., & Freeman, R. D. (1997). Spatiotemporal receptive field organization in the lateral geniculate nucleus of cats and kittens. *Journal of neurophysiology*, 78(2), 1045-1061.
12. Castet, E., Lorenceau, J., & Bonnet, C. (1993). The inverse intensity effect is not lost with stimuli in apparent motion. *Vision Research*, 33(12), 1697-1708.
13. Castet, E. (1994). Effect of the ISI on the visible persistence of a stimulus in apparent motion. *Vision Research*, 34(16), 2103-2114.
14. Clark, A. M., Intoy, J., Rucci, M., & Poletti, M. (2022). Eye drift during fixation predicts visual acuity. *Proceedings of the National Academy of Sciences*, 119(49), e2200256119.
15. Christman, S., Kitterle, F. L., & Hellige, J. (1991). Hemispheric asymmetry in the processing of

- absolute versus relative spatial frequency. *Brain and Cognition*, 16(1), 62-73.
16. Coltheart, M. (1980). Iconic memory and visible persistence. *Perception & psychophysics*, 27, 183-228.
  17. Davis, J., Hsieh, Y. H., & Lee, H. C. (2015). Humans perceive flicker artifacts at 500 Hz. *Scientific reports*, 5(1), 7861.
  18. DeAngelis, G. C., Ohzawa, I., & Freeman, R. D. (1993). Spatiotemporal organization of simple-cell receptive fields in the cat's striate cortex. I. General characteristics and postnatal development. *Journal of neurophysiology*, 69(4), 1091-1117.
  19. DeAngelis, G. C., Ohzawa, I., & Freeman, R. D. (1993). Spatiotemporal organization of simple-cell receptive fields in the cat's striate cortex. II. Linearity of temporal and spatial summation. *Journal of Neurophysiology*, 69(4), 1118-1135.
  20. Denes, G., Jindal, A., Mikhailiuk, A., & Mantiuk, R. K. (2020). A perceptual model of motion quality for rendering with adaptive refresh-rate and resolution. *ACM Transactions on Graphics (TOG)*, 39(4), 133-1.
  21. Deubel, H., & Schneider, W. X. (1996). Saccade target selection and object recognition: Evidence for a common attentional mechanism. *Vision research*, 36(12), 1827-1837.
  22. De Lange, O. E. (1952). Propagation studies at microwave frequencies by means of very short pulses. *The Bell System Technical Journal*, 31(1), 91-103.
  23. De Lange Dzn, H. (1958). Research into the dynamic nature of the human fovea→ cortex systems with intermittent and modulated light. I. Attenuation characteristics with white and colored light. *Josa*, 48(11), 777-784.
  24. De Schonen, S., De Diaz, M. G., & Mathivet, E. (1986). Hemispheric asymmetry in face processing in infancy. *Aspects of face processing*, 199-209.
  25. Di Lollo, V., & Woods, E. (1981). Duration of visible persistence in relation to range of spatial frequencies. *Journal of Experimental Psychology: Human Perception and Performance*, 7(4), 754.
  26. Duhamel, J. R., Colby, C. L., & Goldberg, M. E. (1992). The updating of the representation of visual space in parietal cortex by intended eye movements. *Science*, 255(5040), 90-92.
  27. Emoto, M., & Sugawara, M. (2012). Critical fusion frequency for bright and wide field-of-view image display. *Journal of Display Technology*, 8(7), 424-429.
  28. Eisen-Enosh, A., Farah, N., Burgansky-Eliash, Z., Polat, U., & Mandel, Y. (2017). Evaluation of critical flicker-fusion frequency measurement methods for the investigation of visual temporal



- resolution. *Scientific reports*, 7(1), 15621.
29. Farrell, J. E., Pavel, M., & Sperling, G. (1990). The visible persistence of stimuli in stroboscopic motion. *Vision Research*, 30(6), 921-936.
  30. Francis, G., & Grossberg, S. (1996). Cortical dynamics of boundary segmentation and reset: Persistence, afterimages, and residual traces. *Perception*, 25(5), 543-567.
  31. Francis, G. (1999). Spatial frequency and visual persistence: Cortical reset. *Spatial Vision*, 12(1), 31-50.
  32. Freeman, J., & Simoncelli, E. P. (2011). Metamers of the ventral stream. *Nature neuroscience*, 14(9), 1195-1201.
  33. Gazzaniga, M. S. (1985). *Social brain*. Basic Books.
  34. Geisler, W. S., & Albrecht, D. G. (1995). Bayesian analysis of identification performance in monkey visual cortex: nonlinear mechanisms and stimulus certainty. *Vision research*, 35(19), 2723-2730.
  35. Golomb, J. D., & Mazer, J. A. (2021). Visual remapping. *Annual review of vision science*, 7, 257-277.
  36. Golomb, J. D. (2019). Remapping locations and features across saccades: a dual-spotlight theory of attentional updating. *Current opinion in psychology*, 29, 211-218.
  37. Hecht, S., & Smith, E. L. (1936). Intermittent stimulation by light: VI. Area and the relation between critical frequency and intensity. *The Journal of general physiology*, 19(6), 979-989.
  38. Hellige, J. B., & Wong, T. M. (1983). Hemisphere-specific interference in dichotic listening: task variables and individual differences. *Journal of Experimental Psychology: General*, 112(2), 218.
  39. Hershberger, W. A., & Jordan, J. S. (1996). The phantom array. *Behavioral and Brain Sciences*, 19(3), 552-553.
  40. Hershberger, W. A., & Jordan, J. S. (1998). The phantom array: a perisaccadic illusion of visual direction. *The Psychological Record*, 48, 21-32.
  41. Hoffman, D. M., Karasev, V. I., & Banks, M. S. (2011). Temporal presentation protocols in stereoscopic displays: Flicker visibility, perceived motion, and perceived depth. *Journal of the Society for Information Display*, 19(3), 271-297.
  42. Hoffman, D. M., Johnson, P. V., Kim, J. S., Vargas, A. D., & Banks, M. S. (2014). 240 Hz OLED technology properties that can enable improved image quality. *Journal of the Society for Information Display*, 22(7), 346-356.

43. Hoffman, J. E., & Subramaniam, B. (1995). The role of visual attention in saccadic eye movements. *Perception & psychophysics*, 57(6), 787-795.
44. Holtgraves, T., & Felton, A. (2011). Hemispheric asymmetry in the processing of negative and positive words: A divided field study. *Cognition and Emotion*, 25(4), 691-699.
45. Ikeda, M. (1986). Temporal impulse response. *Vision Research*.
46. Intoy, J., & Rucci, M. (2020). Finely tuned eye movements enhance visual acuity. *Nature communications*, 11(1), 795.
47. Keesey, U. T. (1972). Flicker and pattern detection: a comparison of thresholds. *JOSA*, 62(3), 446-448.
48. Kelly, D. H. (1959). Effects of sharp edges in a flickering field. *JOSA*, 49(7), 730-732.
49. Kelly, D. H. (1961). Visual responses to time-dependent stimuli.\* i. amplitude sensitivity measurements. *JOSA*, 51(4), 422-429.
50. Kelly, D. H. (1971). Theory of flicker and transient responses, I. Uniform fields. *JOSA*, 61(4), 537-546.
51. Kim, H., & Francis, G. (1998). A computational and perceptual account of motion lines. *Perception*, 27(7), 785-797.
52. Krekelberg, B., Dannenberg, S., Hoffmann, K. P., Bremmer, F., & Ross, J. (2003). Neural correlates of implied motion. *Nature*, 424(6949), 674-677.
53. Krekelberg, B. (2010). Saccadic suppression. *Current Biology*, 20(5), R228-R229.
54. Kuang, X., Poletti, M., Victor, J. D., & Rucci, M. (2012). Temporal encoding of spatial information during active visual fixation. *Current Biology*, 22(6), 510-514.
55. Kuo, S. P., Schwartz, G. W., & Rieke, F. (2016). Nonlinear spatiotemporal integration by electrical and chemical synapses in the retina. *Neuron*, 90(2), 320-332.
56. Kuroki, Y., Nishi, T., Kobayashi, S., Oyaizu, H., & Yoshimura, S. (2007). A psychophysical study of improvements in motion-image quality by using high frame rates. *Journal of the Society for Information Display*, 15(1), 61-68.
57. Kwak, Y., & Curtis, C. E. (2022). Unveiling the abstract format of mnemonic representations. *Neuron*.
58. Lake, A., Marshall, C., Harris, M., & Blackstein, M. (2000, June). Stylized rendering techniques for scalable real-time 3d animation. In *Proceedings of the 1st international symposium on Non-*

*photorealistic animation and rendering* (pp. 13-20).

59. Lasseter, J. (1987, August). Principles of traditional animation applied to 3D computer animation. In *Proceedings of the 14th annual conference on Computer graphics and interactive techniques* (pp. 35-44).
60. Li, H. H., Barbot, A., & Carrasco, M. (2016). Saccade preparation reshapes sensory tuning. *Current Biology*, 26(12), 1564-1570.
61. Linsenmeier, R. A., Frishman, L. J., Jakiela, H. G., & Enroth-Cugell, C. (1982). Receptive field properties of X and Y cells in the cat retina derived from contrast sensitivity measurements. *Vision research*, 22(9), 1173-1183.
62. Mackin, A., Noland, K. C., & Bull, D. R. (2017). High frame rates and the visibility of motion artifacts. *SMPTE Motion Imaging Journal*, 126(5), 41-51.
63. Mankowska, N. D., Marcinkowska, A. B., Waskow, M., Sharma, R. I., Kot, J., & Winklewski, P. J. (2021). Critical flicker fusion frequency: a narrative review. *Medicina*, 57(10), 1096.
64. Marino, A. C., & Mazer, J. A. (2016). Perisaccadic updating of visual representations and attentional states: linking behavior and neurophysiology. *Frontiers in Systems Neuroscience*, 10, 3.
65. Matin, E. (1974). Saccadic suppression: a review and an analysis. *Psychological bulletin*, 81(12), 899.
66. Masuch, M., Schlechtweg, S., & Schulz, R. (1999). R.: Speedlines: Depicting motion in motionless pictures. In *In: Proceedings of SIGGRAPH 1999. Computer Graphics Proceedings, Annual Conference Series, ACM, ACM Press/ACM SIGGRAPH*.
67. Mayfrank, L., Kimmig, H., & Fischer, B. (1987). The role of attention in the preparation of visually guided saccadic eye movements in man. In *Eye movements from physiology to cognition* (pp. 37-45). Elsevier.
68. Moon, J., Tadin, D., & Kwon, O. S. (2022). A key role of orientation in the coding of visual motion direction. *Psychonomic Bulletin & Review*, 1-11.
69. Mostofi, N., Zhao, Z., Intoy, J., Boi, M., Victor, J. D., & Rucci, M. (2020). Spatiotemporal content of saccade transients. *Current Biology*, 30(20), 3999-4008.
70. West, D. C. (1968). Effect of retinal image motion on critical flicker-fusion measurement. *Optica Acta: International Journal of Optics*, 15(4), 317-328.
71. Schütz, A. C., Braun, D. I., & Gegenfurtner, K. R. (2009). Improved visual sensitivity during smooth pursuit eye movements: Temporal and spatial characteristics. *Visual neuroscience*, 26(3),

329-340.

72. Patel, A. S. (1966). Spatial resolution by the human visual system. The effect of mean retinal illuminance. *JOSA*, 56(5), 689-694.
73. Pelli, D. G., & Vision, S. (1997). The VideoToolbox software for visual psychophysics: Transforming numbers into movies. *Spatial vision*, 10, 437-442.
74. Peyrin, C., Mermillod, M., Chokron, S., & Marendaz, C. (2006). Effect of temporal constraints on hemispheric asymmetries during spatial frequency processing. *Brain and Cognition*, 62(3), 214-220.
75. Poletti, M., Listorti, C., & Rucci, M. (2010). Stability of the visual world during eye drift. *Journal of Neuroscience*, 30(33), 11143-11150.
76. Rashbass, C. (1970). The visibility of transient changes of luminance. *The Journal of Physiology*, 210(1), 165.
77. Rebai, M., Mecacci, L., Bagot, J. D., & Bonnet, C. (1986). Hemispheric asymmetries in the visual evoked potentials to temporal frequency: preliminary evidence. *Perception*, 15(5), 589-594.
78. Roberts, J. E., & Wilkins, A. J. (2013). Flicker can be perceived during saccades at frequencies in excess of 1 kHz. *Lighting Research & Technology*, 45(1), 124-132.
79. Rovamo, J., & Raninen, A. (1984). Critical flicker frequency and M-scaling of stimulus size and retinal illuminance. *Vision Research*, 24(10), 1127-1131.
80. Rust, N. C., Schwartz, O., Movshon, J. A., & Simoncelli, E. P. (2005). Spatiotemporal elements of macaque v1 receptive fields. *Neuron*, 46(6), 945-956.
81. Seitz, A. R., Nanez, J. E., Holloway, S. R., & Watanabe, T. (2005). Visual experience can substantially alter critical flicker fusion thresholds. *Human Psychopharmacology: Clinical and Experimental*, 20(1), 55-60.
82. Sperling, G. (1976). Movement perception in computer-driven visual displays. *Behavior Research Methods & Instrumentation*, 8, 144-151.
83. Sperling, G., Van Santen, J. P., & Burt, P. J. (1985). Three theories of stroboscopic motion detection. *Spatial vision*, 1(1), 47-56.
84. Steinman, R. M., & Levinson, J. Z. (1990). The role of eye movement in the detection of contrast and spatial detail. *Eye movements and their role in visual and cognitive processes*, 4, 115-212.
85. Stromeyer III, C. F., & Martini, P. (2003). Human temporal impulse response speeds up with

- increased stimulus contrast. *Vision Research*, 43(3), 285-298.
86. Swanson, W. H., Ueno, T., Smith, V. C., & Pokorny, J. (1987). Temporal modulation sensitivity and pulse-detection thresholds for chromatic and luminance perturbations. *JOSA A*, 4(10), 1992-2005.
  87. Sweet, A. L. (1953). Temporal discrimination by the human eye. *The American journal of psychology*, 66(2), 185-198.
  88. Tadin, D., Lappin, J. S., Blake, R., & Glasser, D. M. (2010). High temporal precision for perceiving event offsets. *Vision research*, 50(19), 1966-1971.
  89. Tang, M. F., Dickinson, J. E., Visser, T. A., & Badcock, D. R. (2015). The broad orientation dependence of the motion streak aftereffect reveals interactions between form and motion neurons. *Journal of vision*, 15(13), 4-4.
  90. Terao, M., Watanabe, J., Yagi, A., & Nishida, S. Y. (2010). Smooth pursuit eye movements improve temporal resolution for color perception. *PLoS One*, 5(6), e11214.
  91. Thiele, A., Henning, P., Kubischik, M., & Hoffmann, K. P. (2002). Neural mechanisms of saccadic suppression. *Science*, 295(5564), 2460-2462.
  92. Tolhurst, D. J., Walker, N. S., Thompson, I. D., & Dean, A. F. (1980). Non-linearities of temporal summation in neurones in area 17 of the cat. *Experimental Brain Research*, 38, 431-435.
  93. Tong, J., Ramamurthy, M., Patel, S. S., Vu-Yu, L. P., & Bedell, H. E. (2009). The temporal impulse response function during smooth pursuit. *Vision Research*, 49(23), 2835-2842.
  94. Wandell, B. A. (1995). *Foundations of vision*. sinauer Associates.
  95. Wang, L., Tu, Y., Liu, L., Wang, J., Perz, M., & Teunissen, K. (2017, May). P-141: Phantom Array Effect of LED Lighting. In *SID Symposium Digest of Technical Papers* (Vol. 48, No. 1, pp. 1804-1807).
  96. Watson, A. B., & Nachmias, J. (1977). Patterns of temporal interaction in the detection of gratings. *Vision research*, 17(8), 893-902.
  97. Watson, A. B., Ahumada, A. J., & Farrell, J. E. (1986). Window of visibility: a psychophysical theory of fidelity in time-sampled visual motion displays. *JOSA A*, 3(3), 300-307.
  98. Watson, A. B. (2013). High frame rates and human vision: A view through the window of visibility. *SMPTE Motion Imaging Journal*, 122(2), 18-32.
  99. Waugh, S. J., & Bedell, H. E. (1992). Sensitivity to temporal luminance modulation in congenital nystagmus. *Investigative ophthalmology & visual science*, 33(7), 2316-2324.

100. Westheimer, G. (1975). Visual acuity and hyperacuity. *Investigative Ophthalmology*, 14(8), 570-572.
101. Westheimer, G. (1981). Visual hyperacuity. *Progress in sensory physiology*, 1-30.
102. Westheimer, G., & McKee, S. P. (1977). Perception of temporal order in adjacent visual stimuli. *Vision Research*, 17(8), 887-892.
103. Wilcox, L. M., Allison, R. S., Helliker, J., Dunk, B., & Anthony, R. C. (2015). Evidence that viewers prefer higher frame-rate film. *ACM Transactions on Applied Perception (TAP)*, 12(4), 1-12.
104. Wimbauer, S., Wenisch, O. G., Miller, K. D., & van Hemmen, J. L. (1997). Development of spatiotemporal receptive fields of simple cells: I. Model formulation. *Biological cybernetics*, 77(6), 453-461.
105. Winawer, J., & Horiguchi, H. (2015). Population receptive field size estimates in 3 human retinotopic maps.
106. Zanker, J. M., & Harris, J. P. (2002). On temporal hyperacuity in the human visual system. *Vision Research*, 42(22), 2499-2508.
107. Zimmermann, E., Morrone, M. C., & Burr, D. C. (2014). Buildup of spatial information over time and across eye-movements. *Behavioural brain research*, 275, 281-287.

## Appendix

### Supplementary Figure – Part1

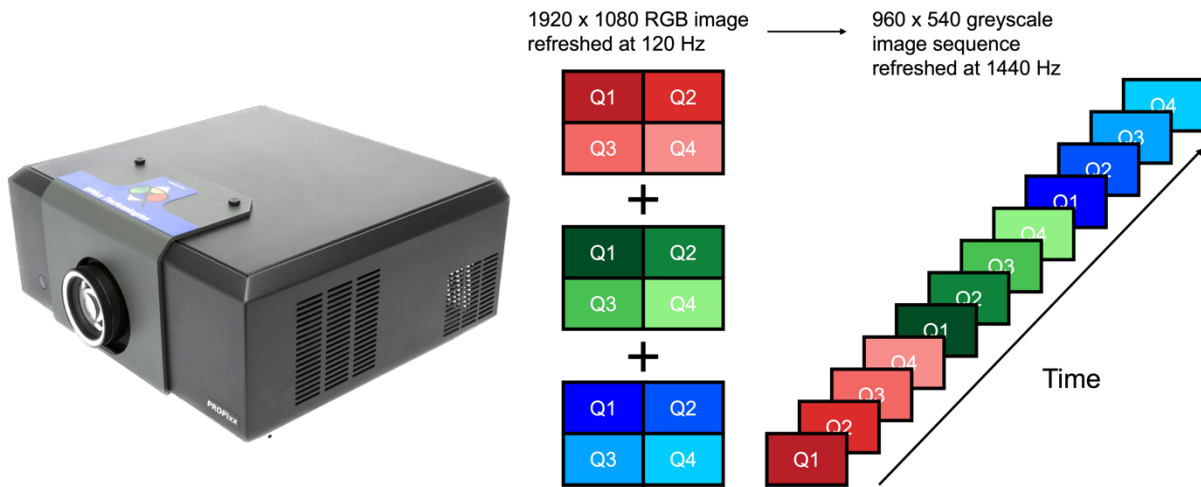


**Figure S1. The PROPixx projector (left) and usage (right) for achieving a refresh rate of 1440 Hz.** The left panel shows the PROPixx projector manufactured by VPixx, while the right panel depicts the method used to generate a visual stimulus flickering at 1440 Hz. The PROPixx projector utilizes a "sequencer" to divide a single 1920 x 1080, 120 Hz RGB video signal into 12 frames displayed sequentially. Initially, the 1920 x 1080 image is divided into four quadrants (960 x 540 images), and each quadrant is magnified to fill the entire screen. Subsequently, each 8-bit RGB color channel is converted to grayscale and displayed separately. The order of appearance is as follows: Quadrant 1 (red), Quadrant 2 (red), Quadrant 3 (red), Quadrant 4 (red), and then this order is repeated for the green and blue channels.

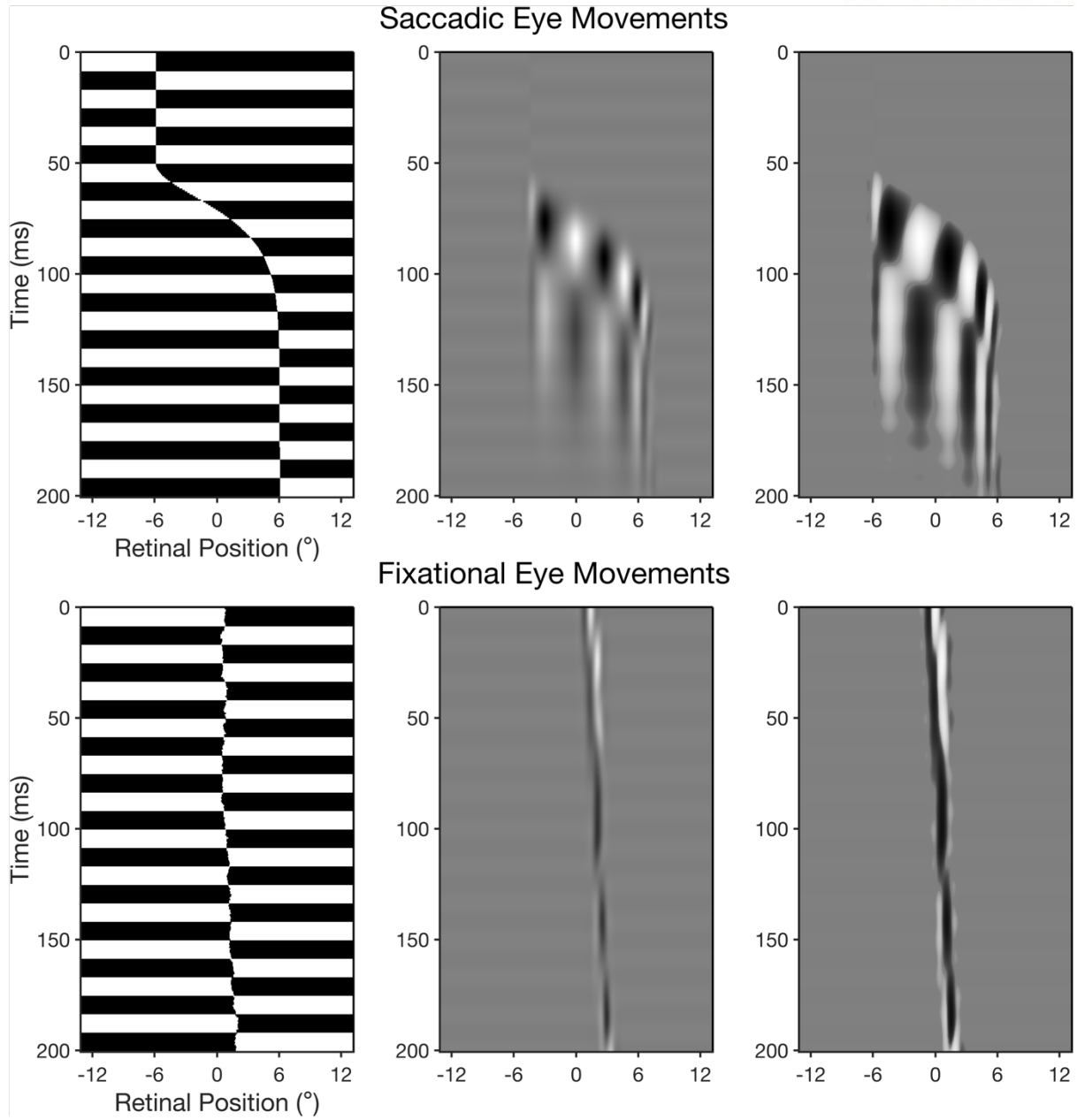


**Figure S2. Model prediction of the retinal responses to FCE stimuli presented at 60 Hz.**



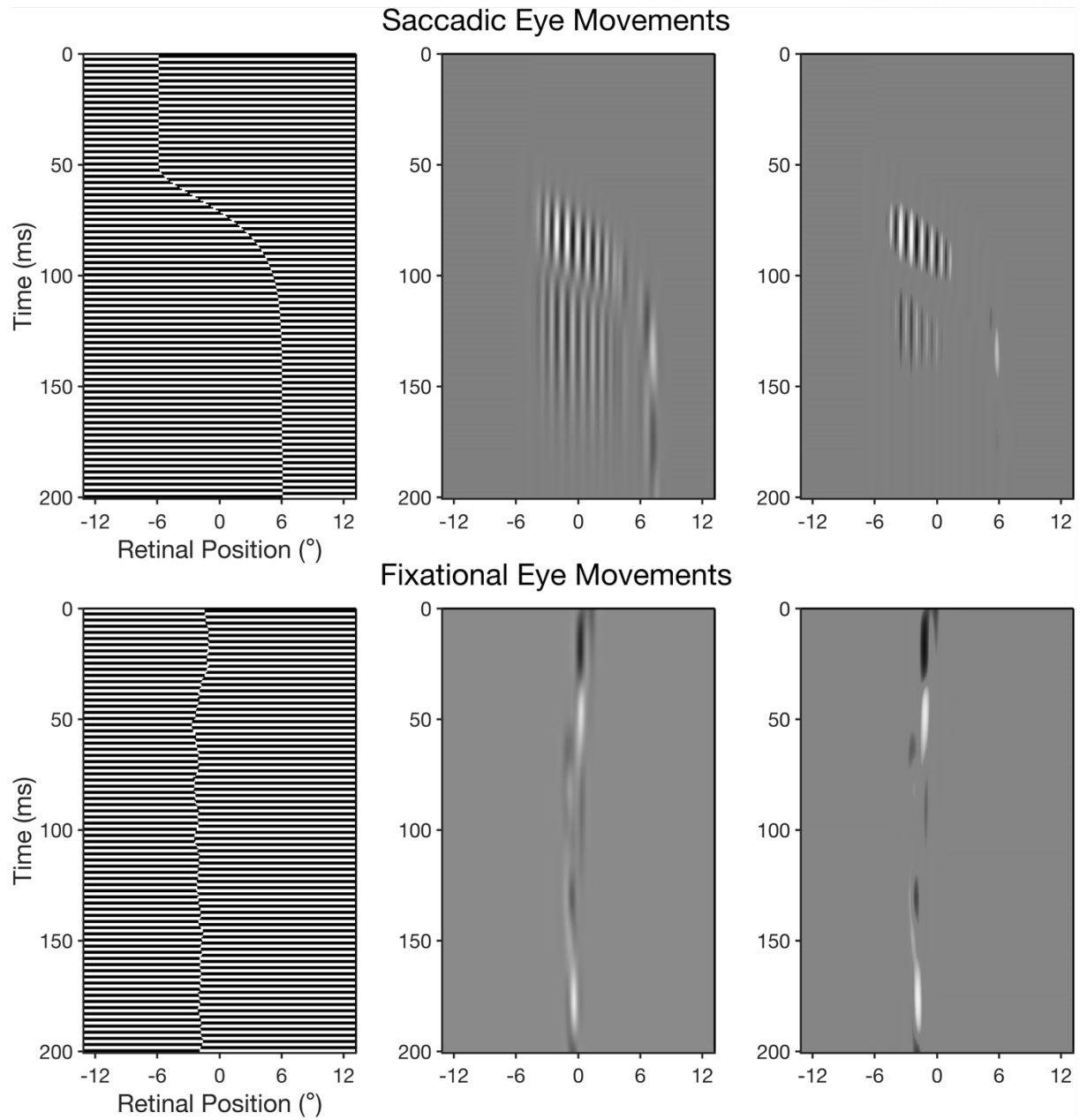


**Figure S3. Model prediction of the retinal responses to FCE stimuli presented at 360 Hz.**

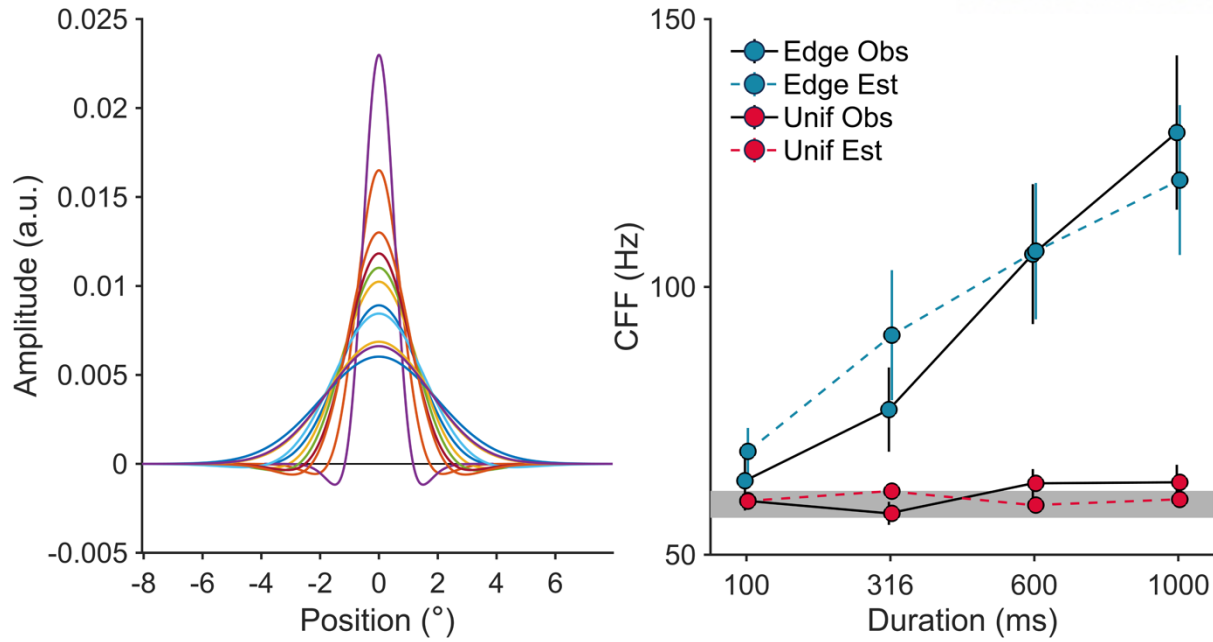


**Figure S4. Estimated CFFs for uniform and FCE stimuli as a function of the stimulus duration.** The left panel demonstrates the fitted spatial filters from different participants ( $N = 11$ ). The right panel shows the CFFs for the two stimuli estimated from behavioral responses collected from psychophysical experiments (solid line) and model prediction on participants' correct responses (dashed line).

#### **Additional Experiment on the effect of the stimulus duration on CFFs for two stimuli.**

We conducted an additional experiment to examine the effect of the stimulus duration on the CFF for uniform and FCE stimuli. In this experiment, the refresh rate of the stimulus was adaptively manipulated according to 2 up 1 down staircase method. The intention was to present the stimulus around the threshold level which is more informative because the retinal responses for the visual stimuli presented at very low and very high refresh rate were not affected by the eye movements. Each stimulus duration was tested in a separate block, within which two staircase chains were performed for 40 trials (total 80 trials, ~10 min). The one is ascending from the lowest refresh rate whereas the other is descending from the highest refresh rate. **Figure S5** and **Figure S6** show the convergence of two parallel staircases in Uniform stimuli and vertical stimuli, respectively. We estimated CFFs from both the ascending and descending chains and then took the average of them. Two stimulus types (uniform and FCE stimuli) and three stimulus duration (100, 316, and 1000 ms) made 6 blocks. Again, we found the consistent pattern that at 100ms there is no significant difference between CFFs for the uniform and FCE stimuli (**Figure S7**).

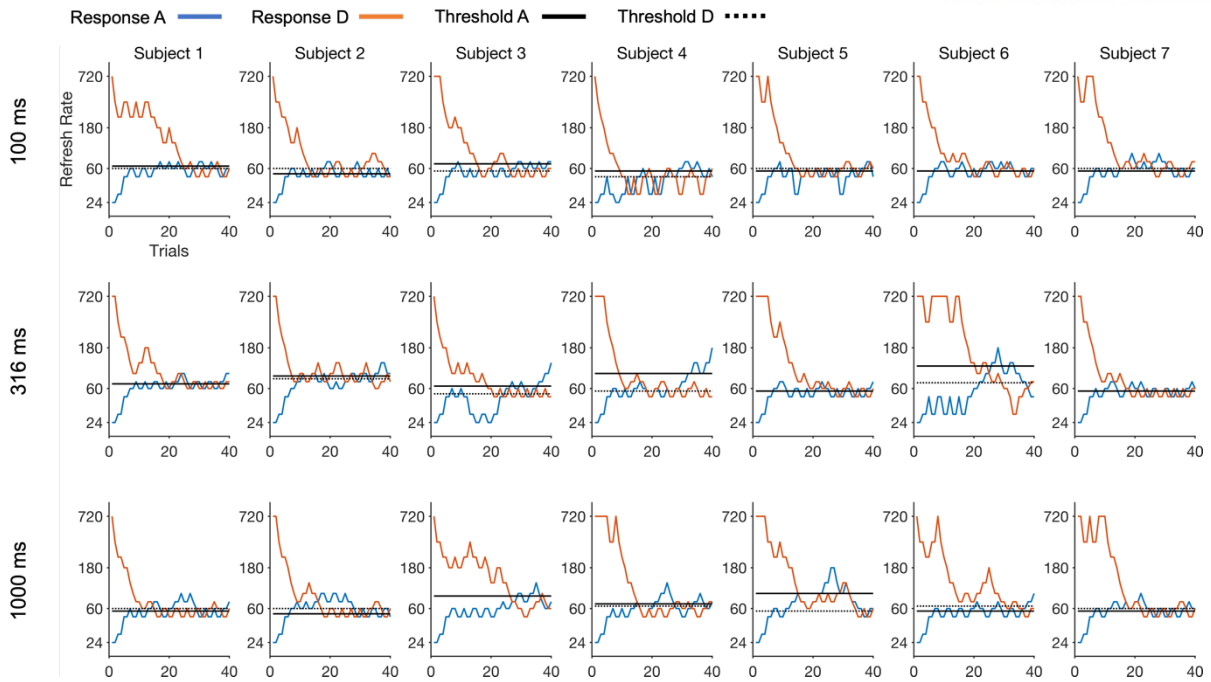


**Figure S5. The convergence of refresh rates for uniform stimuli using the 2up 1down staircase method.** Each row corresponds to a different stimulus duration, while each column represents a different participant. The blue and orange colors indicate the ascending and descending chains, respectively. CFFs were estimated separately from the ascending chain (solid line) and descending chain (dashed line) based on the last three reversals of refresh rates.

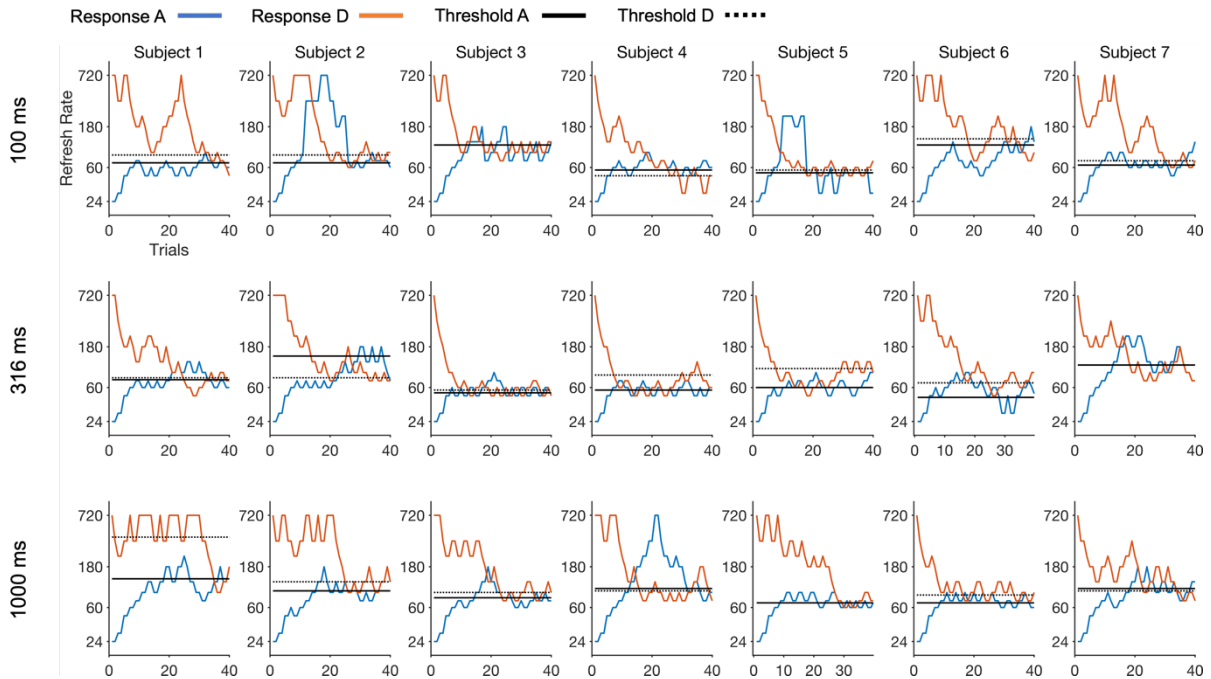


**Figure S6. The convergence of refresh rates for FCE stimuli using the 2up 1down staircase method.**

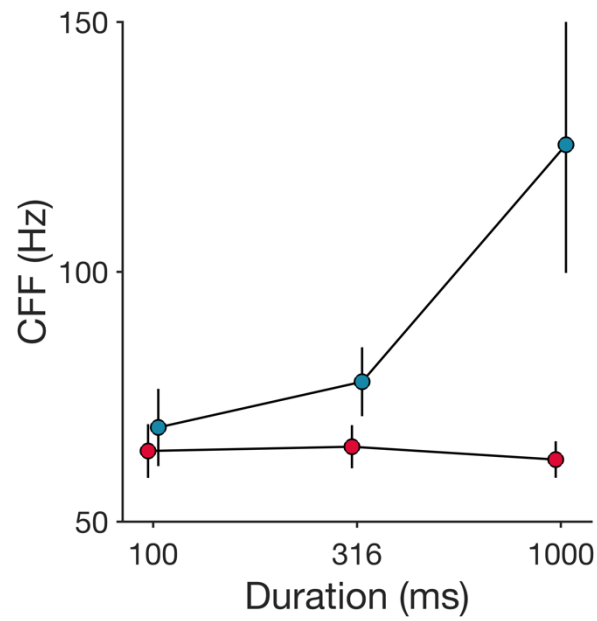


**Figure S7. The effect of the stimulus duration on CFFs for the uniform (red) and vertical edge stimuli (blue) measured using the adaptive method instead.**

Supplementary Figure – Part2

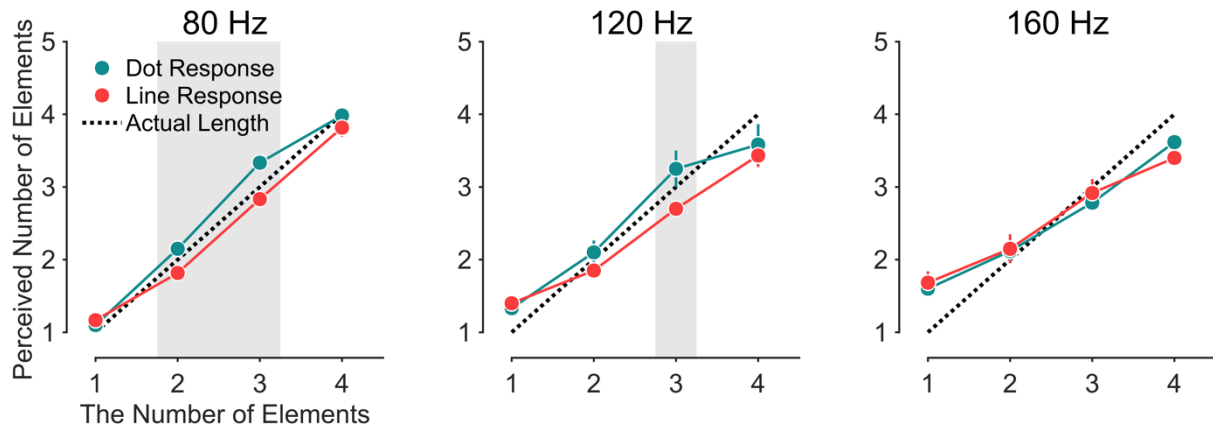


**Figure S8. The perceived number of moving line stimuli (red) and dot stimuli (green) as a function of the number of elements.** Each panel shows the reported number of elements from the different refresh rate conditions. A grey unity line represents the actual number of elements. The physical length of line stimuli and dot stimuli having the same number of elements was set to be the same. The shaded area with gray color represents the refresh rate condition where the perceived number of line stimuli was shorter than that of dot stimuli.

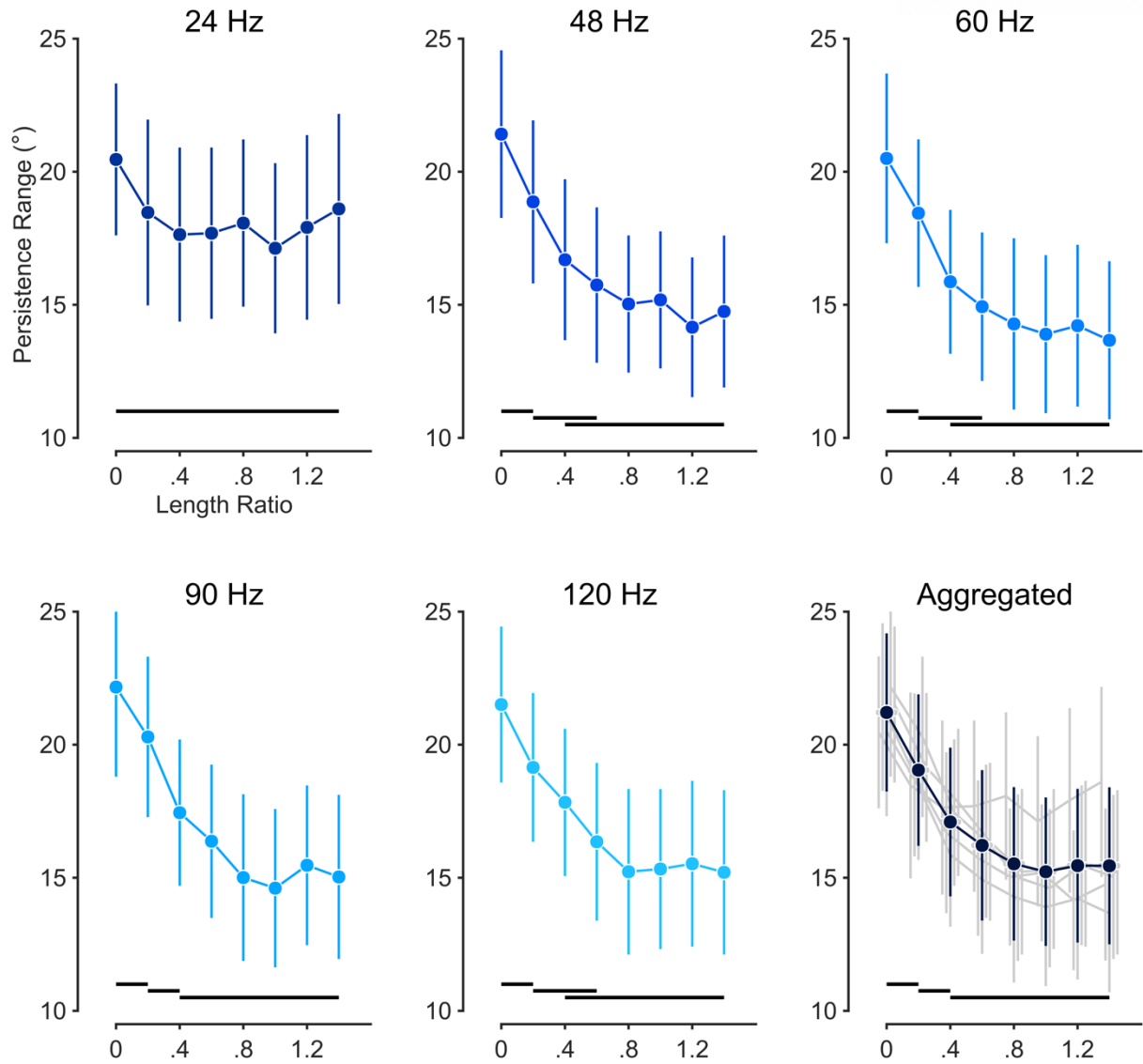


**Figure S9. The range of concurrently perceived persisting images for the different length of line stimuli.** The effect was measured using the intermixed design where different refresh rates were randomly presented within the same block.

## **Additional Experiment on the effect of the stimulus intensity (dot, line, and square)**

### **Participants**

Eleven newly recruited students (2 female, mean age  $25.3 \pm 2.1$ ) participated in the experiment. No participant was excluded. All participants reported normal or corrected-to-normal vision and no history of neurological disorders. All were naïve to the purpose of this study. The study was approved by the Ulsan National Institute of Science and Technology Institutional Review Board. All participants signed a written consent form before the experiment.

### **Apparatus and Stimuli**

The white lines (luminance:  $189.59 \text{ cd/m}^2$ ) moved horizontally at a constant speed ( $120^\circ/\text{s}$ ) and were presented at varied refresh rates (24, 48, 60, 90, 120 Hz). The fast speed and low refresh rates were chosen as the apparent difference between dots and lines was observed in Experiment 1. We produced line stimuli by connecting the positions of two consecutively presented dots. Here, we manipulated the length of line stimuli in 8 steps relative to the distance between two consecutively presented dots (length ratio: 0, 0.2, 0.4, 0.6, 0.8, 1.0, 1.2, 1.4). In the shortest condition (zero-ratio), the line stimulus is as long as the dot diameter. If the ratio is one, the line stimulus is as long as the distance between two dots. The ratio larger than one means that the length of the line stimulus is longer than the distance between two dots and two consecutively presented lines partly overlap although they are never presented at the same time. Depending on refresh rates, the length of the line stimulus varied accordingly (24 Hz: from  $0.2^\circ$  to  $1.42^\circ$ , 48 Hz: from  $0.2^\circ$  to  $1.83^\circ$ , 60 Hz: from  $0.2^\circ$  to  $2.83^\circ$ , 90 Hz: from  $0.2^\circ$  to  $3.50^\circ$ , 120 Hz: from  $0.2^\circ$  to  $7.00^\circ$ , width:  $0.2^\circ$ ).

### **Procedure**

The experimental procedure is as same as that of Experiment 1 with one small modification as described below. Each refresh rate condition was conducted separately in different blocks (5 blocks, 80 trials each, 8 length ratio x 10 repetition, randomized order). The order of blocks was counterbalanced across participants. All blocks were completed within a single day and lasted at most 30 min.

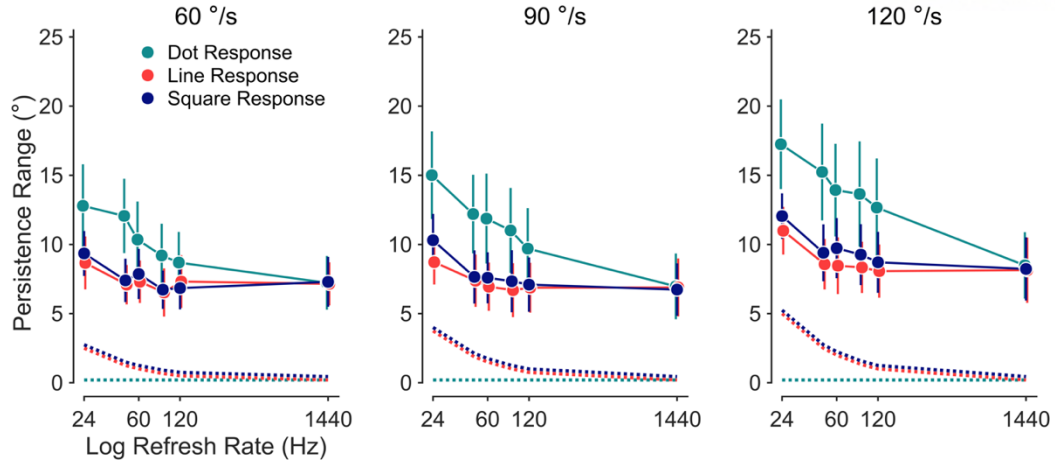


**Figure S10.** The range of concurrently perceived persisting images of a single moving square (navy), line (red), and dot (green). Each panel represents the persistence range against refresh rate collected from different speed conditions. Dashed lines indicate the actual length of two stimuli, and the error bars indicate the standard error of means.

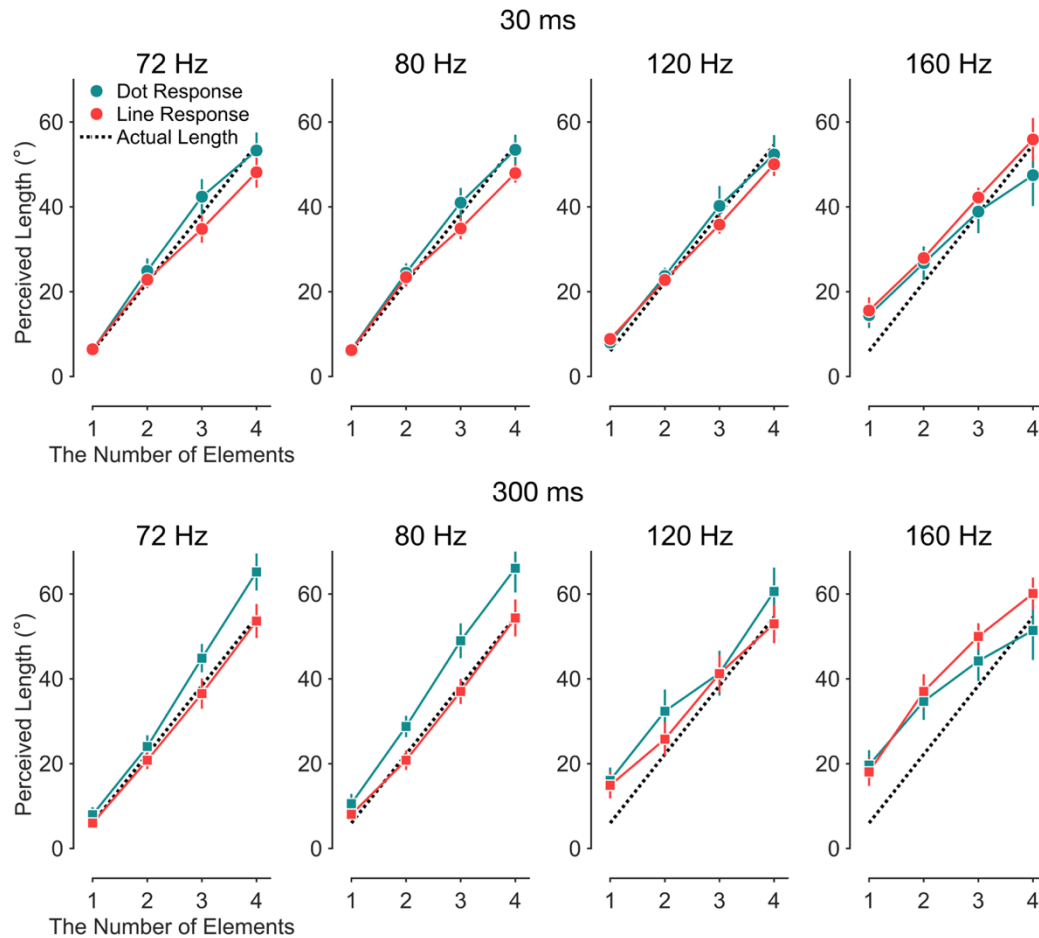


**Figure S11.** The perceived length of moving objects with the different stimulus durations. Each panel represents the perceived length of moving stimuli against the number of elements.





**Figure S12. Jwibulnori stimuli.** In Experiment 5, the participants were then asked to report moving stimuli that they perceived as more realistic and similar to the Jwibulnori stimuli.

## ANOVA Table – Part1

Table S1. Results of ANOVA in Experiment 1. The effect of the stimulus type on CFFs in the fixation condition.

Variable	F	$df_1$	$df_2$	MSE	P	$\eta_p^2$
Stimulus type	23.93	2	34	7664	$3.26e^{-07}$	0.58

Table S2. Multiple comparison results of Tukey's test

Stimulus type	Means (Hz)	G1	G2
Uniform	58.65	a	
Vertical FCE	93.40		b
Horizontal FCE	95.30		b

Table S3. Results of ANOVA in Experiment 2. The effect of the stimulus type on CFFs in the saccade condition.

Variable	F	$df_1$	$df_2$	MSE	P	$\eta_p^2$
Stimulus type	87.12	2	34	432048	$4.16e^{-14}$	0.84

Table S4. Multiple comparison results of Tukey's test

Stimulus type	Means (Hz)	G1	G2
Uniform	61.50	a	
Vertical FCE	351.43		b
Horizontal FCE	111.80	a	

Table S5. Results of ANOVA for data obtained from Experiment 1 and Experiment 2. The effect of the stimulus type and eye movements on CFFs.

Variable	F	$df_1$	$df_2$	MSE	P	$\eta_p^2$
Stimulus type	89.55	2	34	1016973	$2.81e^{-14}$	0.840
Eye movements	77.75	1	17	923276	$9.47e^{-08}$	0.736
Stimulus type x Eye movements	76.2	2	34	741876	$2.84e^{-13}$	0.816

Table S6. Results of ANOVA for Experiment 3. The effect of the stimulus type and stimulus duration on CFFs.

Variable	F	$df_1$	$df_2$	MSE	P	$\eta_p^2$
Stimulus type	11.22	1	10	35783	$7.38e^{-03}$	0.529
Stimulus duration	7.59	3	30	11327	$6.40e^{-04}$	0.432
Stimulus type x Stimulus duration	6.00	3	30	9346	0.0025	0.375

Table S7. Multiple comparison results of Tukey's test on all data collected from both the uniform and vertical FCE stimuli.

Stimulus duration	Means (Hz)	G1	G2
100 ms	61.05	a	
316 ms	67.69	a	b
600 ms	83.73		b
1000 ms	112.02		b

Table S8. Multiple comparison results of Tukey's test on all data collected from vertical FCE stimuli.

Stimulus duration	Means (Hz)	G1	G2
100 ms	62.59	a	
316 ms	77.59	a	b
600 ms	104.12		b
1000 ms	160.85		b

Table S9. Multiple comparison results of Tukey's test on all data collected from uniform stimuli.

Stimulus duration	Means (Hz)	G1	G2
100 ms	59.51	a	
316 ms	57.80	a	
600 ms	63.33	a	
1000 ms	63.18	a	

Table S10. Results of ANOVA for Experiment 5. The effect of the stimulus type and eccentricity on CFFs.

Variable	F	$df_1$	$df_2$	MSE	P	$\eta_p^2$
Stimulus type	80.99	1	17	8235	$7.09e^{-08}$	0.729
Eccentricity	11.24	1	17	1321.9	$3.77e^{-03}$	0.303
Stimulus type x Eccentricity	17.89	1	17	3213	$5.65e^{-04}$	0.513

## ANOVA Table – Part2

Table S11. Results of ANOVA in Experiment 1. The effect of the stimulus type (dot and line, 2 levels), refresh rate (24, 48, 60, 90, 120, 240, 360, and 1440 Hz, 8 levels), and speed on the range of concurrently perceived persisting images.

Variable	F	$df_1$	$df_2$	MSE	P	$\eta_p^2$
Stimulus type	20.80	1	8	391.0	0.00185	0.763
Speed	17.89	1	17	3213	$5.65e^{-04}$	0.513
Stimulus type x Refresh rate	11.30	6	48	27.905	$7.80e^{-07}$	0.579
Stimulus type x Speed	9.57	2	16	66.98	0.00185	0.524
Stimulus type x Refresh rate x Speed	2.605	12	96	3.299	0.00479	0.246

Table S12. Results of ANOVA in Experiment 1. The effect of the stimulus type (dot and line, 2 levels) and refresh rate (24, 48, 60, 90, 120, 240, 360, and 1440 Hz, 8 levels) on the persistence range when speed is 60 °/s.

Variable	F	$df_1$	$df_2$	MSE	P	$\eta_p^2$
Stimulus type	4.52	1	8	21.143	0.0662	0.361
Stimulus type x Refresh rate	3.459	6	48	3.941	0.00639	0.302

Table S13. Results of ANOVA in Experiment 1. The effect of the stimulus type and refresh rate on the persistence range when speed is 90 °/s.

Variable	F	$df_1$	$df_2$	MSE	P	$\eta_p^2$
Stimulus type	12.31	1	8	83.87	0.00798	0.606
Stimulus type x Refresh rate	5.826	6	48	10.167	$1.28e^{-04}$	0.421

Table S14. Results of ANOVA in Experiment 1. The effect of the stimulus type and refresh rate on the persistence range when speed is 120 °/s.

Variable	F	$df_1$	$df_2$	MSE	P	$\eta_p^2$
Stimulus type	19.71	1	8	419.9	0.00217	0.606
Stimulus type x Refresh rate	9.632	6	48	10.167	$6.00e^{-07}$	0.546

Table S15. Results of ANOVA in Experiment 2. The effect of the stimulus type (dot, horizontal line, and vertical line, 3 levels) and refresh rate (24, 48, 60, 90, 120, and 1440 Hz, 6 levels) on the persistence range.

Variable	F	$df_1$	$df_2$	MSE	P	$\eta_p^2$
Stimulus type	9.511	2	22	208908	0.00106	0.46
Refresh rate	4.653	6	66	59821	$5.31e^{-04}$	0.30
Stimulus type x Refresh rate	2.275	12	132	10.167	0.0117	0.17

Table S16. Multiple comparison results of Tukey's test on the effect of the stimulus type.

Stimulus type	Means (°)	G1	G2
Vertical Speedline	6.8552	a	
Horizontal Speedline	10.2597		b
Dot	11.4848		b

Table S17. Results of ANOVA in Experiment 3. The effect of the length ratio (0, 0.2, 0.4, 0.6, 0.8, 1.0, 1.2, and 1.4, 7 levels) and refresh rate (60 and 240 Hz, 2 levels) on the persistence range. Data from 60 and 240 Hz are pooled.

Variable	F	$df_1$	$df_2$	MSE	P	$\eta_p^2$
Length ratio	5.831	1	12	230.97	0.0326	0.33
Refresh rate	17.04	7	84	78.28	$7.99e^{-14}$	0.59
Length ratio x Refresh rate	2.999	7	84	19.079	0.00735	0.20

Table S18. Multiple comparison results of Tukey's test on the length ratio effect for 60 Hz.

Length Ratio	Means (°)	G1	G2
1	13.19	a	
2	11.96	a	
3	9.81	a	
4	8.22		b
6	7.19		b
5	7.04		b
8	7.00		b
7	6.35		b

Table S19. Multiple comparison results of Tukey's test on the length ratio effect for 240 Hz.

Length Ratio	Means (°)	G1	G2	G3
1	8.67	a		
2	7.63	a	b	
3	6.96	a	b	c
6	6.56		b	c
7	6.25		b	c
5	6.18		b	c
8	6.00		b	c
4	5.65			c

Table S20. Multiple comparison results of Tukey's test on the length ratio effect for 1440 Hz condition.

Line Length (°)	Means (°)	G1
Dot diameter (0.2)	7.68	a
60 Hz min (0.4)	7.72	a
60 Hz Max (2.8)	7.94	a
240 Hz min (0.2)	8.19	a
240 Hz Max (0.7)	7.95	a

Table S21. Results of ANOVA in Experiment 4. The effect of the stimulus type (dot and line, 2 levels), the number of elements (1, 2, 3, and 4, 4 levels), and refresh rate (72, 80, 120, and 160 Hz, 4 levels, equivalently, 4 speeds) on the persistence range. Data from 60 and 240 Hz are pooled.

Variable	F	$df_1$	$df_2$	MSE	P	$\eta_p^2$
Stimulus type	7.676	1	5	5540	0.0393	1.00
# of elements	77.32	2	10	78.28	$8.27e^{-07}$	1.00
Refresh rate	2.113	3	15	460.0	0.141	0.3
Stimulus type x # of elements	4.345	2	10	439.5	0.0438	1.00
Stimulus type x Refresh rate	2.342	3	15	386.3	0.114	0.32
# of elements x Refresh rate	5.751	6	30	346.2	$4.47e^{-04}$	0.53
Stimulus type x # of elements x Refresh rate	1.015	6	30	67.97	0.434	0.17



Table S22. Results of ANOVA for Figure S8.

Variable	F	$df_1$	$df_2$	MSE	P	$\eta_p^2$
Stimulus type	6.811	1	5	0.7951	0.0477	1.00
# of elements	227.4	3	15	35.89	$1.01e^{-12}$	1.00
Refresh rate	0.249	2	10	0.0859	0.784	0.05
Stimulus type x # of elements	4.207	3	15	0.22637	0.024	1.00
Stimulus type x Refresh rate	2.171	2	10	0.2221	0.165	0.3
# of elements x Refresh rate	9.132	6	30	0.5212	$1.04e^{-05}$	0.65
Stimulus type x # of elements x Refresh rate	2.884	6	30	0.10928	0.0243	0.37

Table S23. Results of ANOVA for Figure S10.

Variable	F	$df_1$	$df_2$	MSE	P	$\eta_p^2$
Stimulus type	4.053	2	14	716.6	0.0409	0.3667
Refresh rate	19.6	4	28	116.41	$8.66e^{-08}$	0.7368
Speed	7.321	2	14	214.84	0.00667	0.5112
Stimulus type x Refresh rate	2.237	8	56	8.210	0.0379	0.2422
Stimulus type x Speed	2.327	4	28	15.660	0.0809	0.2495
Refresh rate x Speed	1.099	8	56	1.519	0.378	0.1357
Stimulus type x Refresh rate x Speed	0.369	16	112	0.7157	0.987	0.005

## Acknowledgment

I would like to express my gratitude to Dr. Oh-Sang Kwon for his support and guidance throughout my graduate studies. I discovered my passion for vision science during his undergraduate courses, which ultimately led me to pursue a PhD. Dr. Kwon has been an exceptional mentor who not only nurtured me as a scientist but also as a person. I am truly grateful for his mentorship.

I am grateful to Dr. Kwak for steering me in the right direction and ensuring that my research remained focused. I would like to express my appreciation to Dr. Chung for providing me with numerous constructive comments and critical considerations that I may have otherwise overlooked. I would also like to extend my thanks to Dr. Chong for his invaluable advice and constructive comments. His insightful perspectives greatly enriched my PhD studies. I would like to thank Dr. Joo for his suggestions and diverse viewpoints in interpreting the data, as well as for his encouragement.

I am grateful to all of my lab mates. Their assistance ranged from helping with experimental setup to interpreting results and deriving meaningful conclusions from my study. I sincerely value the friendship that blossomed during this challenging yet enlightening experience. Special thanks go to the members of my soccer club, Earth Cops, for their invaluable emotional support and camaraderie.

I would like to express my sincere gratitude to my family for their patience and support. Lastly, my deepest appreciation goes to Hyolim for her boundless patience. Her belief in me and her constant encouragement were essential for me to overcome the challenges of my PhD studies. Thank you for always being there for me.